

Supporting Information

Synthesis of 3,4-dihydroisoquinolin-1(2*H*)-one derivatives and their antioomycete activity against the phytopathogen *Pythium recalcitrans*

Delong Wang[#], Min Li[#], Jing Li, Yali Fang^{*} and Zhijia Zhang^{*}

Department of Pharmaceutical Engineering, College of Plant Protection, Shanxi Key Laboratory of Integrated Pest Management in Agriculture, Shanxi Agricultural University, Taiyuan 030031, China

[#] These authors contributed equally to this work and share the first authorship.

^{*} Correspondence: fang_august@163.com (Y. F.) and Zhang770504@126.com (Z. Z.)

Contents:

1. X-ray diffraction data for compound **I6** (**Table S1**).....Page **S1**
2. The relative configuration ratios of the synthesized target compounds in the present study (**Table S2**).....Page **S2**
3. Experimental and predicted activities of compounds **I1–I34**, **II1–II20** and **III1–III5** for the 3D-QSAR models (**Table S3**).....Page **S3**
4. *In vivo* control efficacy of compound **I23** against *Pythium recalcitrans* on *Nicotiana benthamiana* seedlings in pot experiment (**Table S4**).....Page **S4**
5. The results of molecular superposition based on the common backbone of the most potent compound **I23** (**Figure S1**).....Page **S5**
6. The representative photos of the inhibition effect of compounds **I23** and hymexazol on the mycelial growth of *Pythium recalcitrans* at different concentrations (**Figure S2**).....Page **S5**
7. The correlation plots of the experimental versus predicted activities (pEC₅₀ values) of training and test set based on the CoMFA (**a**) and CoMSIA (**b**) models (**Figure S3**).....Page **S6**
8. Effect of **I23** on cell membrane permeability of *P. recalcitrans* (**Figure S4**).....Page **S6**
9. Comparison between the mean levels of the different lipid classes with the contents higher than 1% (**Figure S5**).....Page **S7**
10. The distribution of the chain lengths and degrees of unsaturation of lipid classes Cer, PI and PC (**Figure S6**).....Page **S8**
11. The ¹H and ¹³C NMR spectra of compounds **I1–I34**, **II1–II20** and **III1–III5**.....Pages **S9–S68**

Table S1. X-ray diffraction data for compound **I6** (CCDC Deposition No. 2180985)

Compound I6	
Chemical formula	C ₂₁ H ₁₇ NO ₄
Chemical formula weight	347.36
Temperature (K)	120.01(10)
Wavelength	1.54184 Å
Crystal system	monoclinic
Space group	<i>P</i> 1 2 ₁ / <i>n</i> 1
Unit cell dimension	<i>a</i> =8.61550(10) Å, <i>b</i> =13.21640(10) Å, <i>c</i> =15.09880(10) Å <i>α</i> =90°, <i>β</i> =99.6980(10)°, <i>γ</i> =90°
Volume (Å ³)	1694.67(3)
<i>Z</i>	4
Calculated density (g/cm ³)	1.361
Radiation type	Cu <i>Kα</i>
Absorpt coefficient (mm ⁻¹)	0.776
Crystal description	colourless block
Crystal size (mm)	0.3 × 0.2 × 0.1
Diffractometer	XtaLAB Synergy R, HyPix
Absorpt correction type	multi-scan
<i>T</i> _{max}	1.00000
<i>T</i> _{min}	0.87479
Theta range for data collection	4.474° to 67.684°
<i>F</i> (000)	728
Limiting indices	-10 ≤ <i>h</i> ≤ 10, -15 ≤ <i>k</i> ≤ 16, -18 ≤ <i>l</i> ≤ 17
Reflection number/cell	16914/14765
measurement reflection used	
<i>R</i> _{int} , <i>R</i> _{sigma}	0.0151, 0.0087
Refinement method	Full-matrix
No. of refinement reflections	3424
No. of reflections (<i>I</i> > 2σ(<i>I</i>))	3340
No. of parameters	236
No. of restraints	0
H-atom treatment	H-atom parameters constrained
Goodness-of-fit on <i>F</i> ²	1.041
<i>R</i> indices (all data)	<i>R</i> ₁ = 0.0388, <i>wR</i> ₂ = 0.1000
Final <i>R</i> indices (<i>I</i> > 2σ(<i>I</i>))	<i>R</i> ₁ = 0.0380, <i>wR</i> ₂ = 0.0995
Extinction method	none
Δρ _{max} , Δρ _{min} (e Å ⁻³)	0.304, -0.252

Table S2. The relative configuration ratios of the synthesized target compounds in the present study

Compd.	<i>trans/cis</i> ratio	Compd.	<i>trans/cis</i> ratio
I1	1:0 (<i>trans</i> only)	I31	0:1
I2	1:0	I32	0:1
I3	1:0	I33	0:1
I4	0:1 (<i>cis</i> only)	I34	0:1
I5	1:0	II1	0:1
I6	1:0	II2	0:1
I7	1:0	II3	0:1
I8	1:0	II4	1:6.3
I9	5.6:1	II5	0:1
I10	1:0	II6	1:9
I11	1:0	II7	0:1
I12	1:0	II8	0:1
I13	1:0	II9	1:3.1
I14	1:0	II10	1:6.3
I15	0:1	II11	0:1
I16	0:1	II12	1:0
I17	0:1	II13	1:7.1
I18	0:1	II14	0:1
I19	0:1	II15	0:1
I20	0:1	II16	0:1
I21	0:1	II17	1:5.3
I22	1:0	II18	0:1
I23	0:1	II19	1:4.8
I24	0:1	II20	1:3.2
I25	1:6.6	III1	1:0
I26	0:1	III2	1:0
I27	0:1	III3	1:0
I28	0:1	III4	1:0
I29	0:1	III5	1:0
I30	0:1		

Table S3. Experimental and predicted activities of compounds **I1–I34**, **II1–II20** and **III1–III5** for the 3D-QSAR models

Compd.	EC ₅₀ (× 10 ⁻³ mM)	Actual pEC ₅₀	CoMFA		CoMSIA	
			Predicated	Residual	Predicated	Residual
I1*	46.6	1.332	1.311	-0.021	1.340	0.008
I2	45.8	1.339	1.359	0.020	1.335	-0.004
I3*	29.5	1.530	1.405	-0.125	1.412	-0.118
I4	45.4	1.343	1.362	0.019	1.357	0.014
I5	53.7	1.270	1.365	0.095	1.319	0.049
I6	46.8	1.330	1.178	-0.152	1.238	-0.092
I7	43.6	1.360	1.359	-0.001	1.354	-0.006
I8*	59.8	1.223	1.130	-0.093	1.190	-0.033
I9	57.4	1.241	1.406	0.165	1.380	0.139
I10	54.0	1.268	1.310	0.042	1.313	0.045
I11	46.5	1.333	1.315	-0.018	1.320	-0.013
I12	67.8	1.169	1.351	0.182	1.323	0.154
I13	65.1	1.187	1.292	0.105	1.308	0.121
I14*	40.6	1.392	1.347	-0.045	1.334	-0.058
I15*	42.8	1.369	1.585	0.216	1.531	0.162
I16	20.9	1.681	1.518	-0.163	1.456	-0.225
I17*	23.2	1.635	1.643	0.008	1.578	-0.057
I18	25.1	1.601	1.710	0.109	1.599	-0.002
I19	21.5	1.668	1.653	-0.015	1.581	-0.087
I20	23.2	1.635	1.533	-0.102	1.578	-0.057
I21	14.7	1.833	1.593	-0.240	1.620	-0.213
I22	20.8	1.682	1.544	-0.138	1.634	-0.048
I23	14.0	1.855	1.537	-0.318	1.54	-0.315
I24	38.9	1.411	1.506	0.095	1.498	0.087
I25	33.2	1.479	1.566	0.087	1.543	0.064
I26	29.6	1.528	1.574	0.046	1.553	0.025
I27	26.0	1.585	1.592	0.007	1.569	-0.016
I28	29.4	1.532	1.646	0.114	1.588	0.056
I29	41.7	1.380	1.351	-0.029	1.368	-0.012
I30*	26.0	1.585	1.541	-0.044	1.463	-0.122
I31	36.3	1.440	1.465	0.025	1.418	-0.022
I32	26.9	1.570	1.648	0.078	1.547	-0.023
I33	43.1	1.365	1.399	0.034	1.513	0.148
I34	40.9	1.389	1.424	0.035	1.374	-0.015
II1*	18.2	1.739	1.636	-0.103	1.609	-0.13
II2	27.7	1.558	1.555	-0.003	1.558	0
II3	32.0	1.494	1.552	0.058	1.578	0.084
II4	38.5	1.415	1.562	0.147	1.588	0.173
II5*	45.3	1.344	1.472	0.128	1.515	0.171

II6	43.0	1.366	1.430	0.064	1.400	0.034
II7	31.5	1.502	1.472	-0.030	1.540	0.038
II8	47.1	1.327	1.424	0.097	1.477	0.150
II9	31.3	1.504	1.473	-0.031	1.523	0.019
II10	41.3	1.384	1.502	0.118	1.534	0.150
II11	16.9	1.773	1.615	-0.158	1.613	-0.160
II12*	35.8	1.446	1.529	0.083	1.567	0.121
II13	29.6	1.529	1.511	-0.018	1.500	-0.029
II14	47.8	1.321	1.366	0.045	1.434	0.113
II15*	31.3	1.505	1.397	-0.108	1.391	-0.114
II16*	48.7	1.313	1.287	-0.026	1.444	0.131
II17	30.3	1.519	1.573	0.054	1.548	0.029
II18	33.1	1.480	1.511	0.031	1.523	0.043
II19*	32.2	1.492	1.514	0.022	1.509	0.017
II20	34.0	1.469	1.506	0.037	1.523	0.054
III1	951.4	0.022	-0.185	-0.207	-0.094	-0.116
III2	1258.1	-0.097	0.066	0.163	0.007	0.104
III3	874.3	0.060	0.035	-0.025	-0.034	-0.094
III4*	895.7	0.051	0.186	0.135	0.141	0.090
III5	1055.2	-0.021	0.174	0.195	0.132	0.153

* The compounds were in the test set for external validation of the optimal 3D-QSAR models.

Table S4. *In vivo* control efficacy of compound **I23** against *Pythium recalcitrans* on *Nicotiana benthamiana* seedlings in pot experiment

Compound	Dose (mg/pot)	Control efficacy (%)	
		Preventive effect	Curative effect
I23	1.0	37.8 ± 10.7c	3.3 ± 2.9c
	2.0	75.4 ± 12.6b	33.3 ± 12.6ab
	5.0	96.5 ± 3.1a	55.0 ± 10.0a
Hymexazol	2.0	63.9 ± 3.5b	21.7 ± 10.4b

The results were expressed as the mean ± SD of three independent replicates.

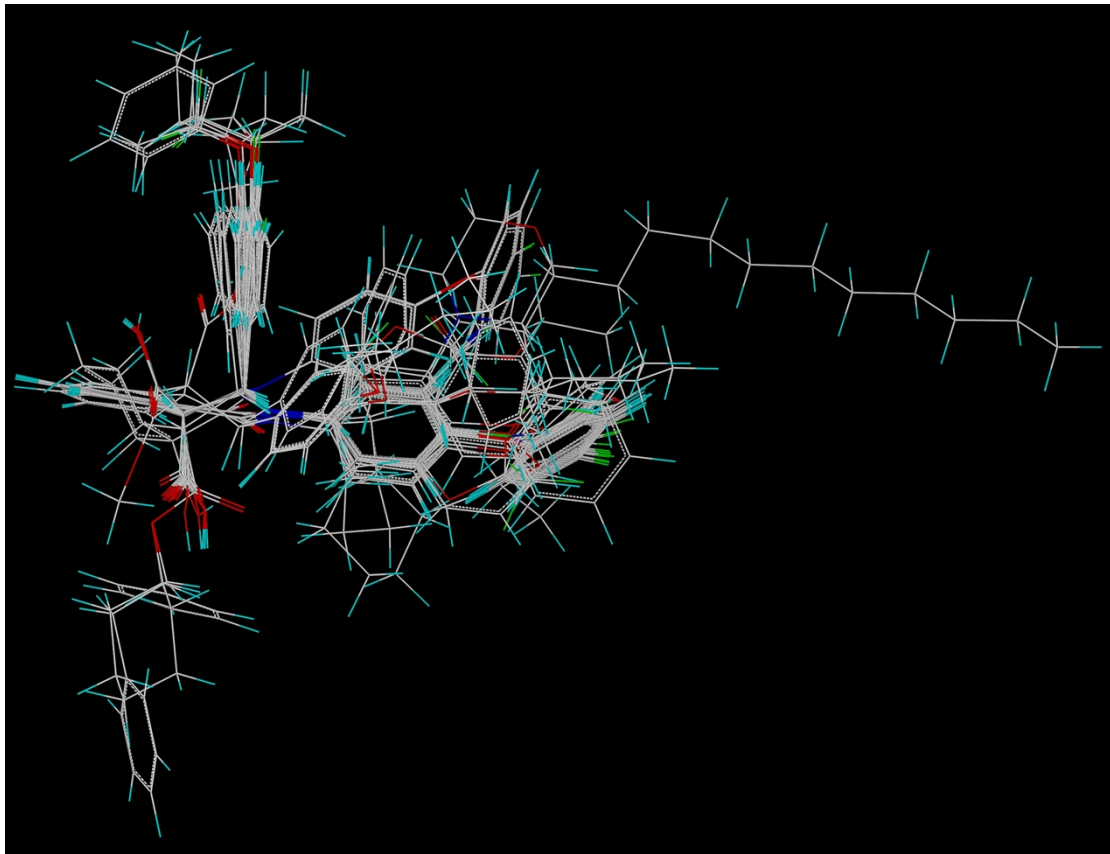


Figure S1. The results of molecular superposition based on the common backbone of the most potent compound **I23**.

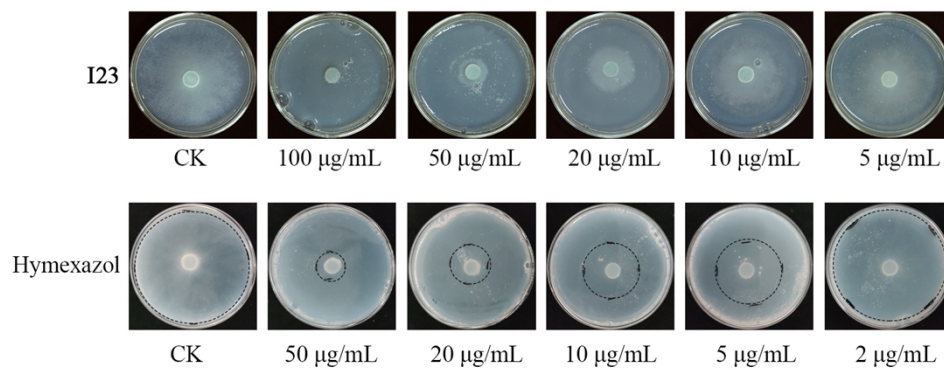


Figure S2. The representative photos of the inhibition effect of compounds **I23** and hymexazol on the mycelial growth of *Pythium recalcitrans* at different concentrations.

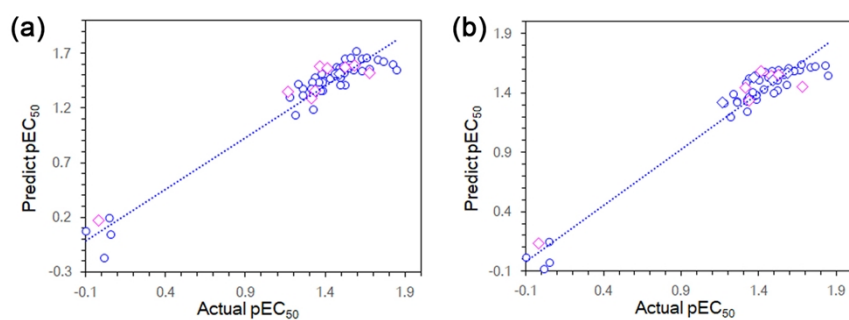


Figure S3. The correlation plots of the experimental versus predicted activities (pEC₅₀ values) of training (○) and test (*) set based on the CoMFA (a) and CoMSIA (b) models.

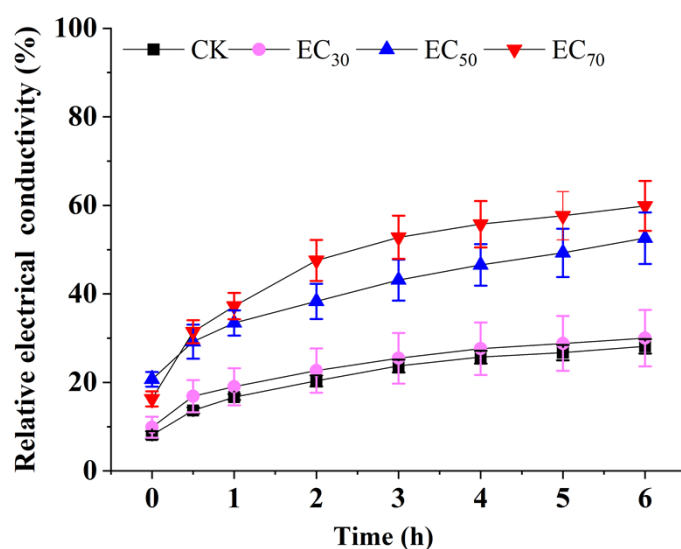


Figure S4. Effect of I23 on cell membrane permeability of *P. recalcitrans*.

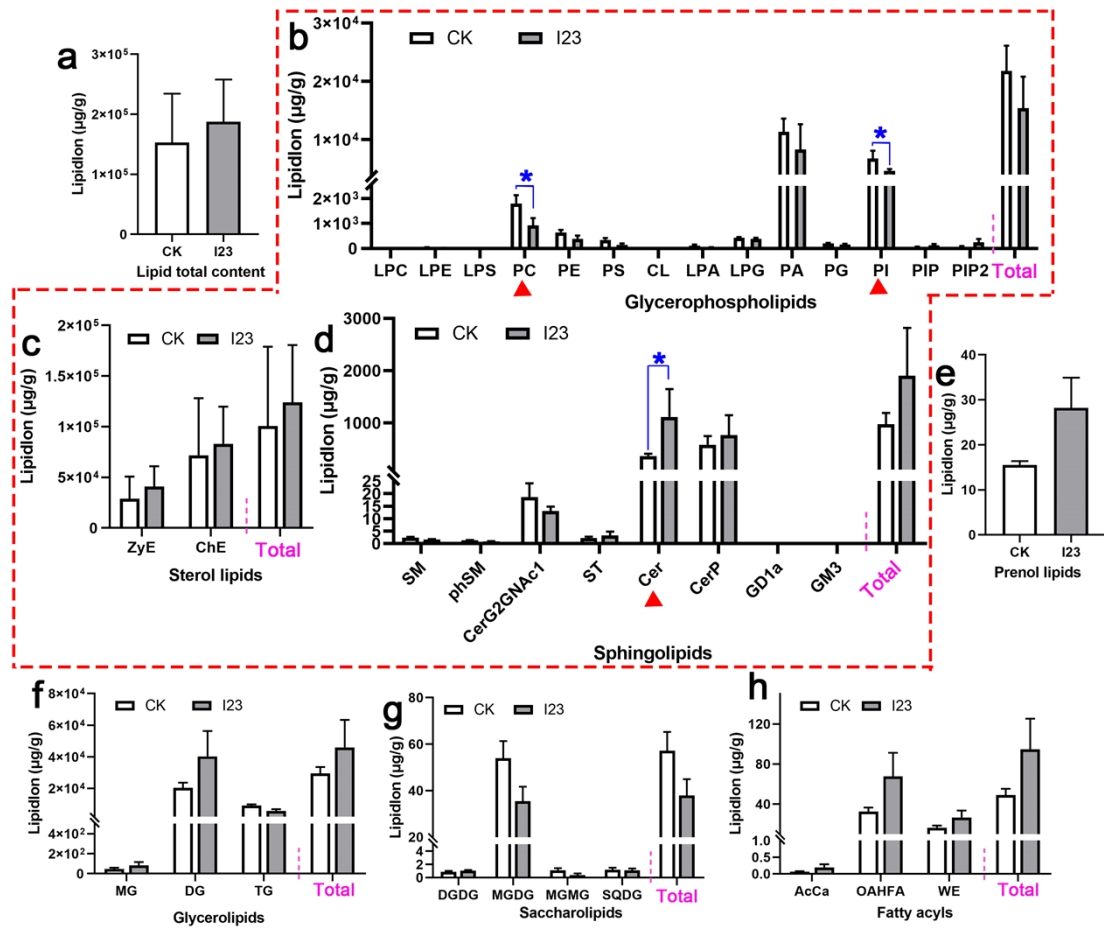


Figure S5. Comparison between the mean levels of the different lipid classes with the contents higher than 1%.

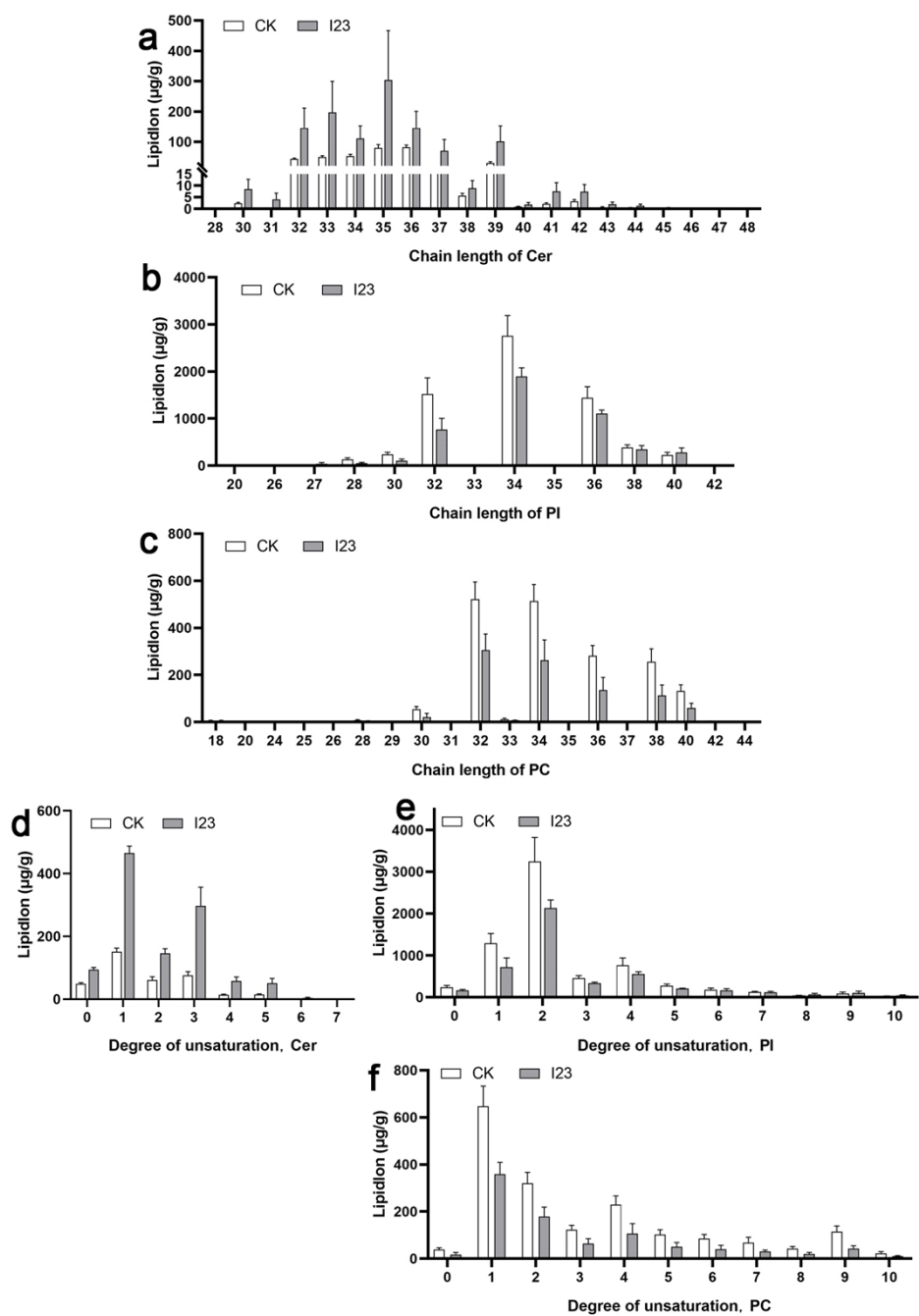


Figure S6. The distribution of the chain lengths and degrees of unsaturation of lipid classes Cer, PI and PC.

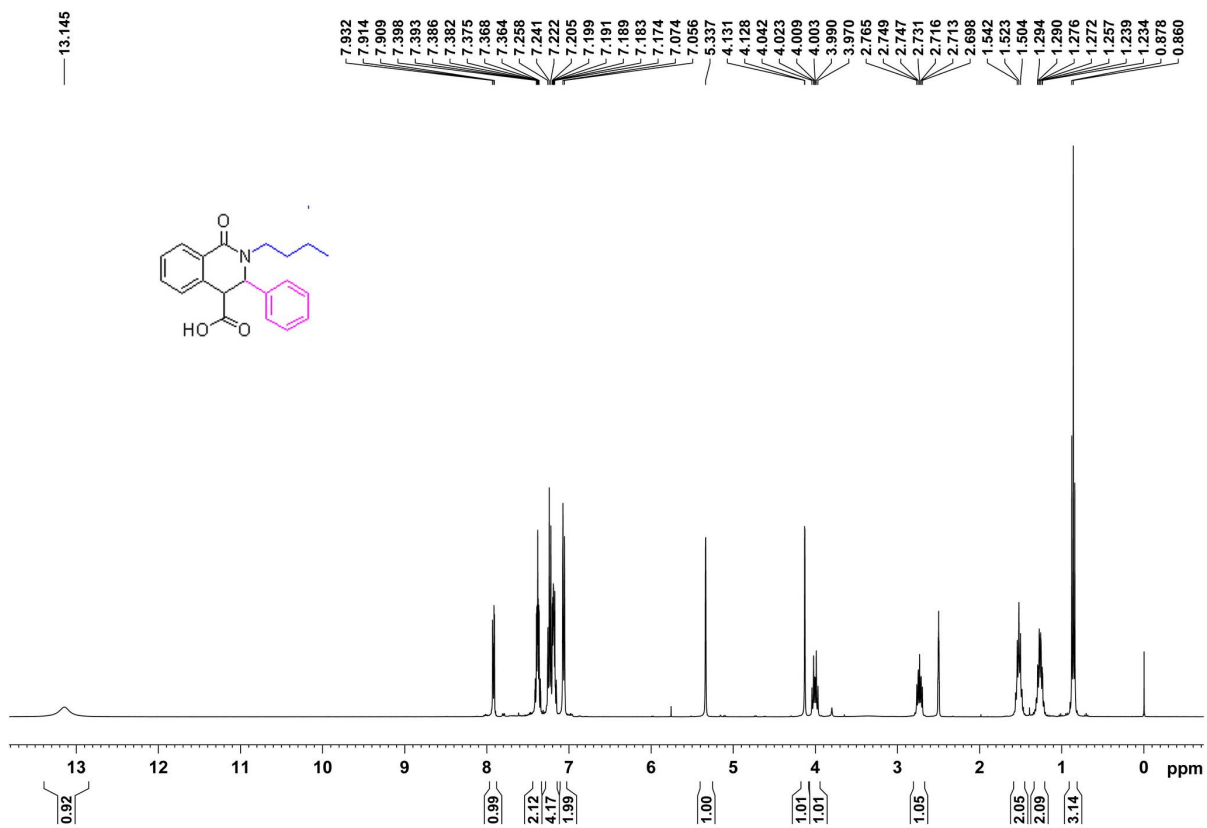


Figure S7. The ^1H NMR spectrum of compound II

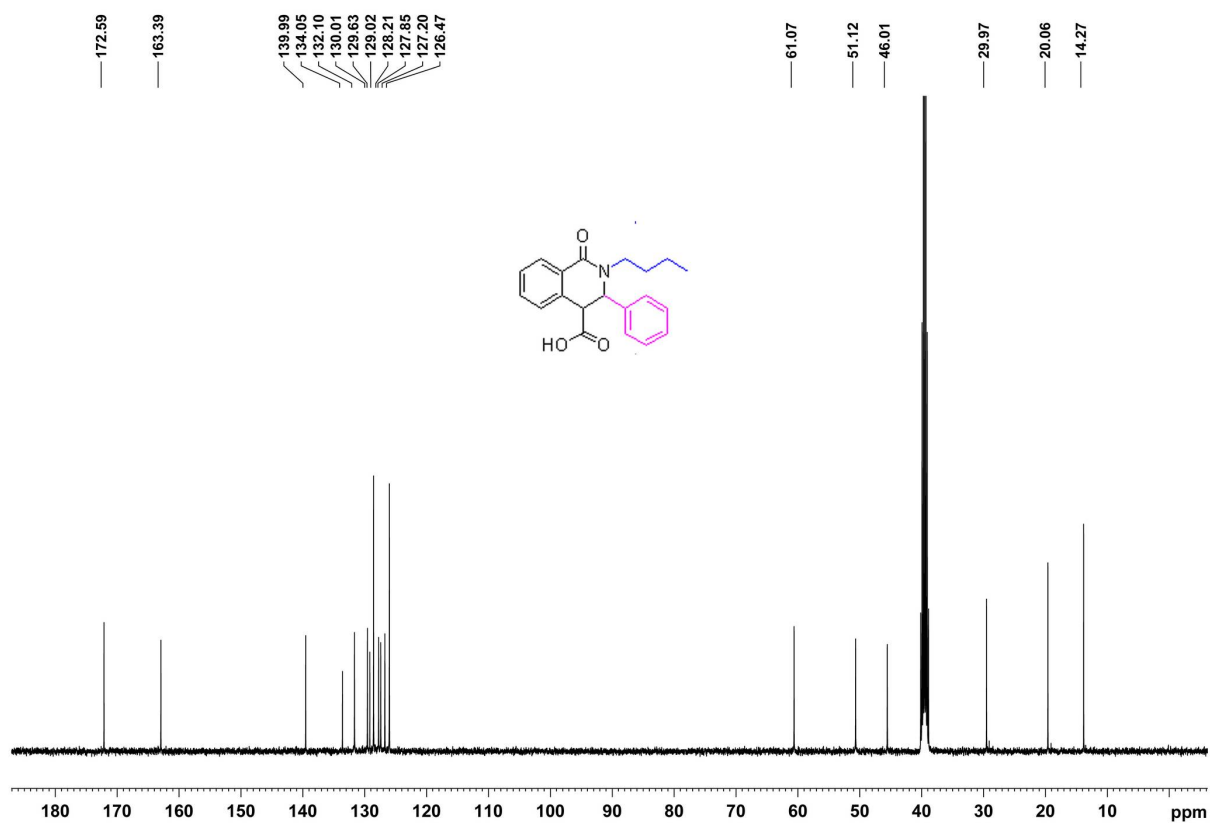


Figure S8. The ^{13}C NMR spectrum of compound II

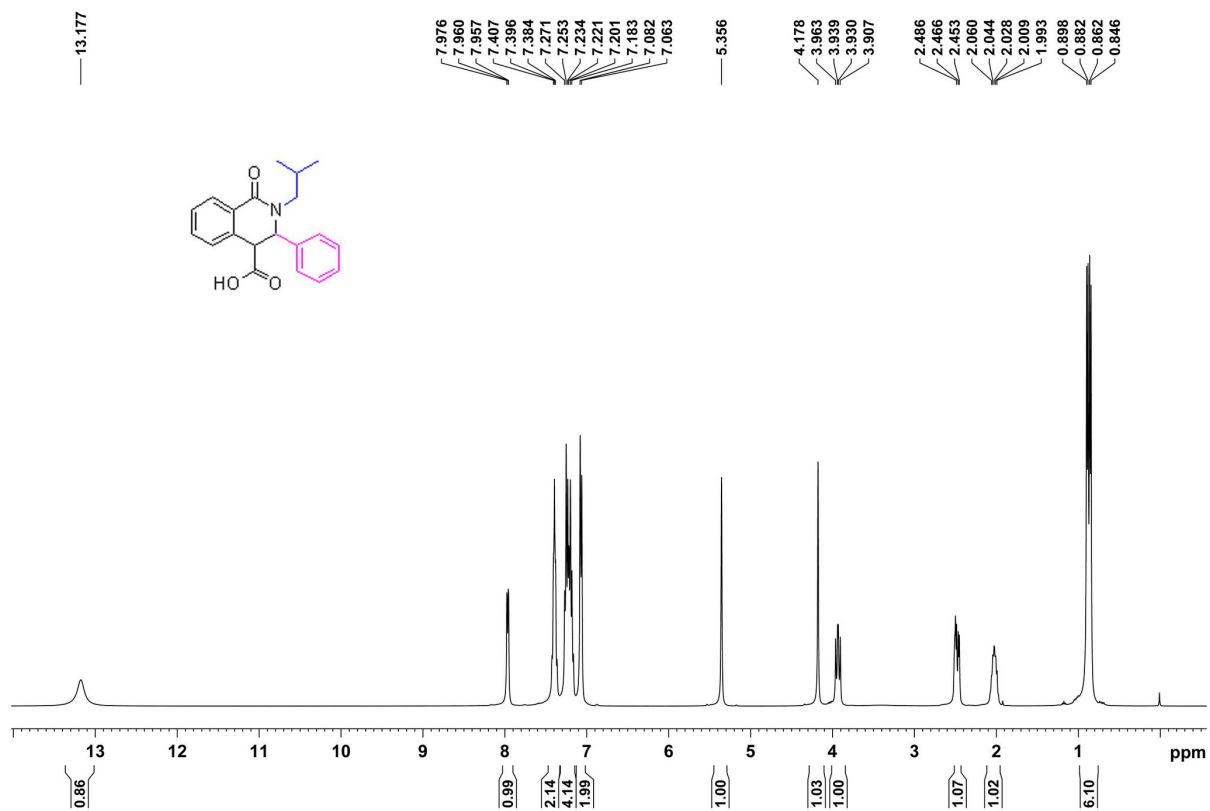


Figure S9. The ¹H NMR spectrum of compound I2

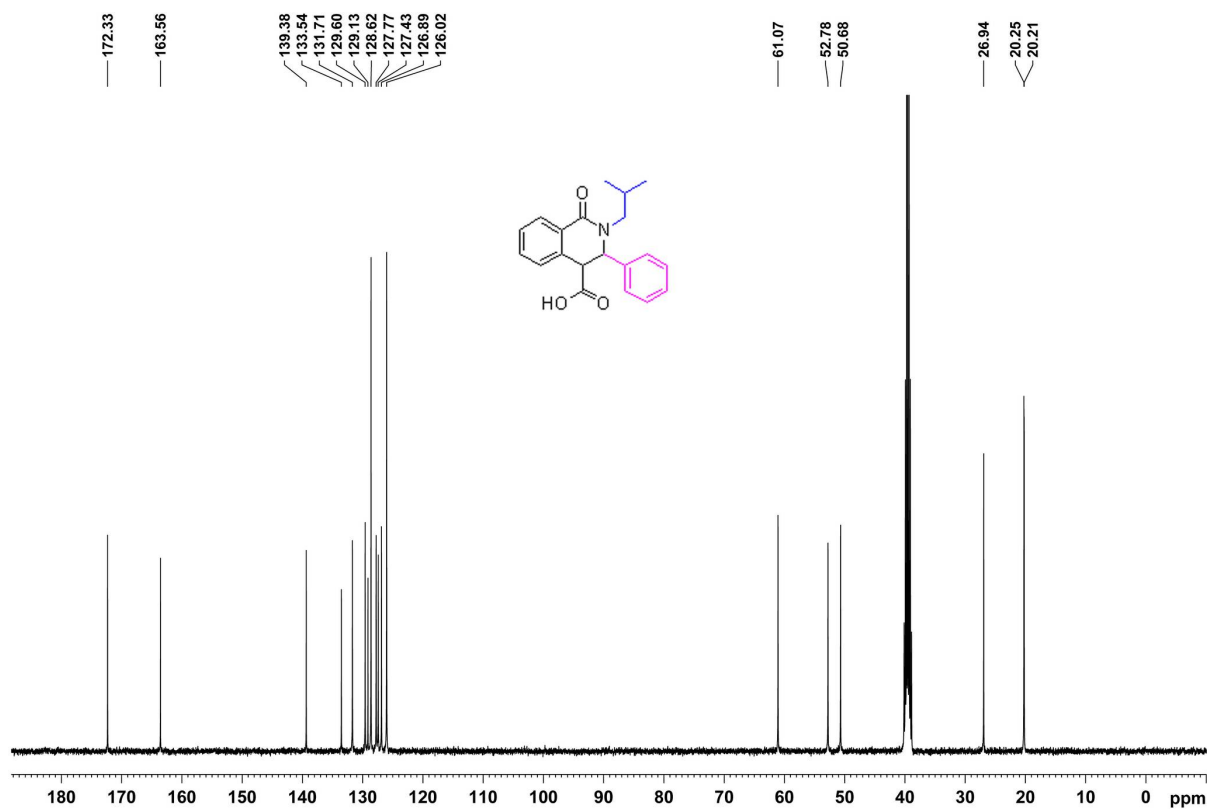


Figure S10. The ¹³C NMR spectrum of compound I2

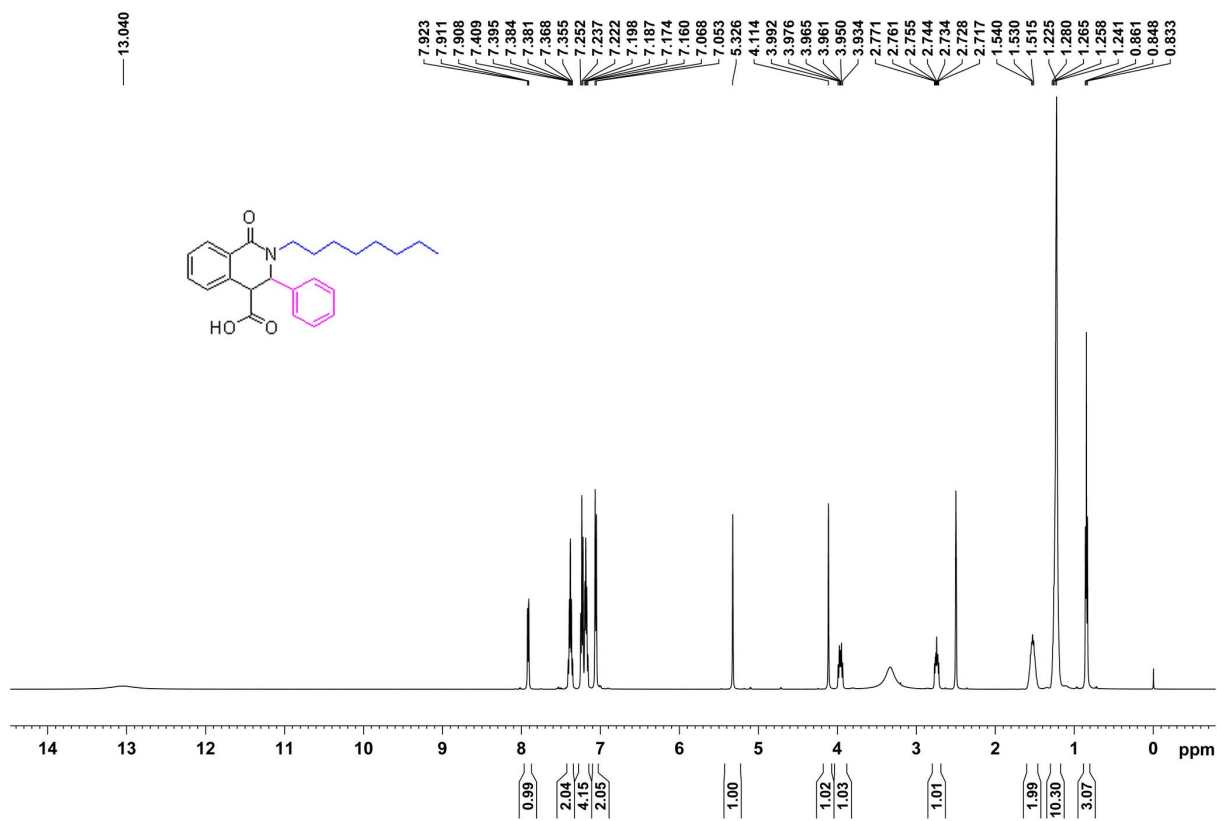


Figure S11. The ^1H NMR spectrum of compound **I3**

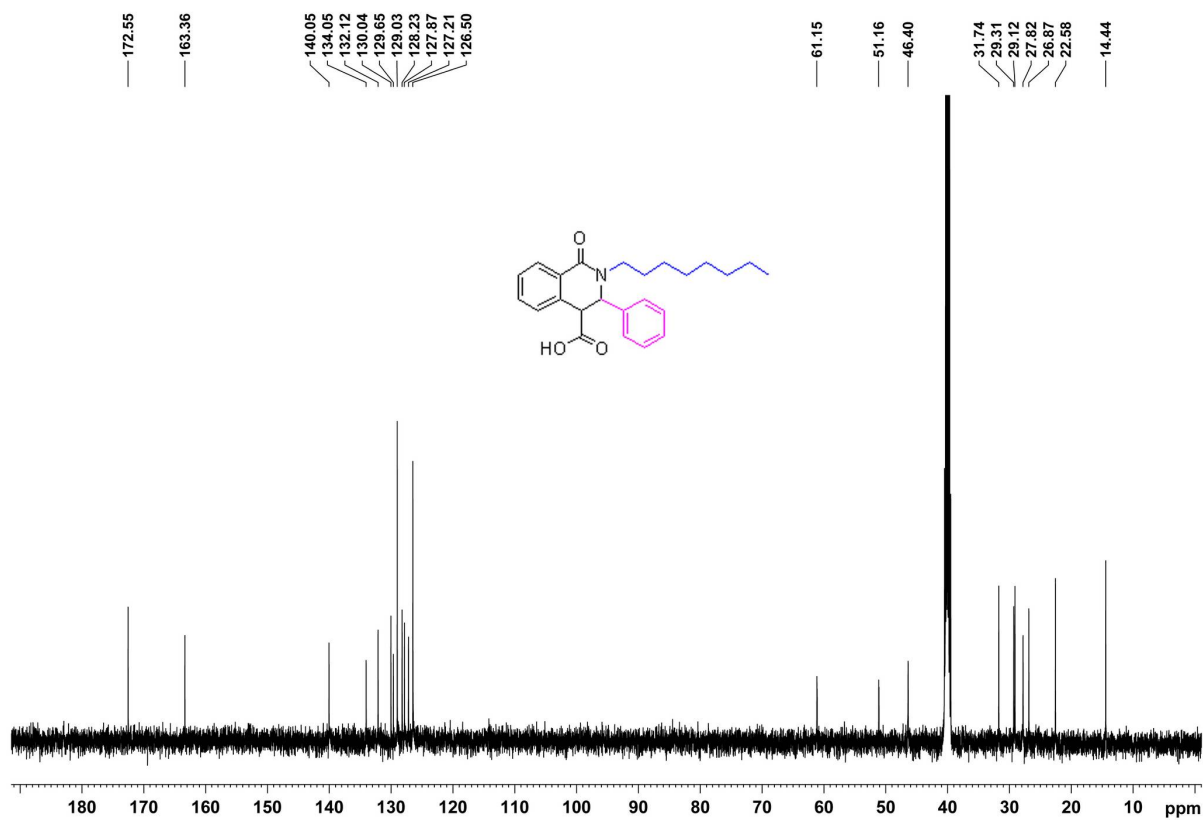


Figure S12. The ^{13}C NMR spectrum of compound **I3**

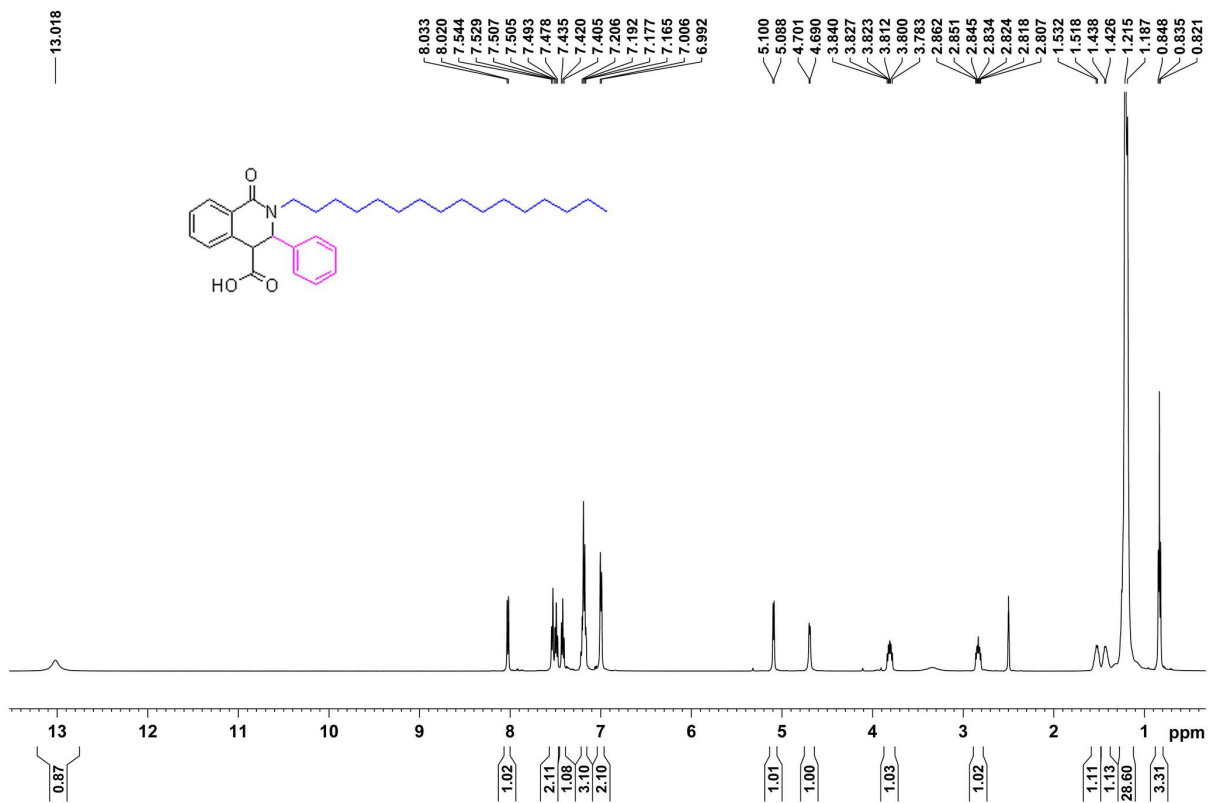


Figure S13. The ¹H NMR spectrum of compound I4

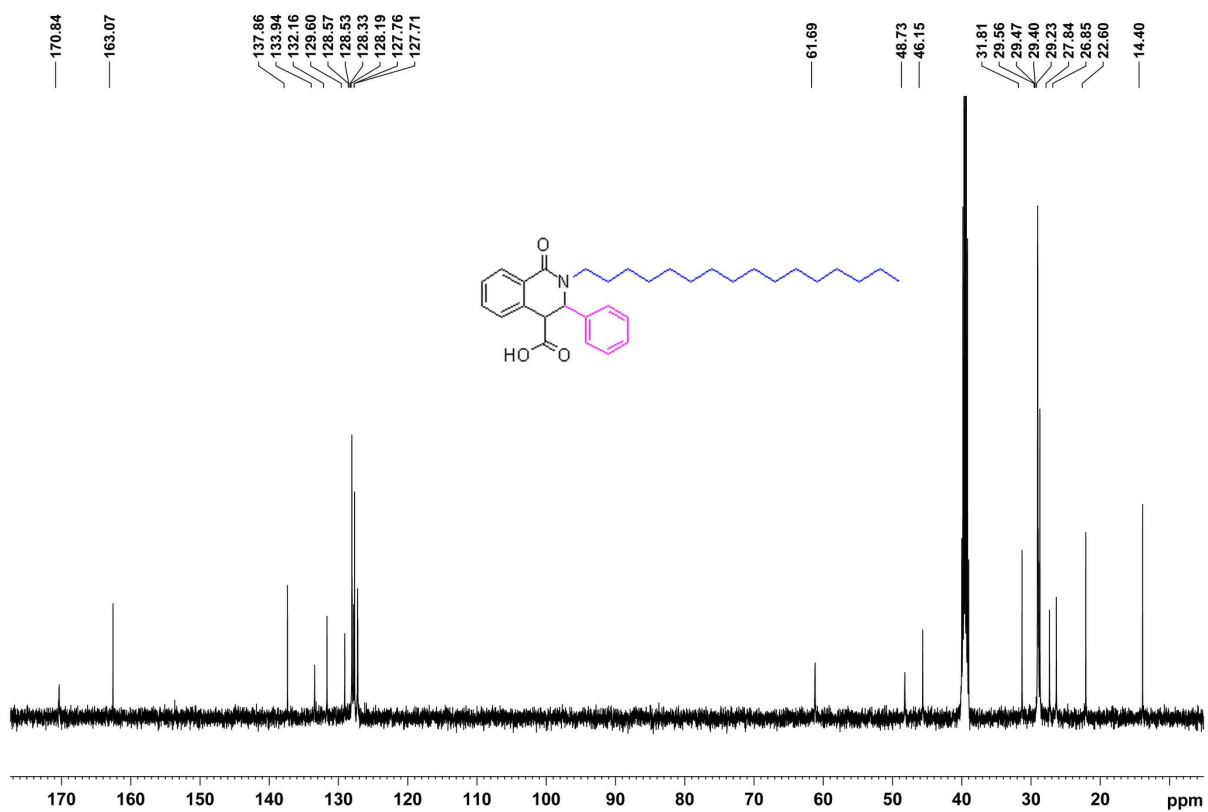


Figure S14. The ¹³C NMR spectrum of compound I4

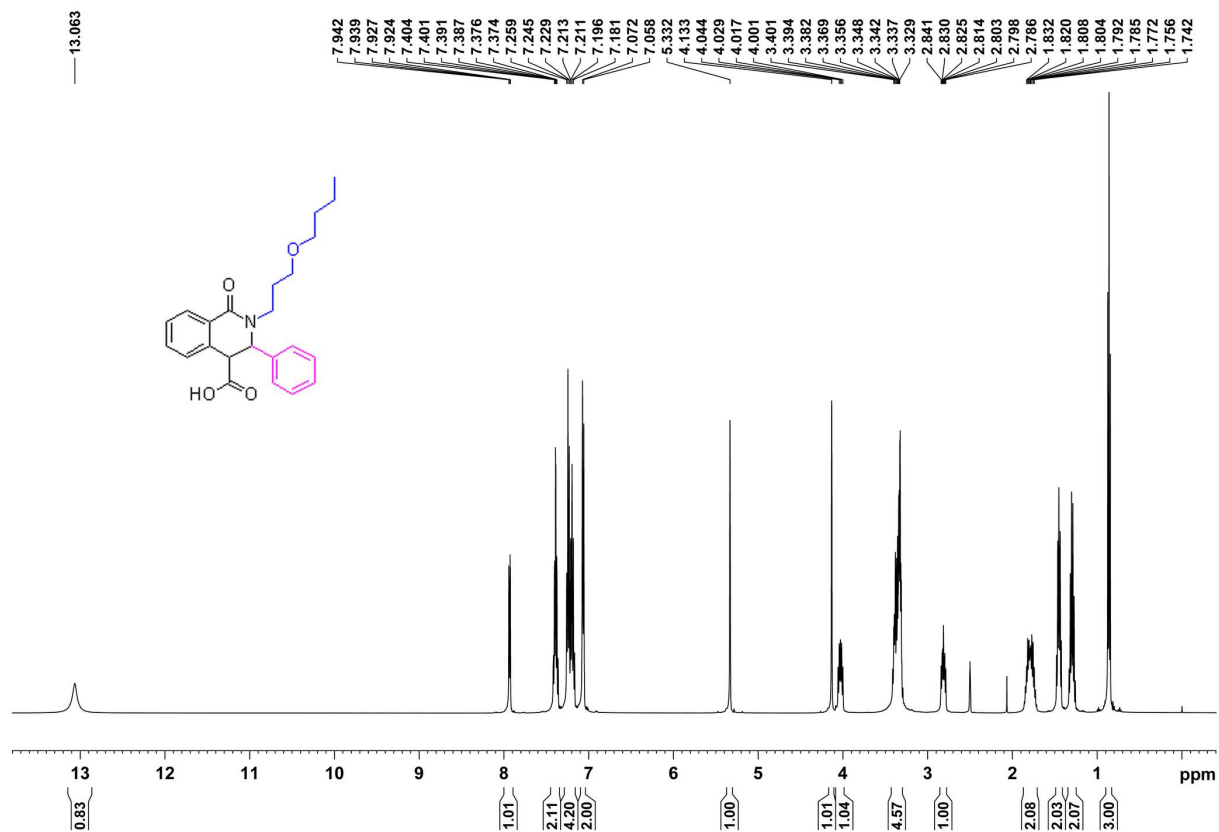


Figure S15. The ¹H NMR spectrum of compound I5

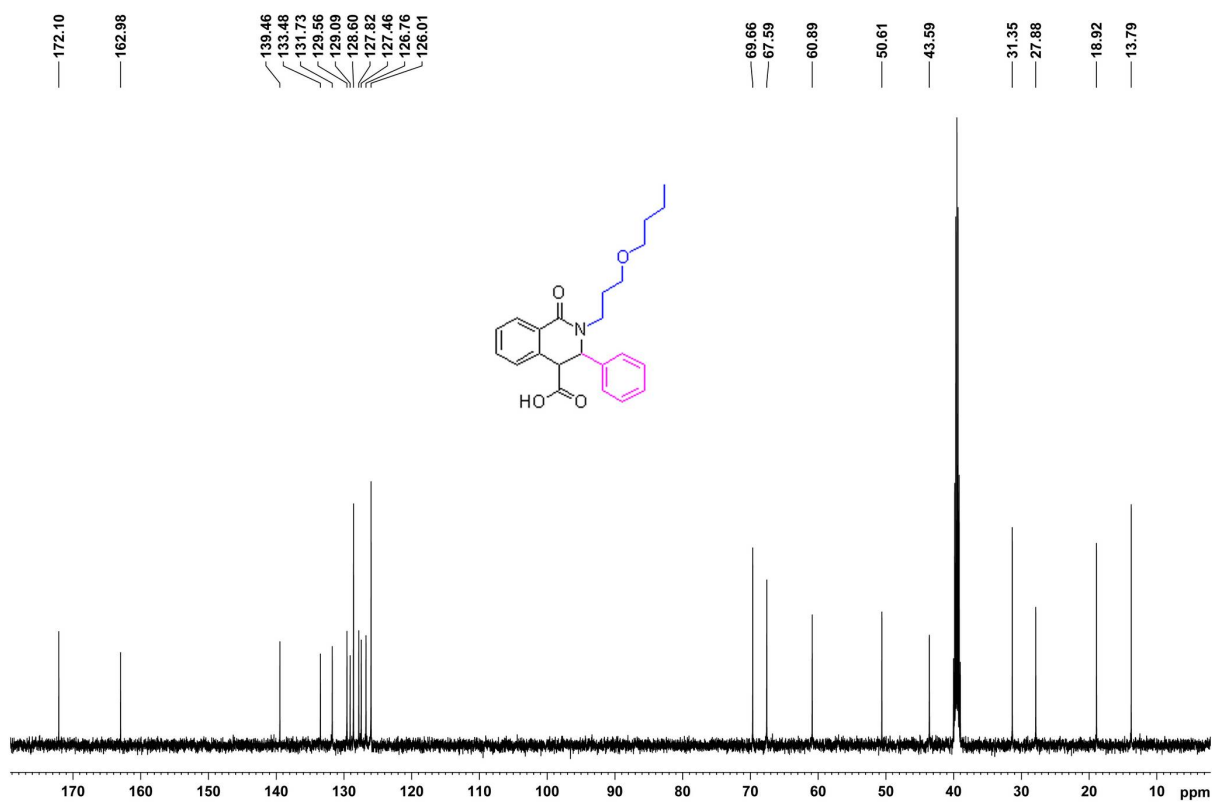


Figure S16. The ¹³C NMR spectrum of compound I5

PROTON DMSO {D:\2020-3} ZHL 26

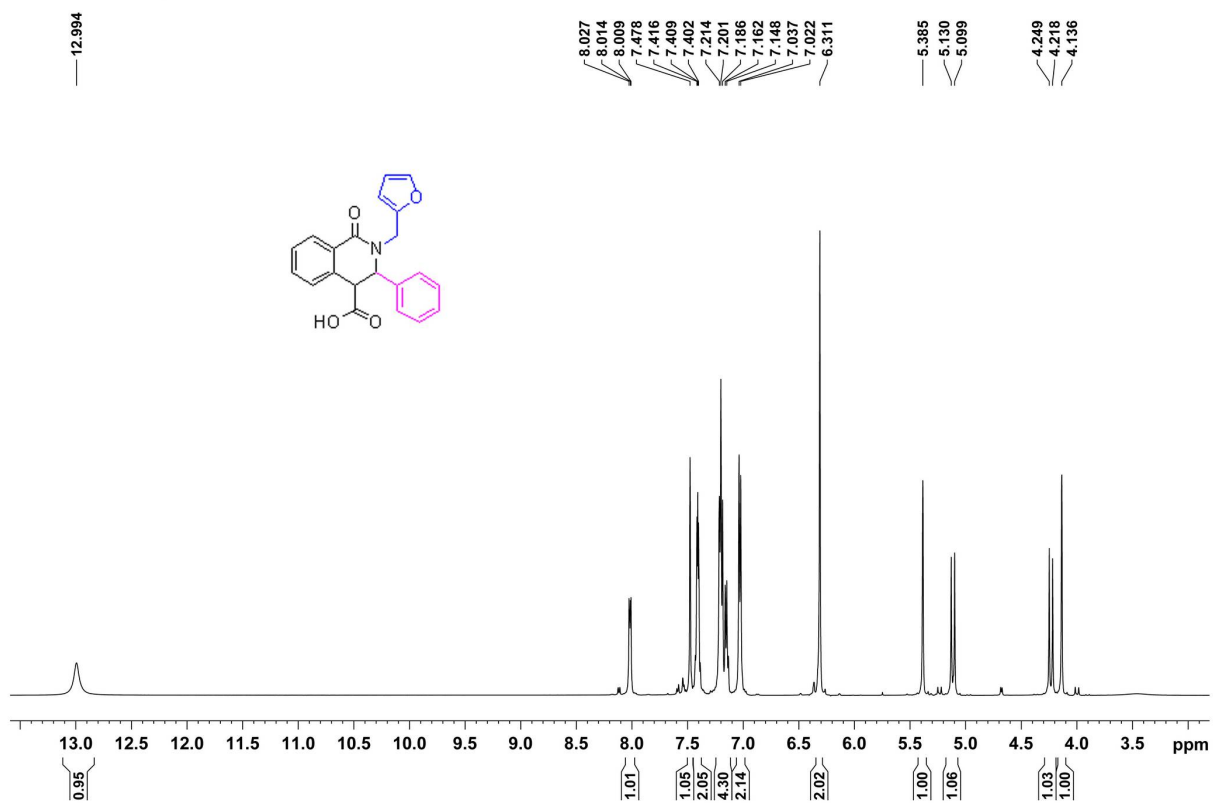


Figure S17. The ¹H NMR spectrum of compound I6

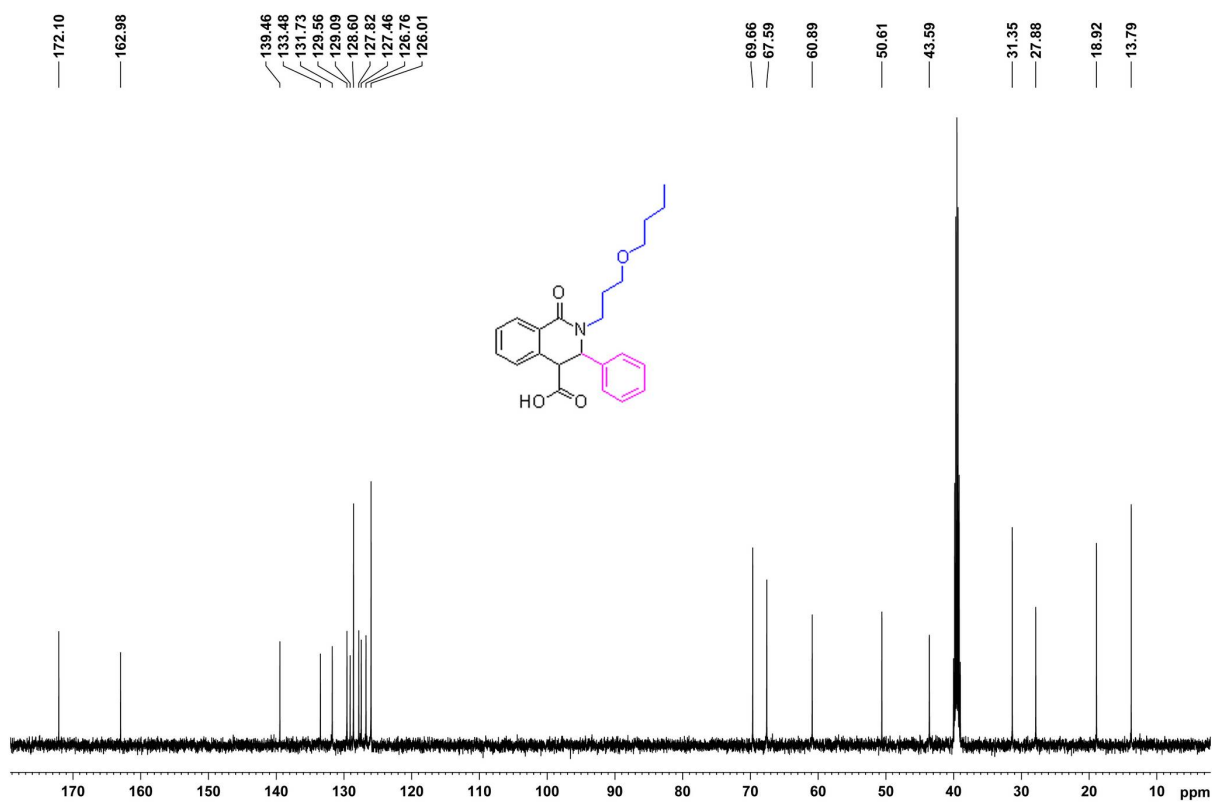


Figure S18. The ¹³C NMR spectrum of compound I6

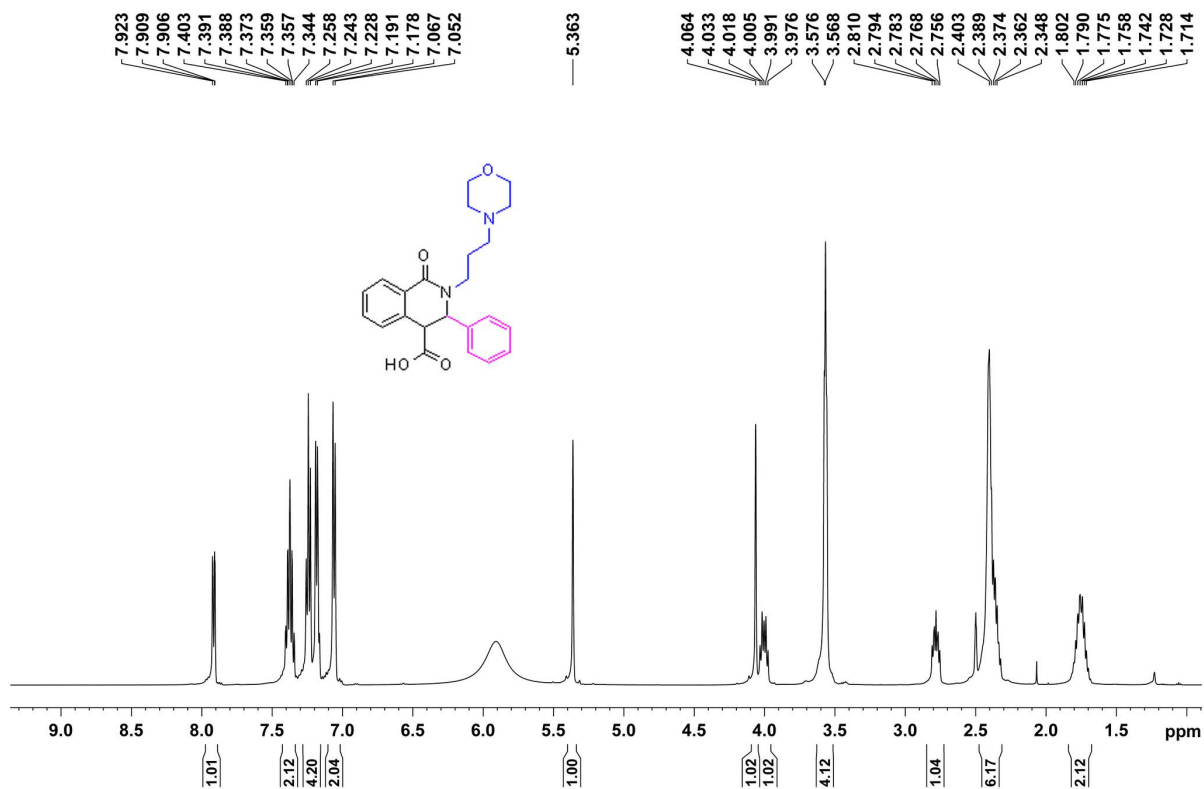


Figure S19. The ¹H NMR spectrum of compound I7

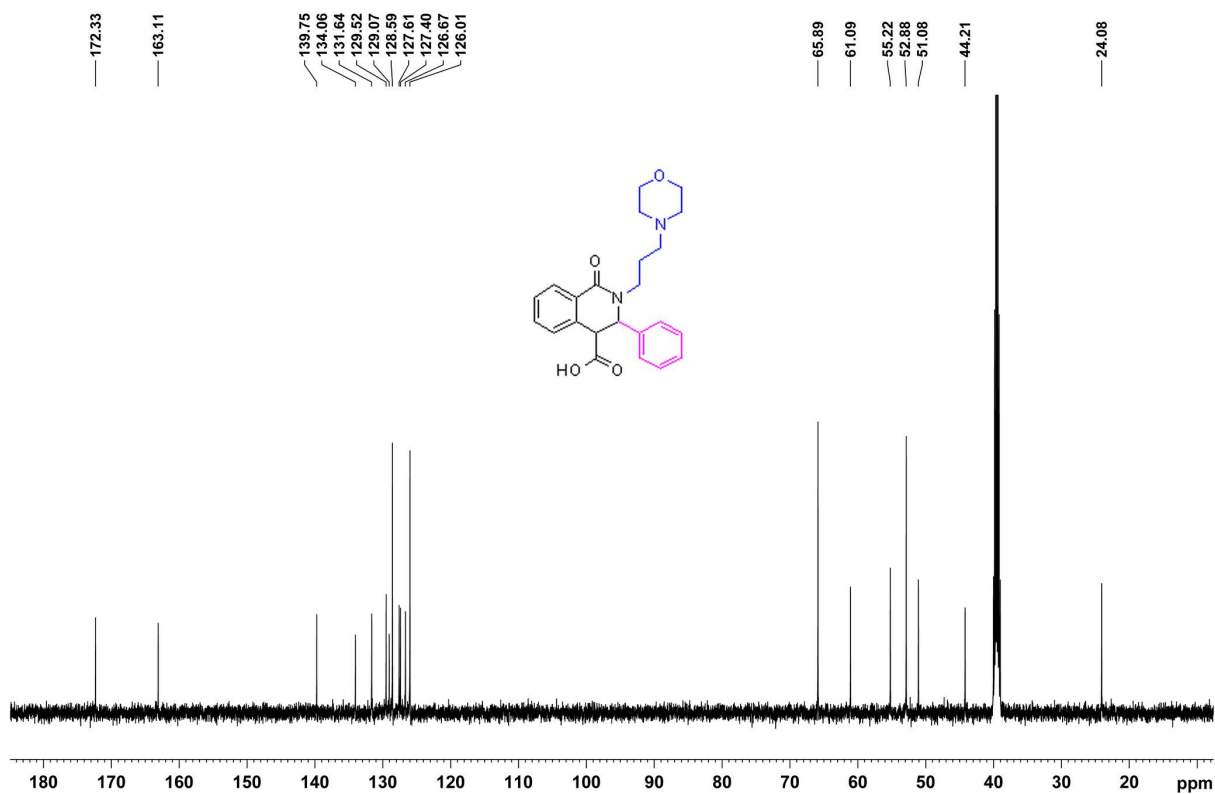


Figure S20. The ¹³C NMR spectrum of compound I7

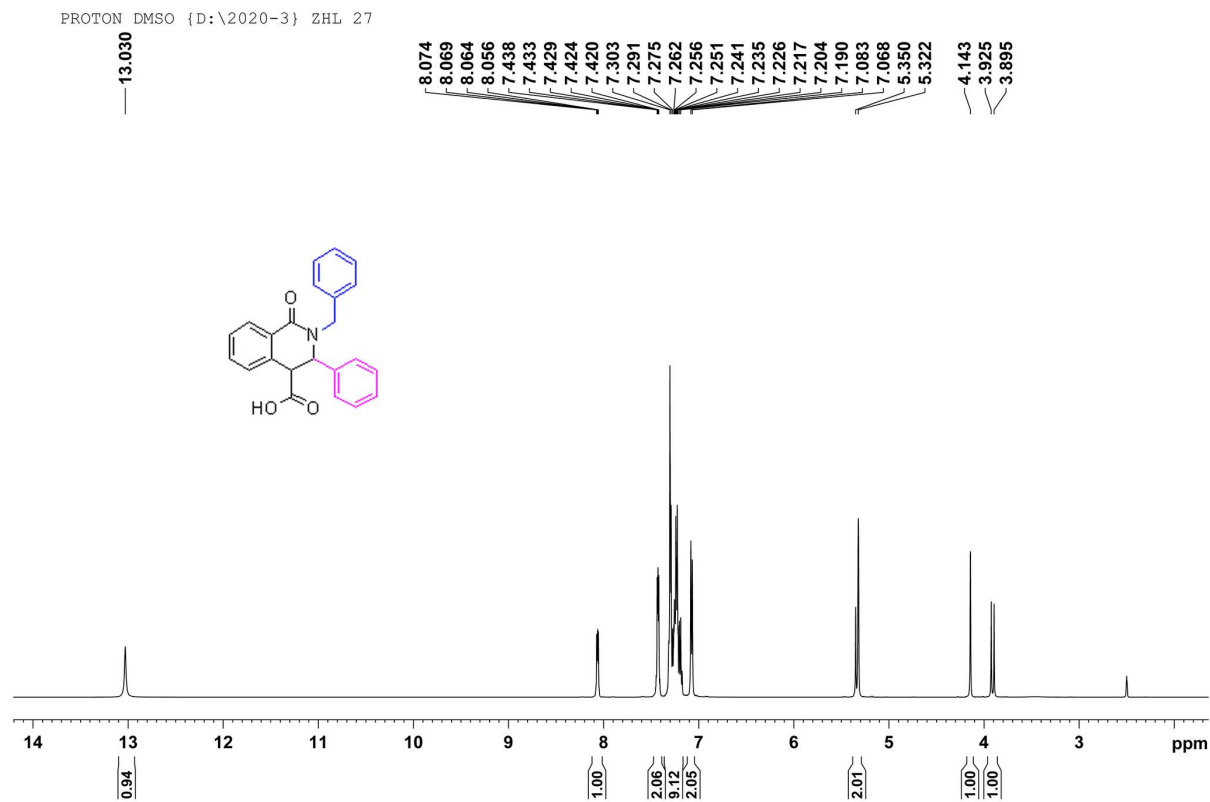


Figure S21. The ^1H NMR spectrum of compound I8

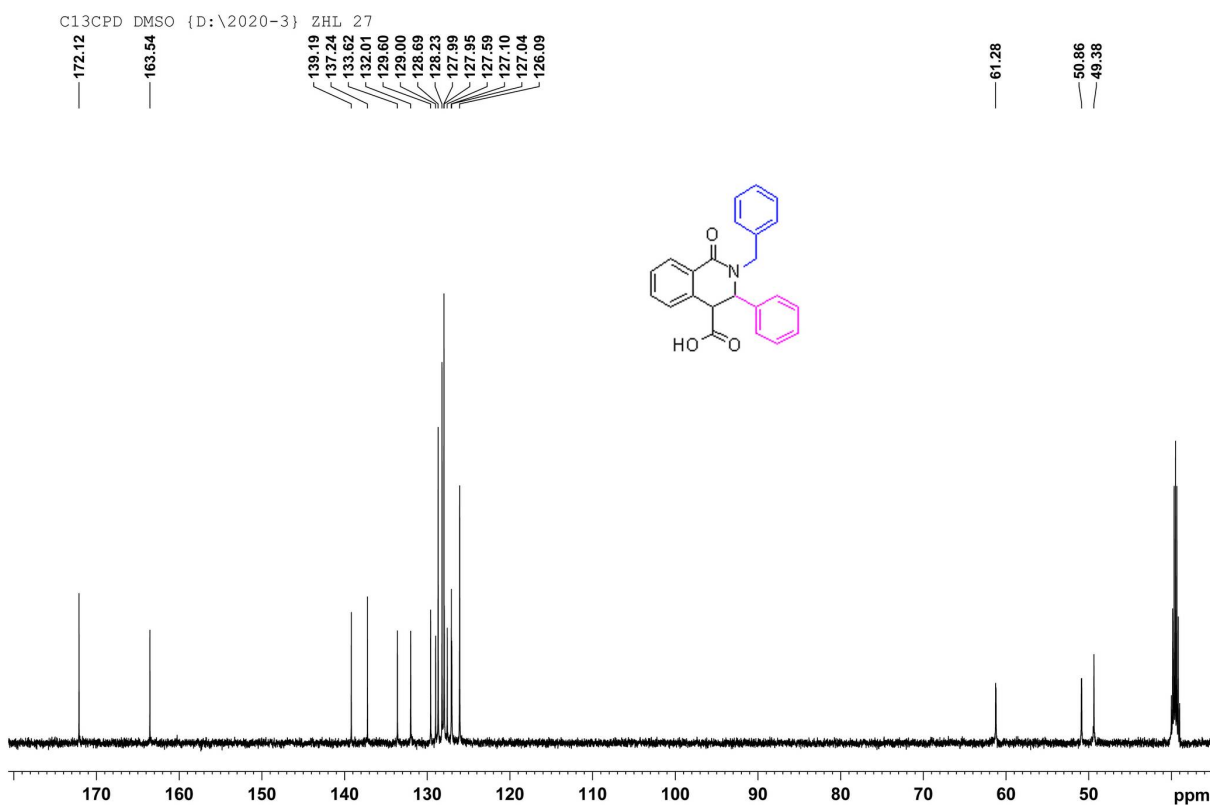


Figure S22. The ^{13}C NMR spectrum of compound I8

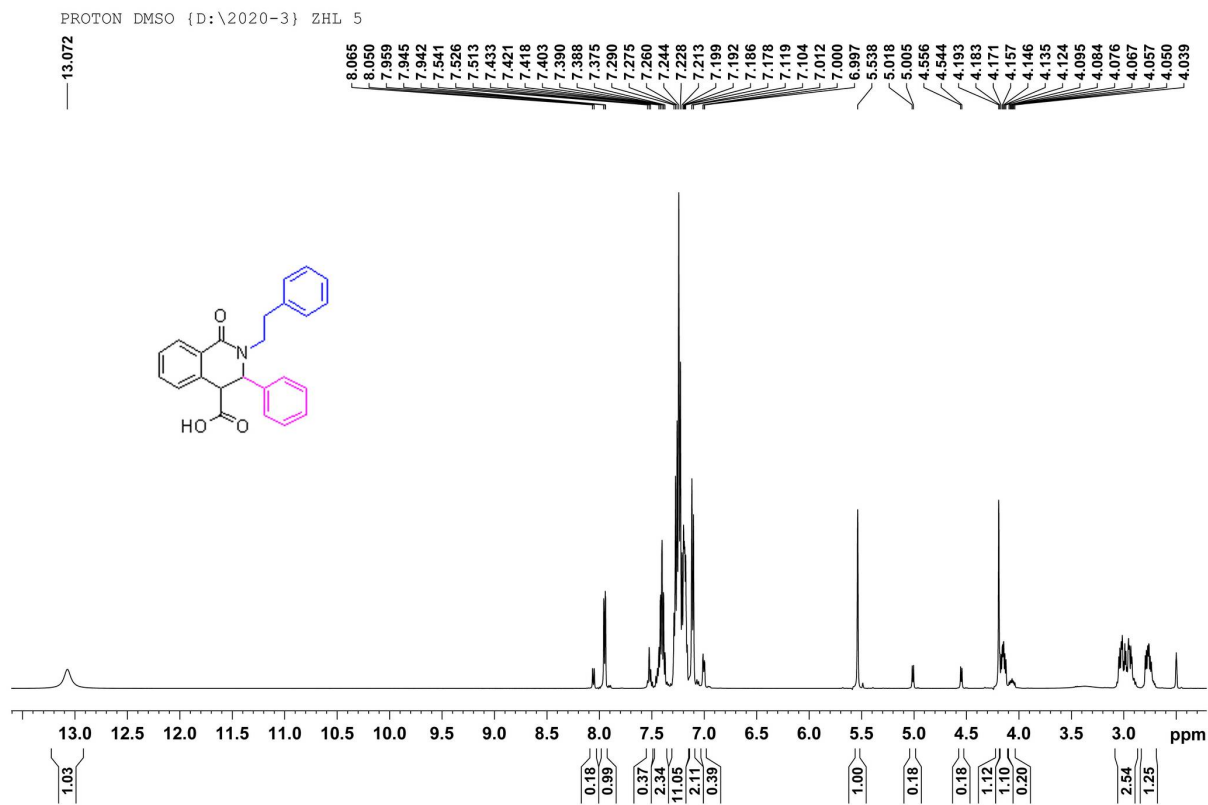


Figure S23. The ^1H NMR spectrum of compound **I9**

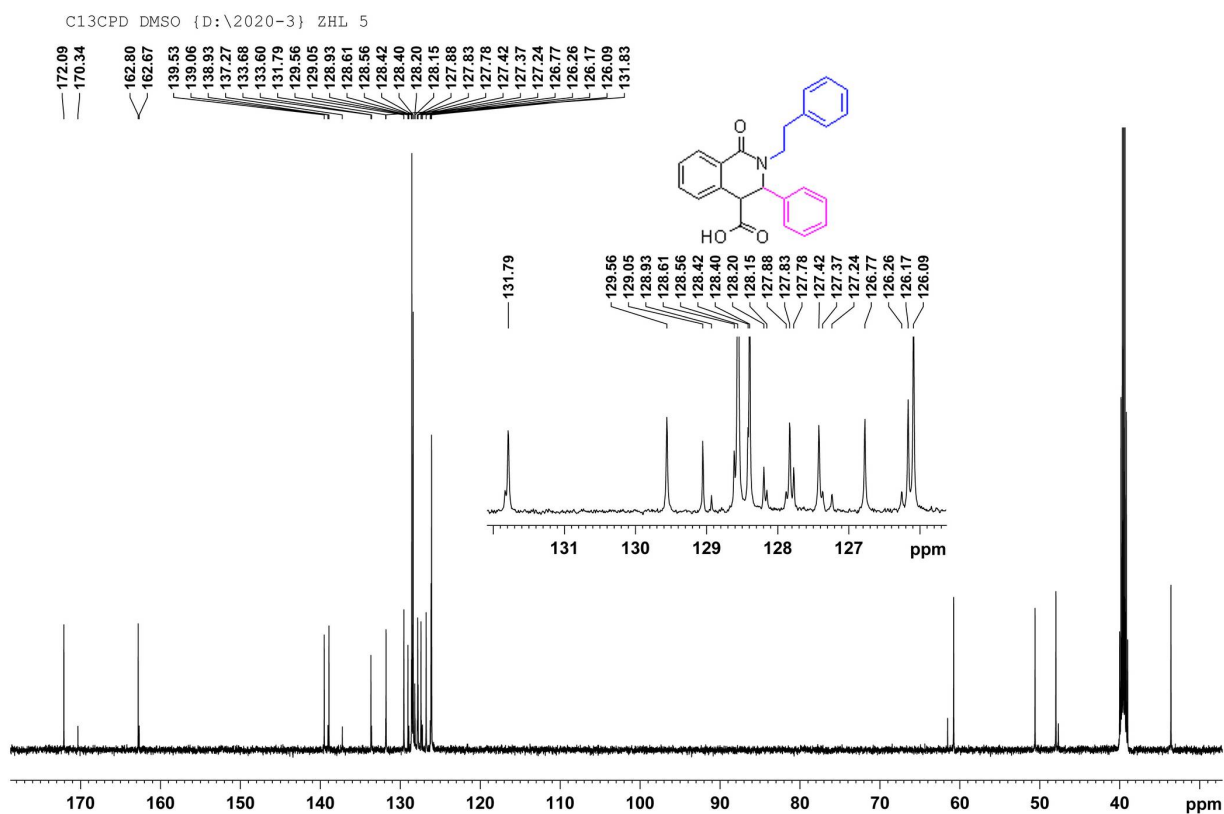


Figure S24. The ^{13}C NMR spectrum of compound **I9**

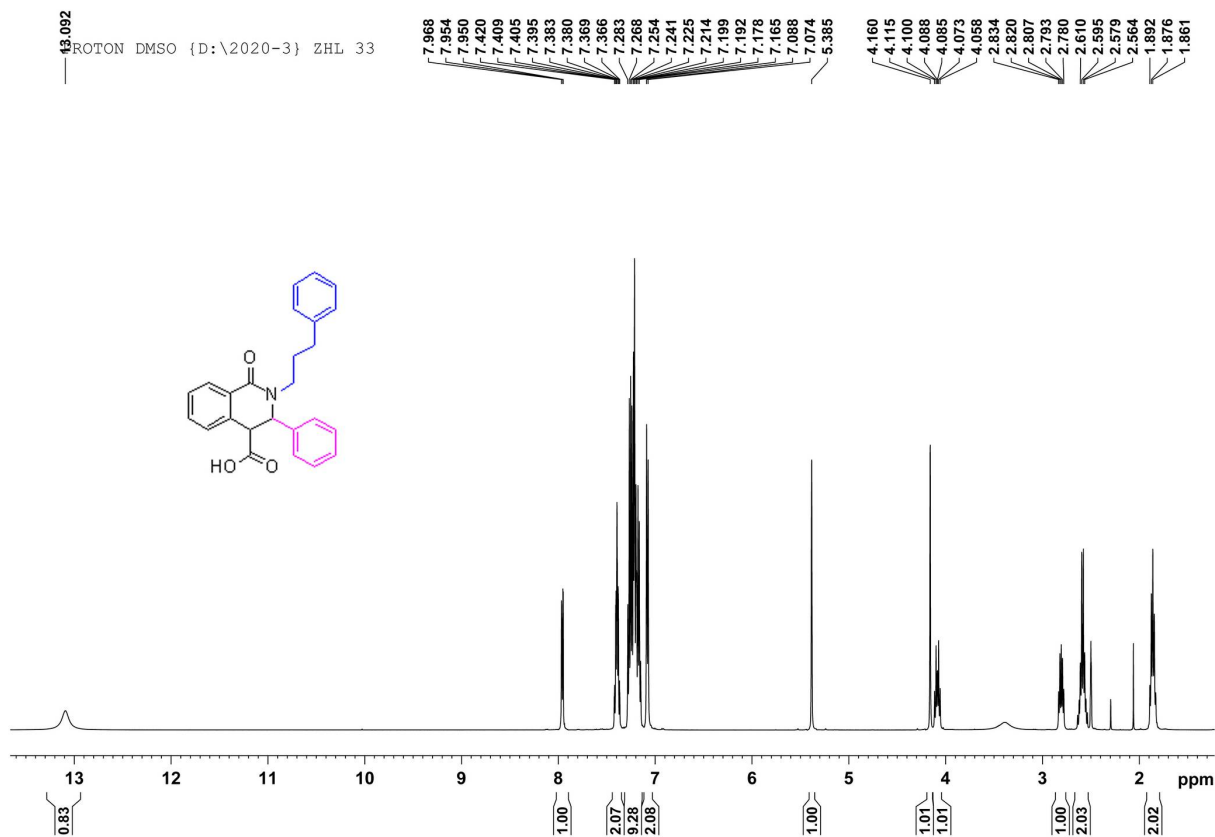


Figure S25. The ^1H NMR spectrum of compound I10

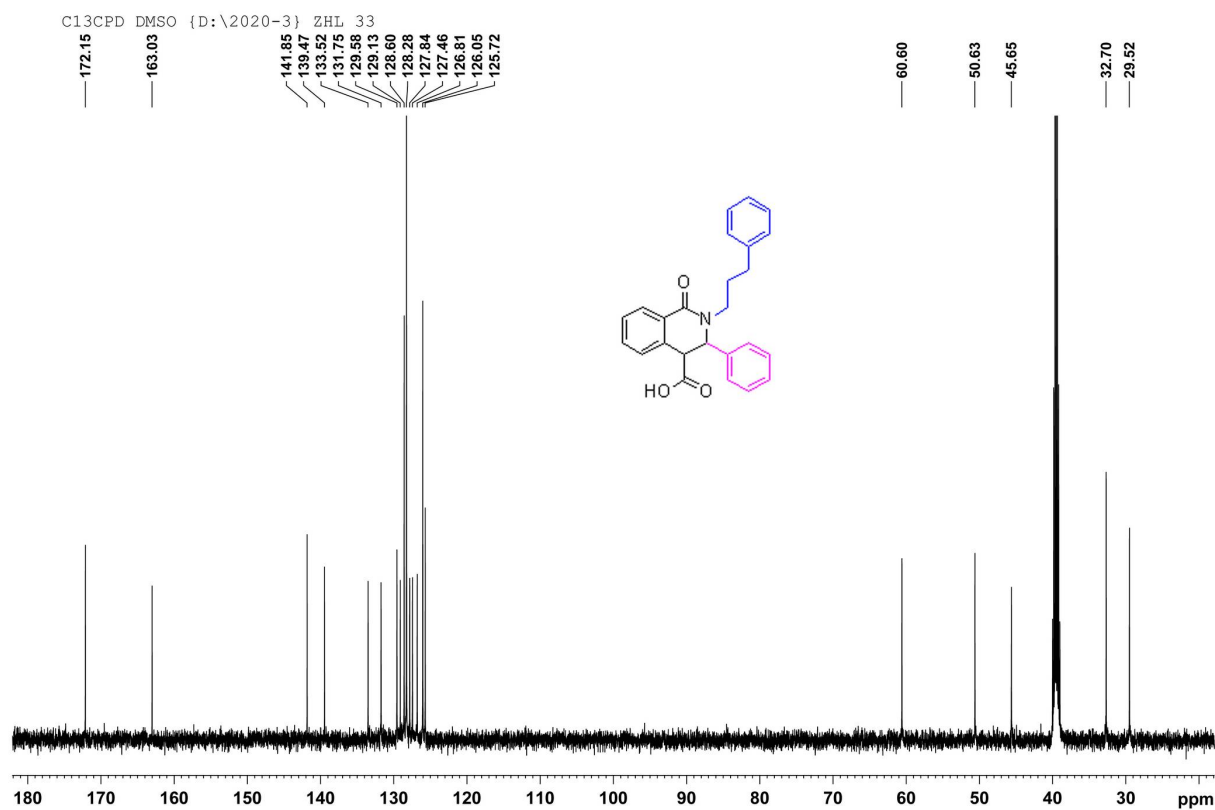


Figure S26. The ^{13}C NMR spectrum of compound I10

PROTON DMSO {D:\2020-3} ZHL 6

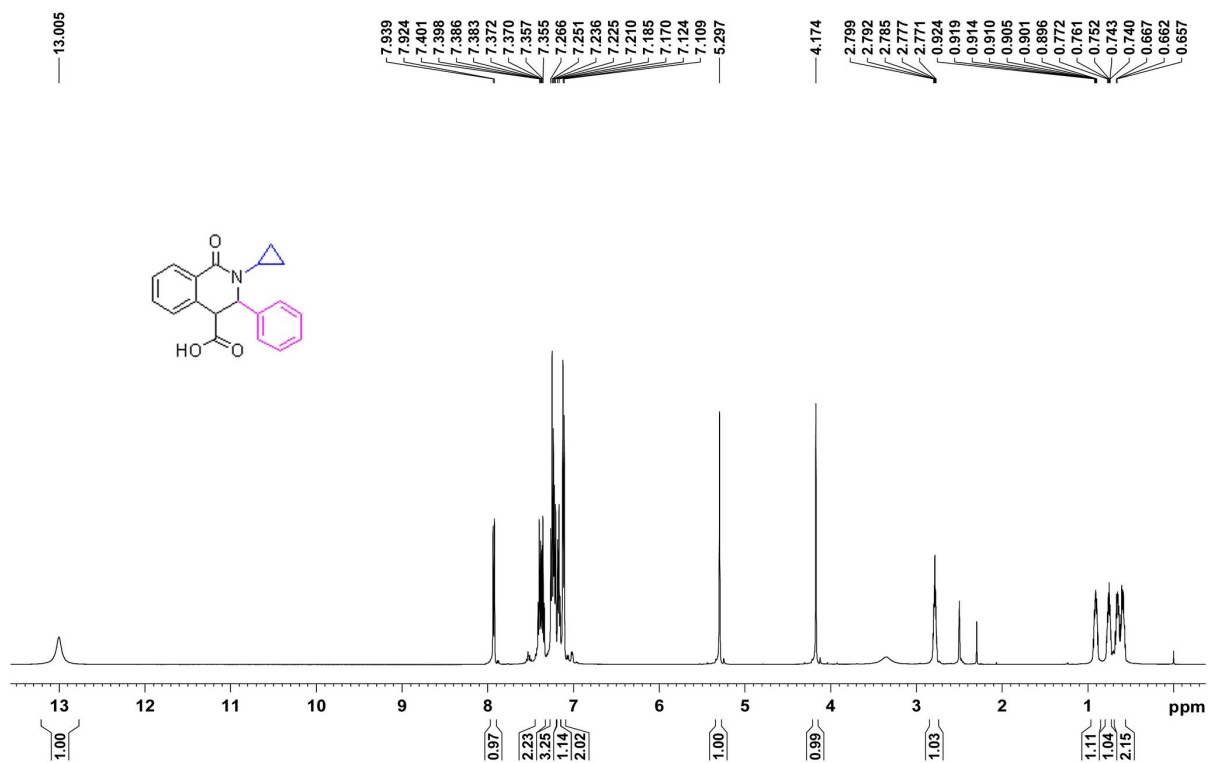


Figure S27. The ^1H NMR spectrum of compound I11

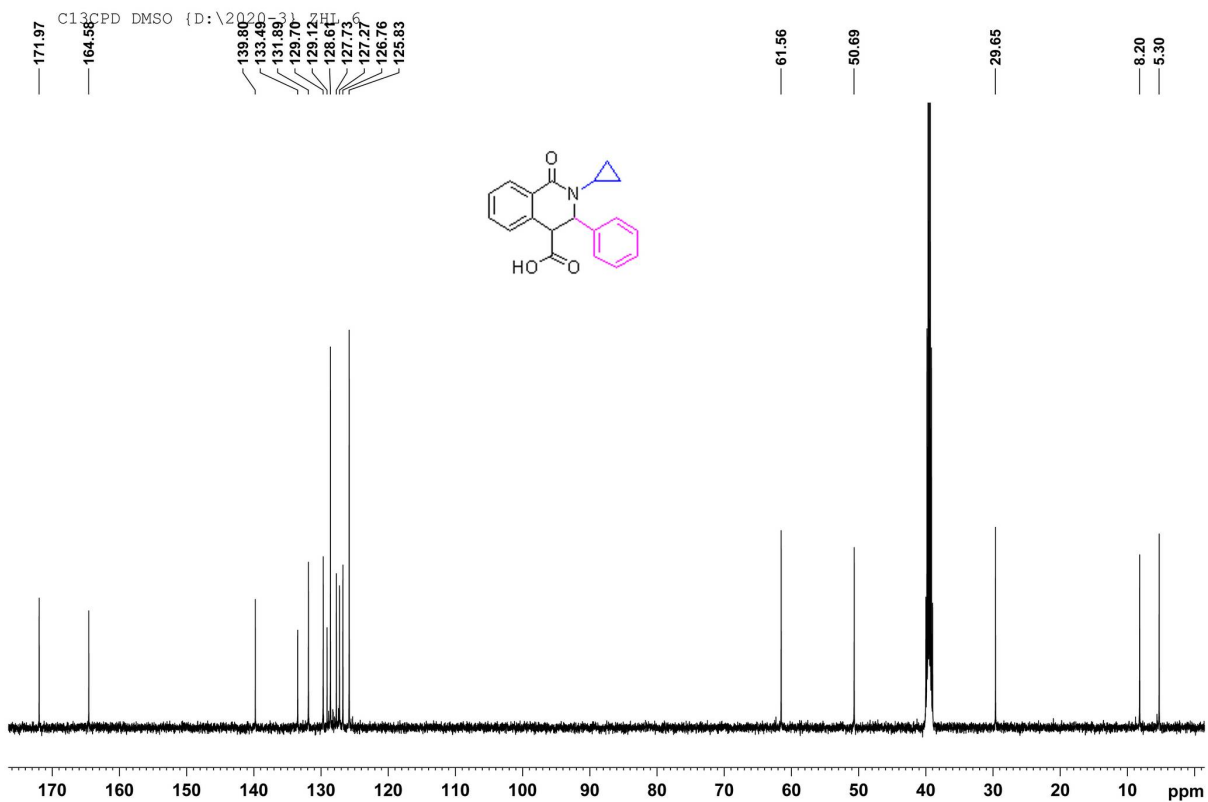


Figure S28. The ^{13}C NMR spectrum of compound I11

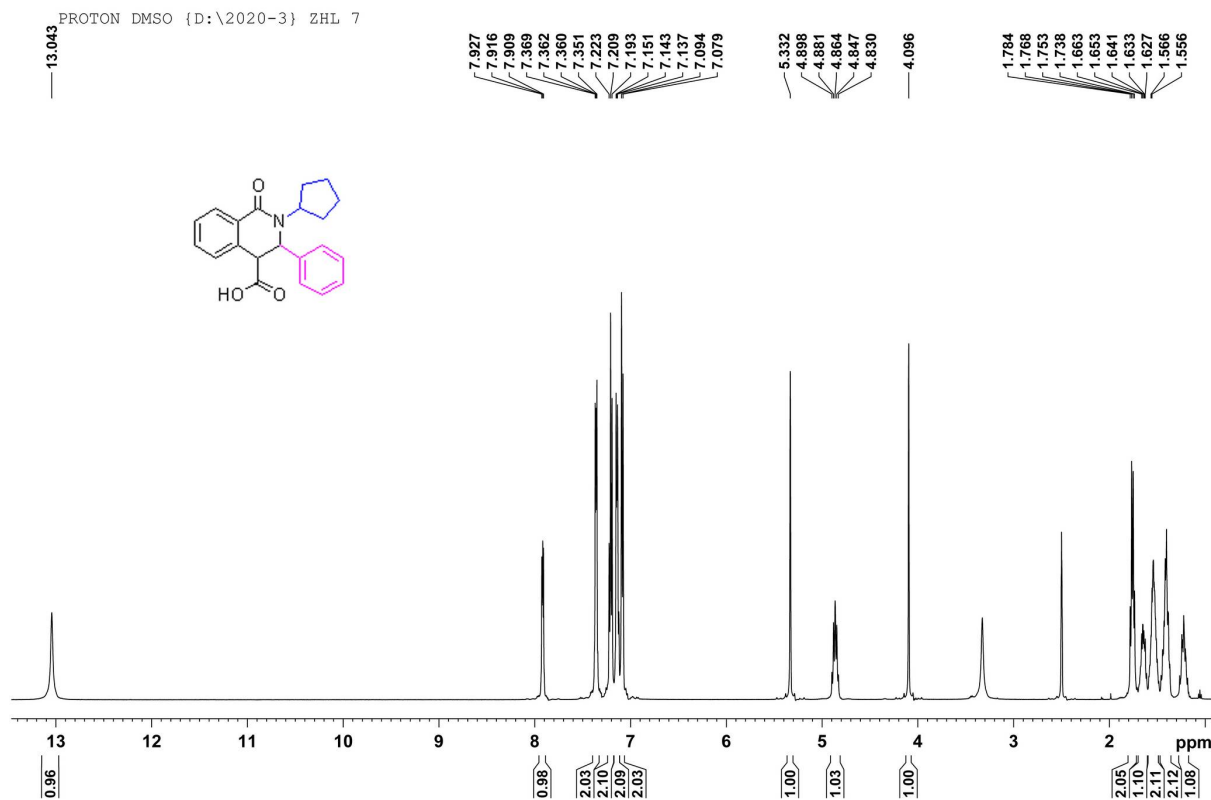


Figure S29. The ^1H NMR spectrum of compound I12

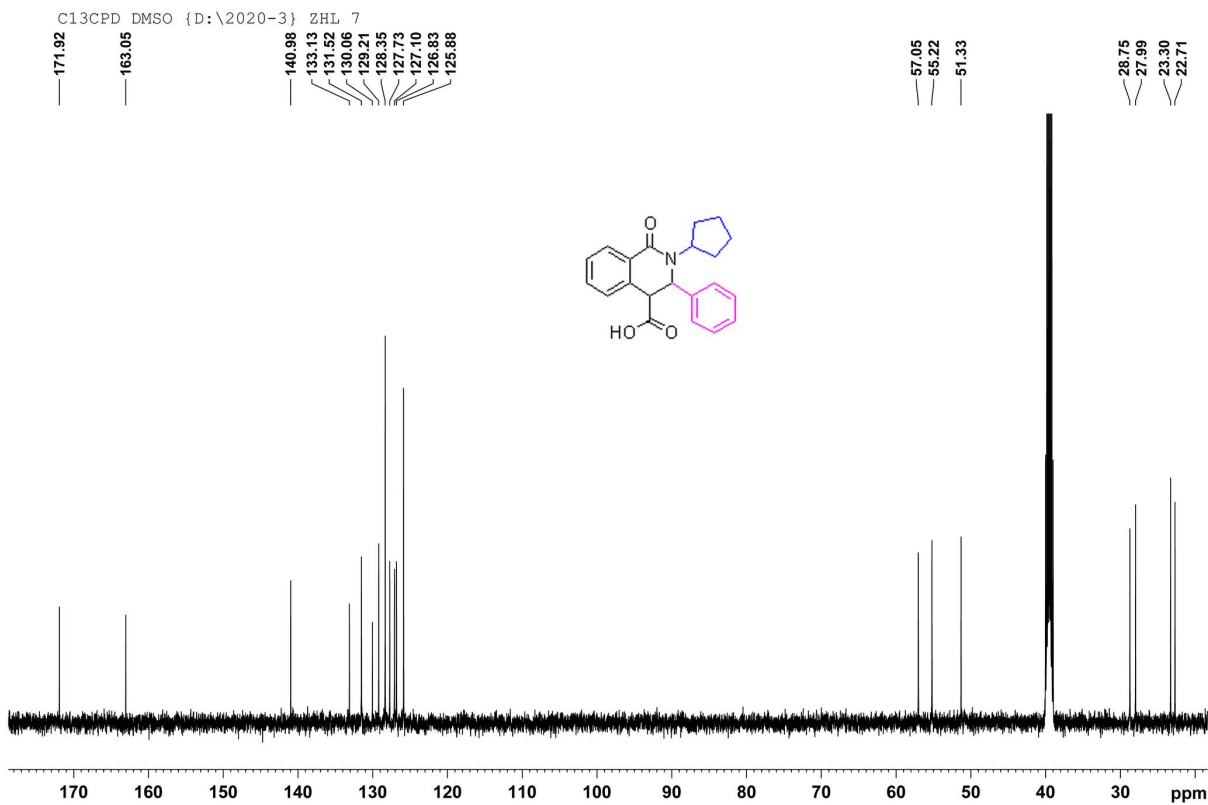


Figure S30. The ^{13}C NMR spectrum of compound I12

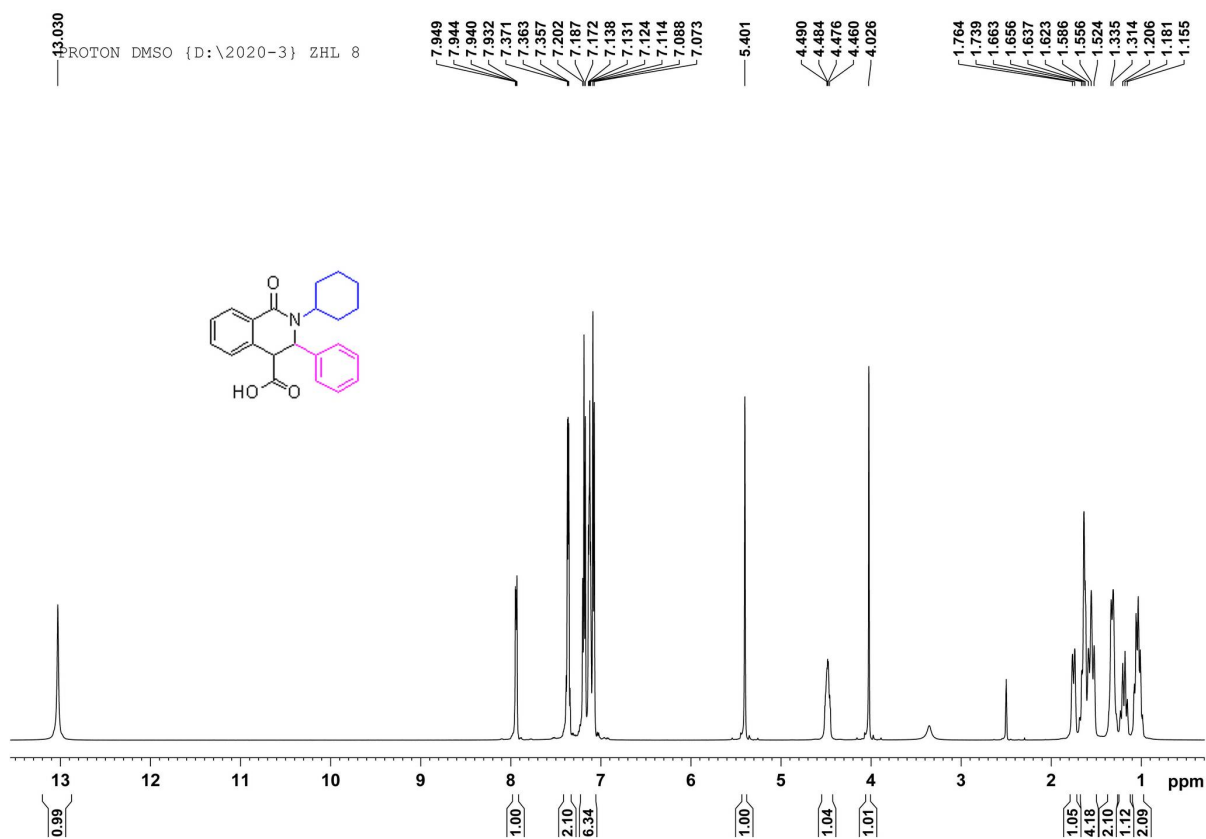


Figure S31. The ^1H NMR spectrum of compound I13

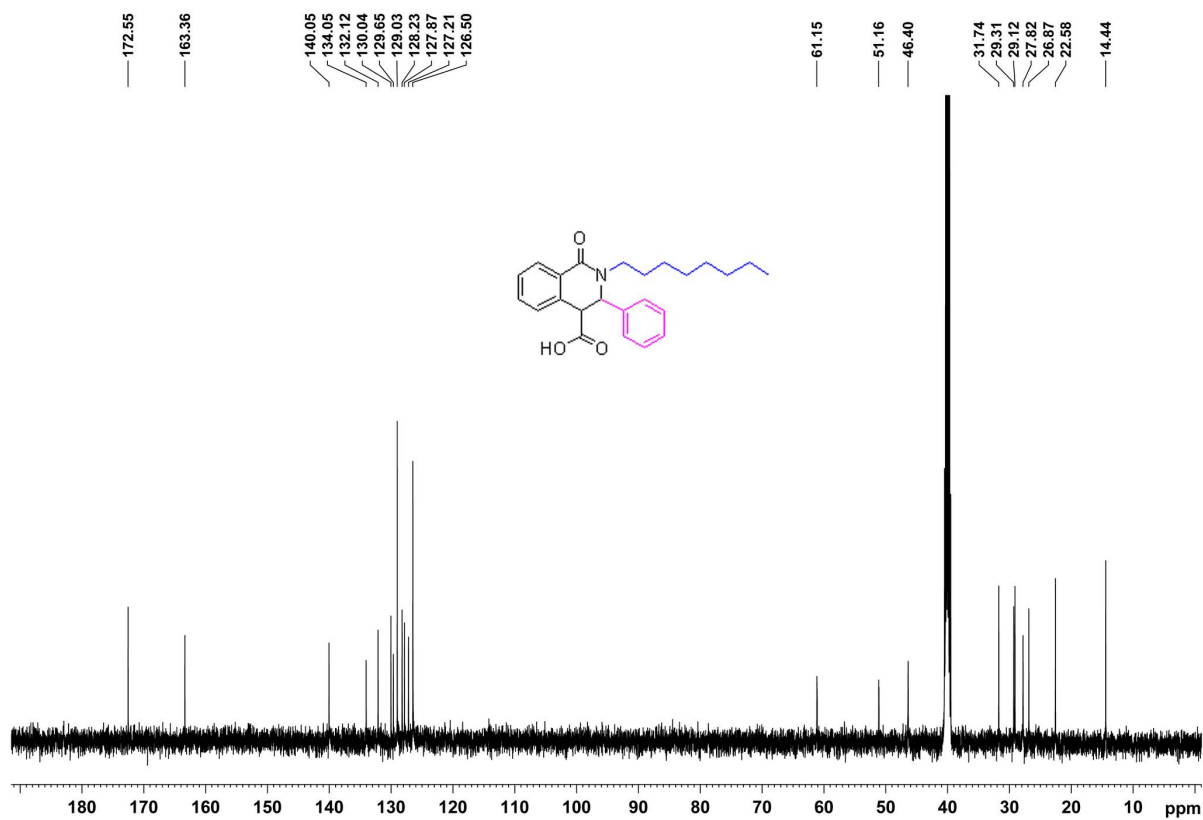


Figure S32. The ^{13}C NMR spectrum of compound I13

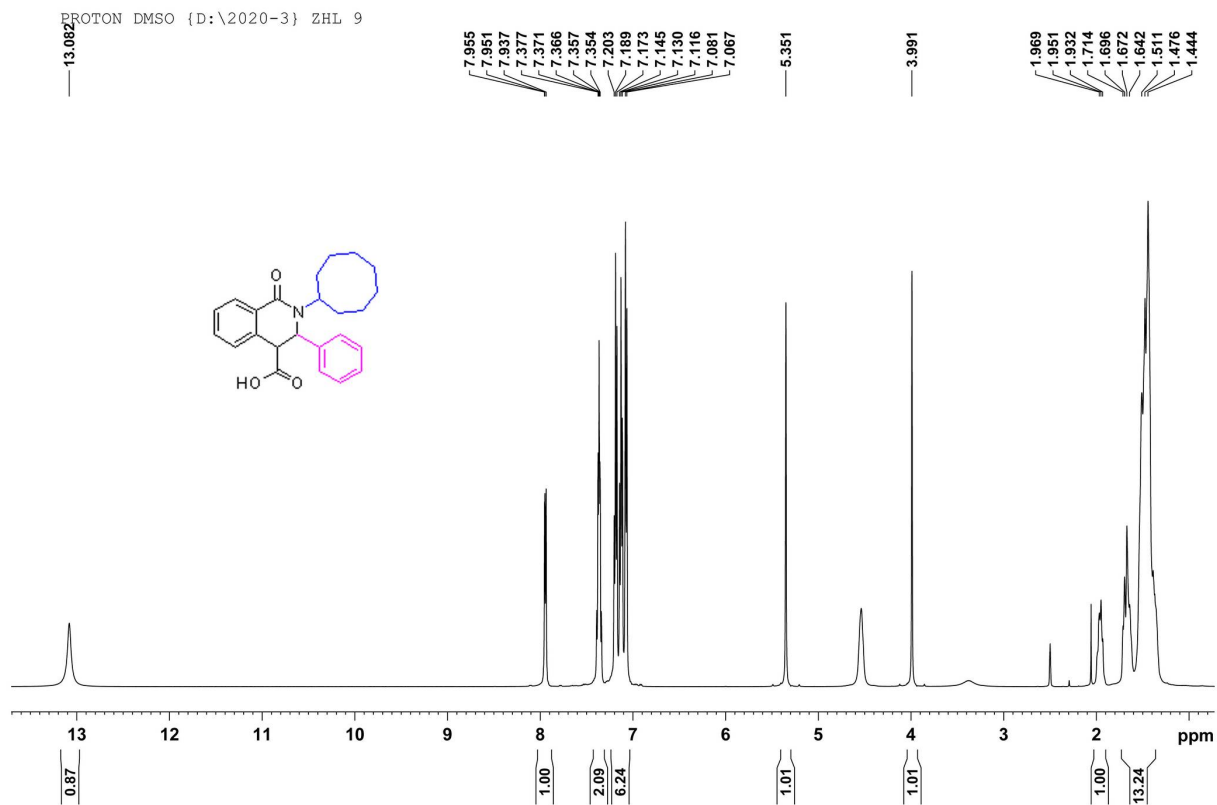


Figure S33. The ^1H NMR spectrum of compound I14

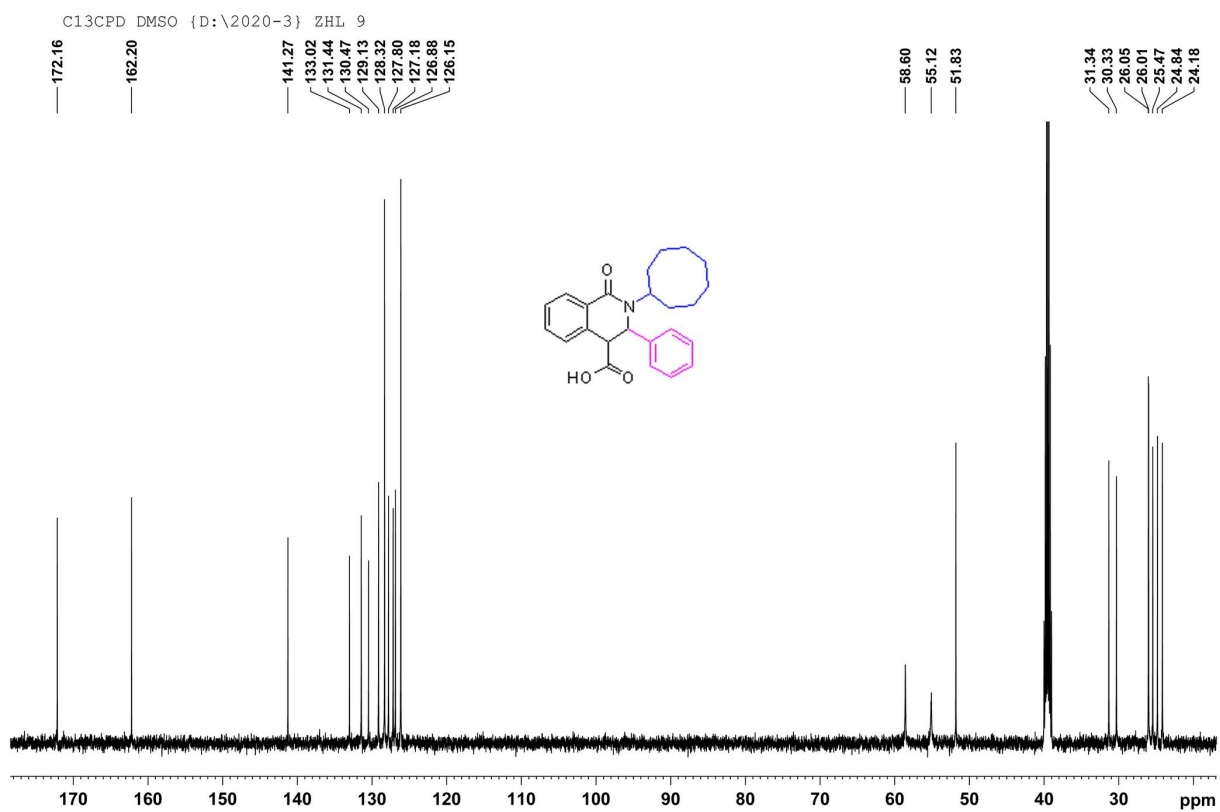


Figure S34. The ^{13}C NMR spectrum of compound I14

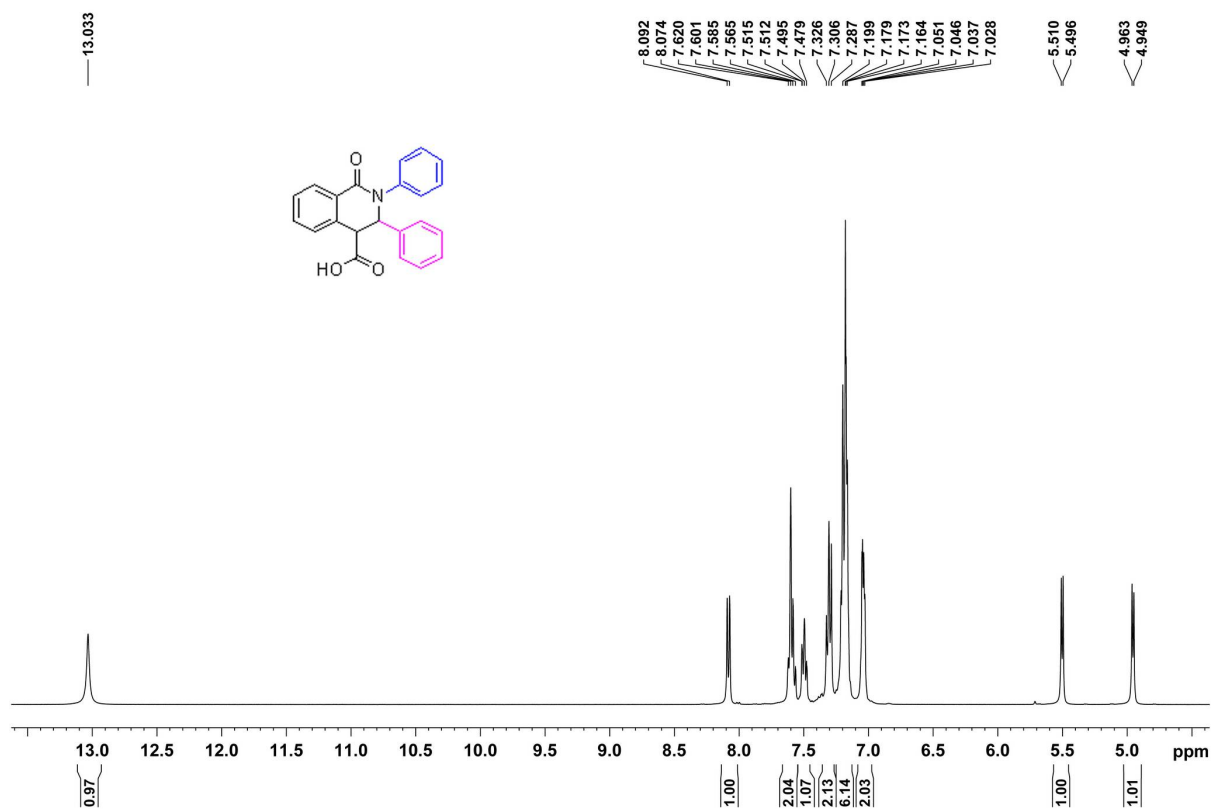


Figure S35. The ^1H NMR spectrum of compound I15

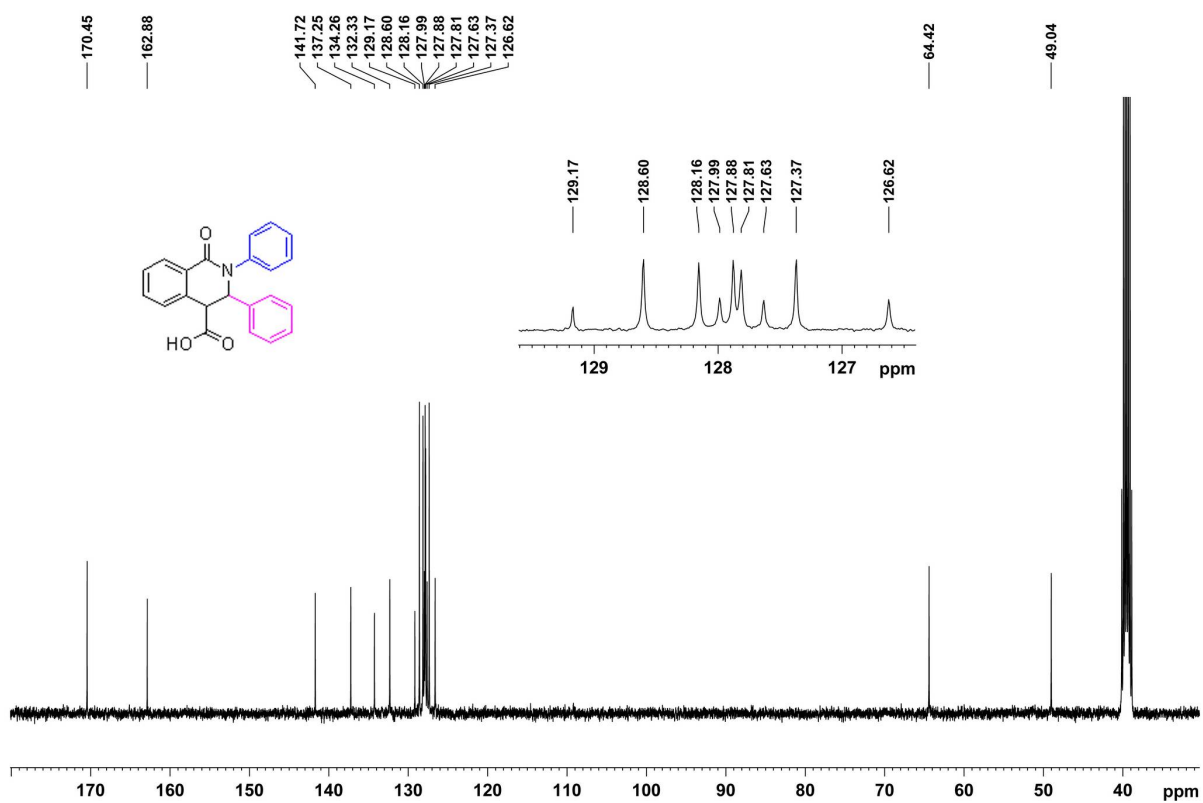


Figure S36. The ^{13}C NMR spectrum of compound I15

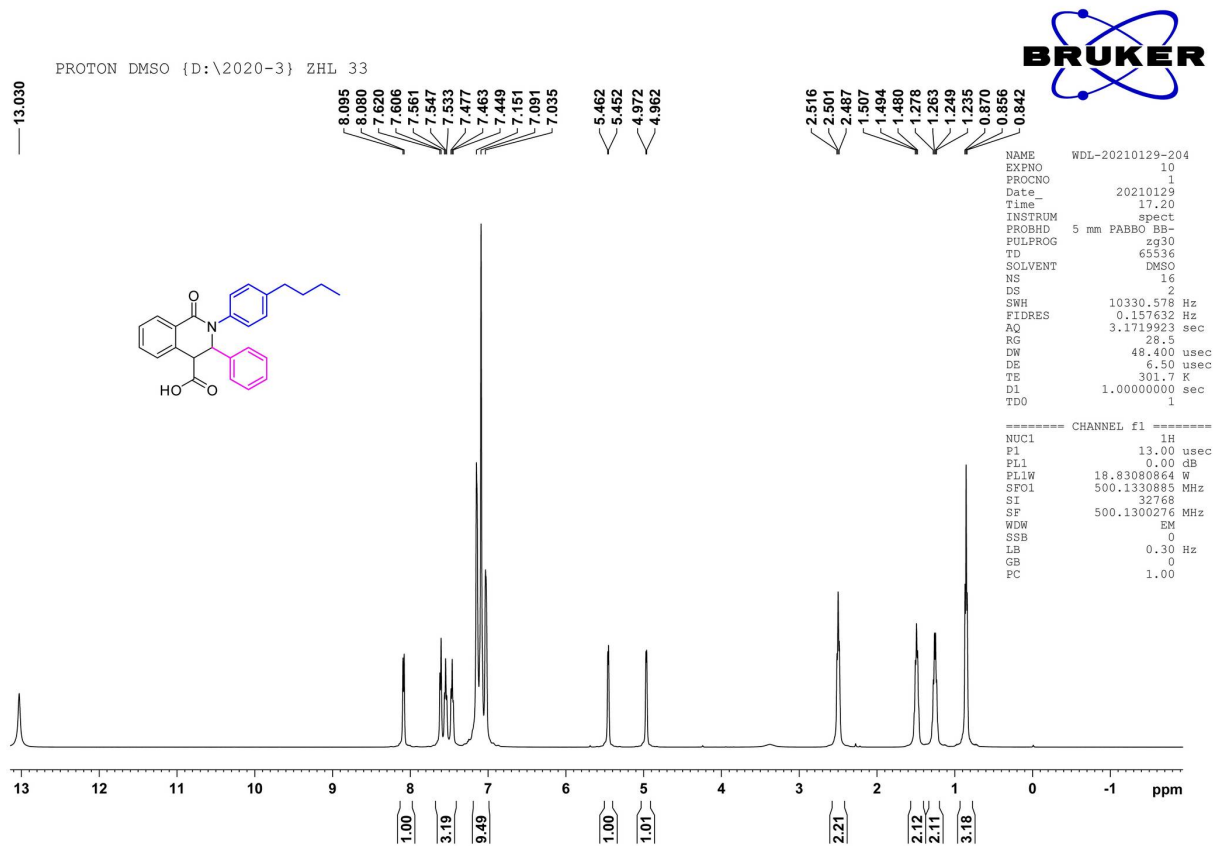


Figure S37. The ^1H NMR spectrum of compound I16

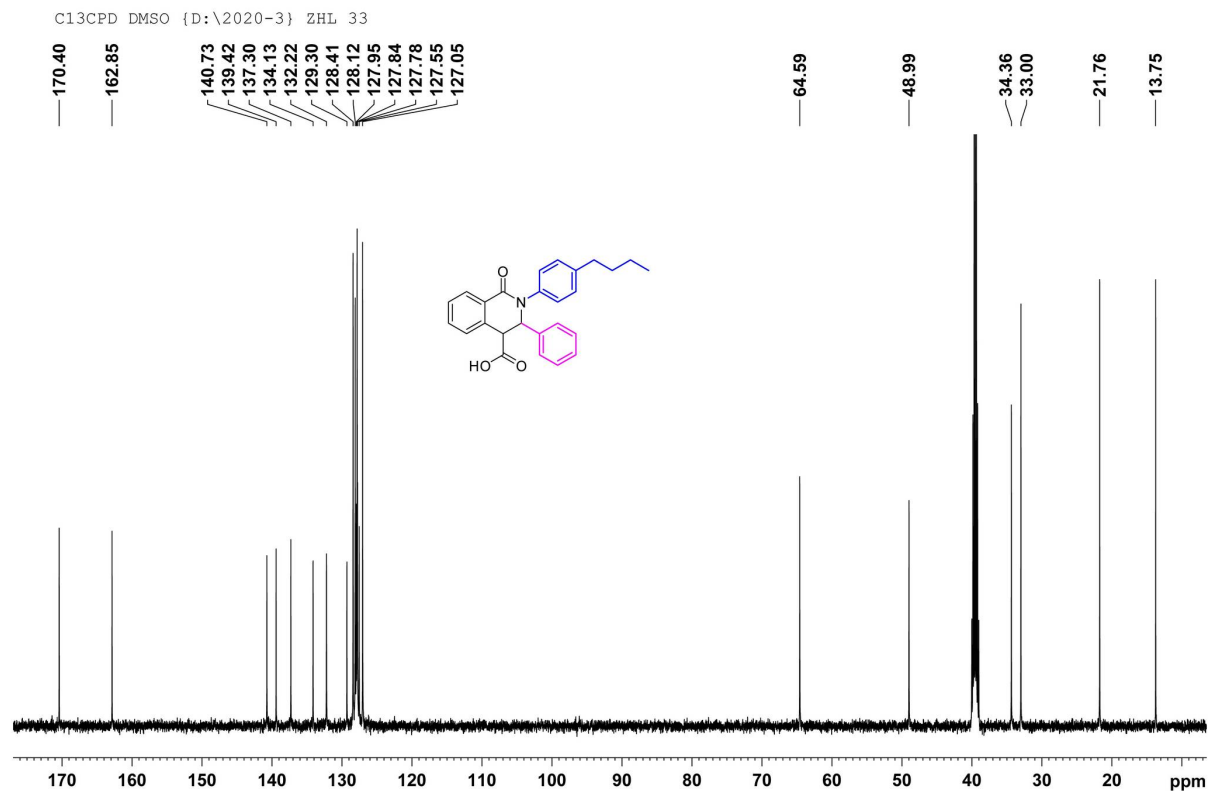


Figure S38. The ^{13}C NMR spectrum of compound I16

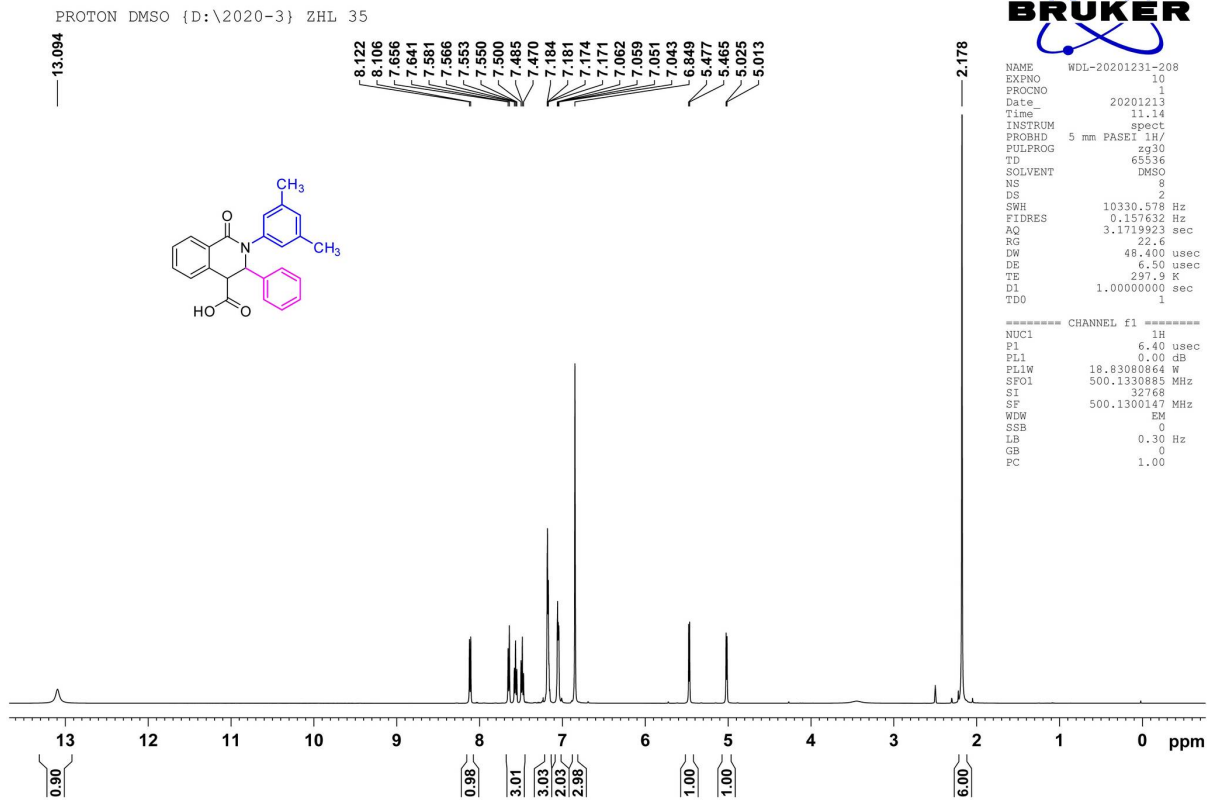


Figure S39. The ^1H NMR spectrum of compound I17

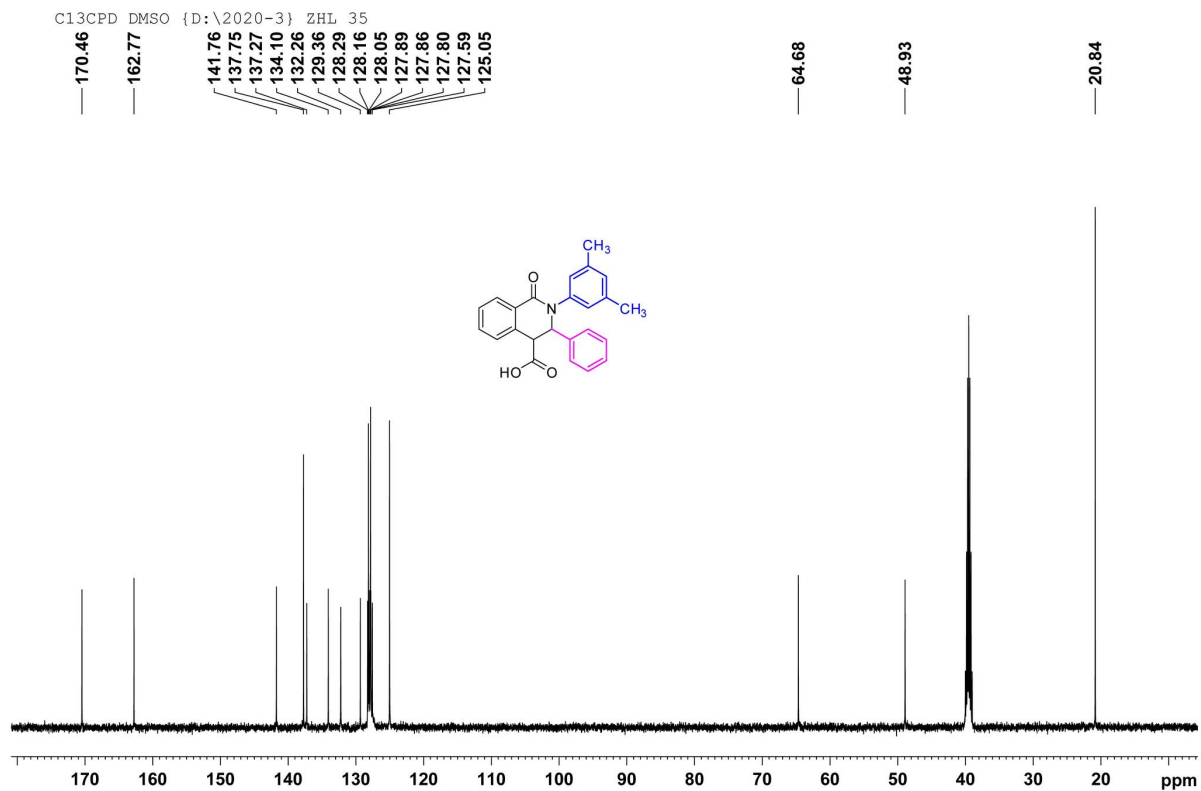


Figure S40. The ^{13}C NMR spectrum of compound I17

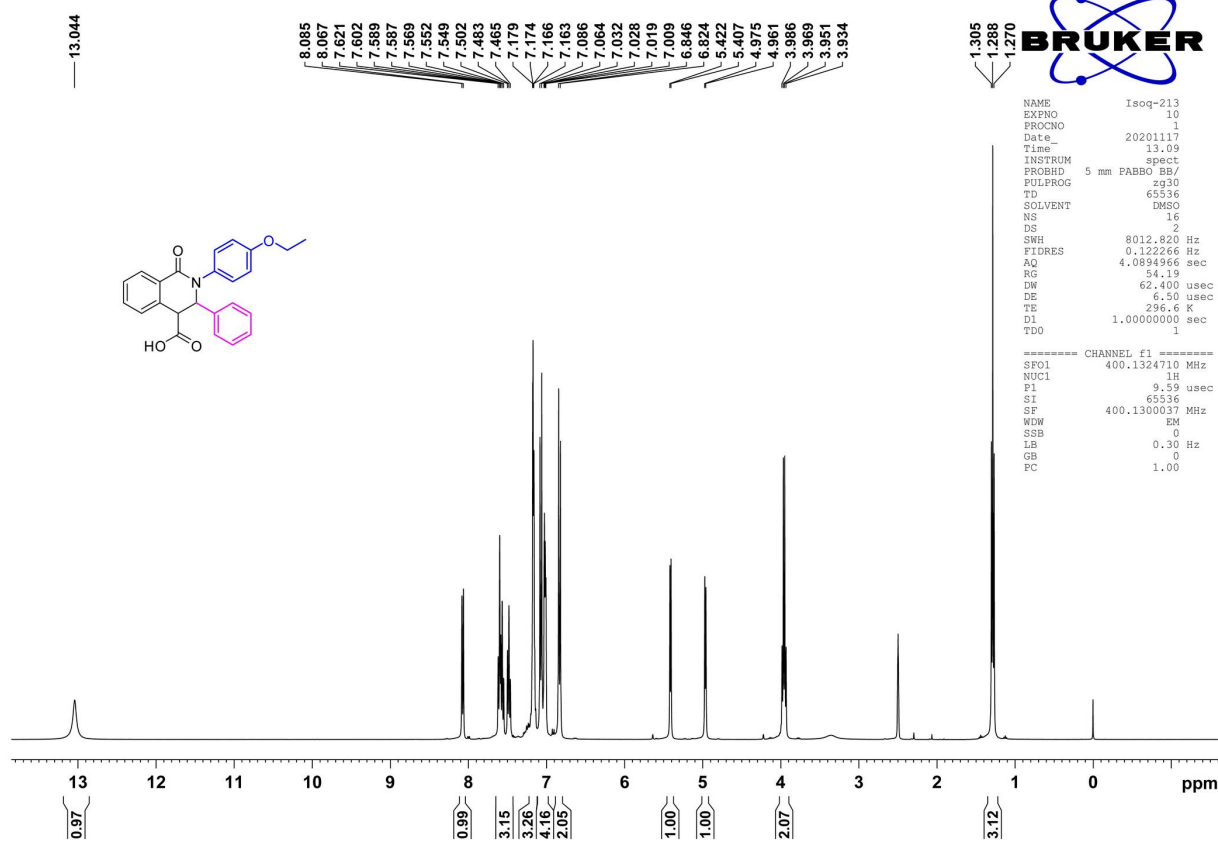


Figure S41. The ^1H NMR spectrum of compound I18

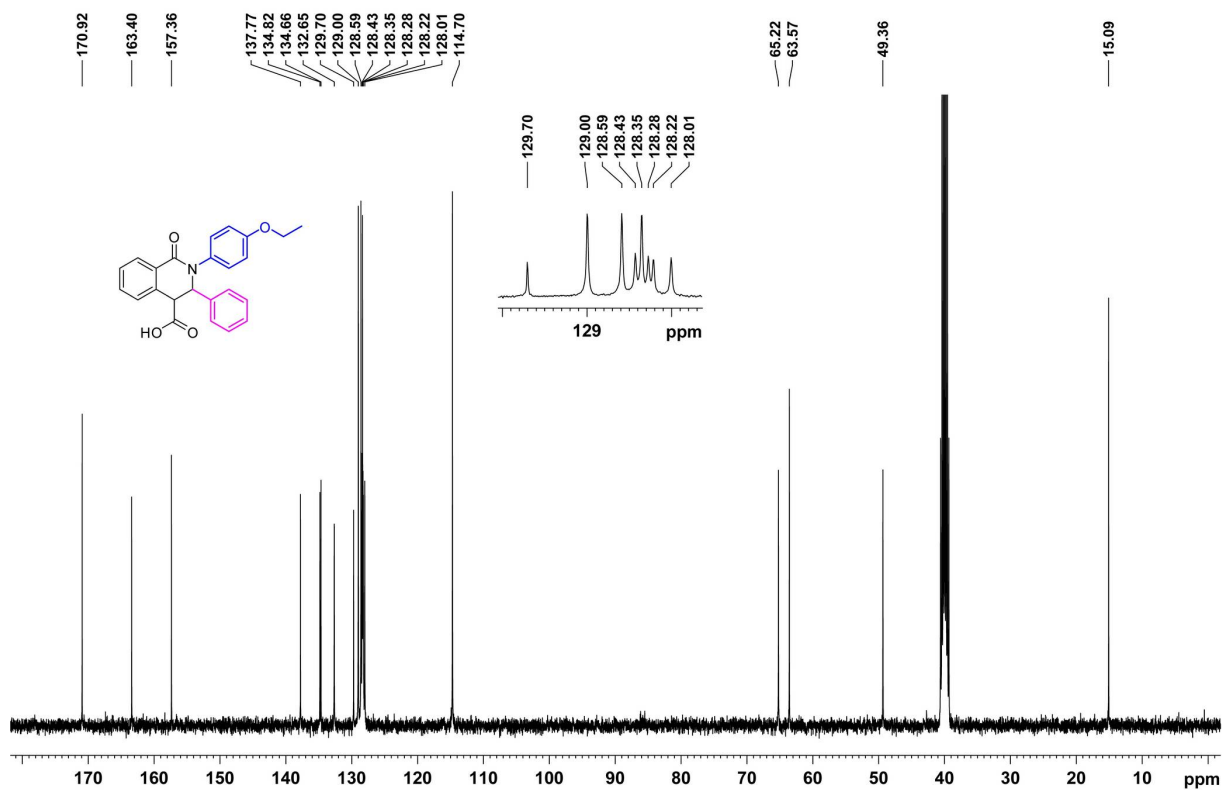


Figure S42. The ^{13}C NMR spectrum of compound I18

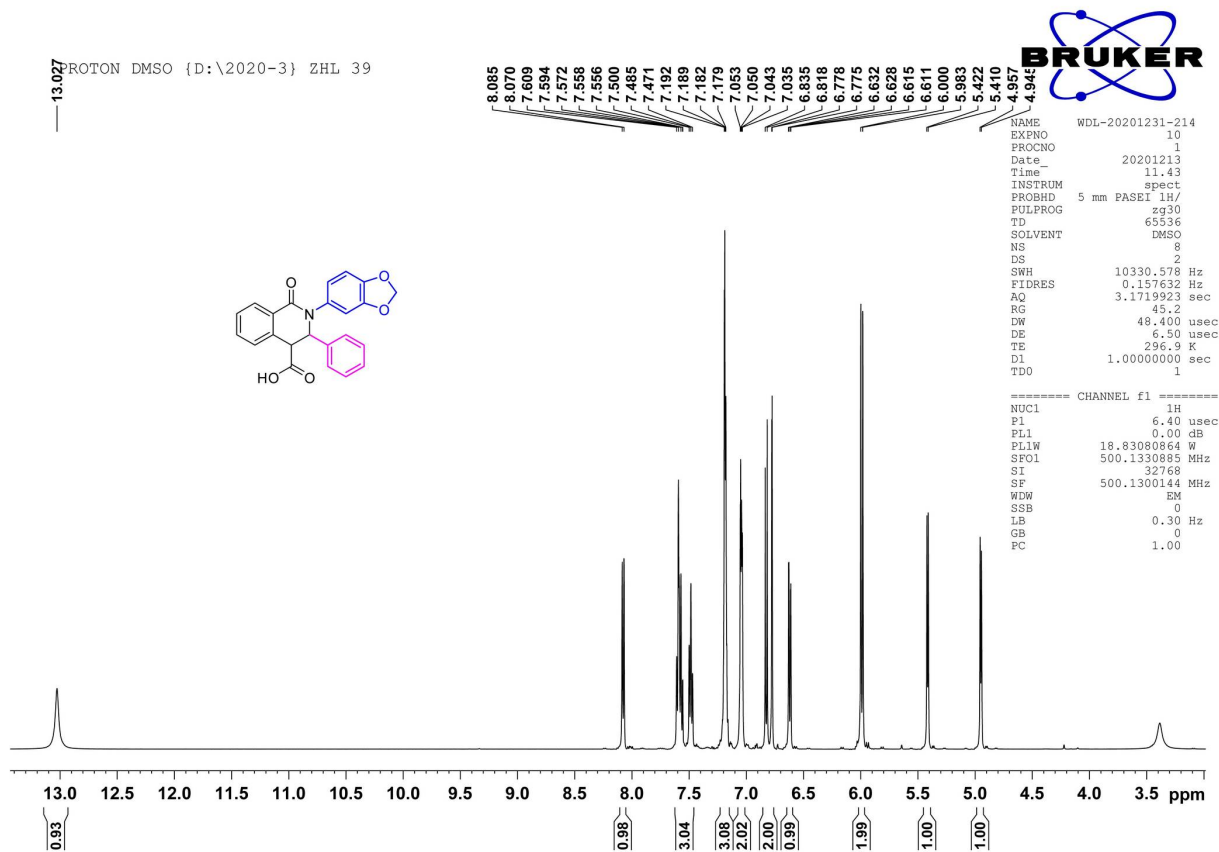


Figure S43. The ^1H NMR spectrum of compound I19

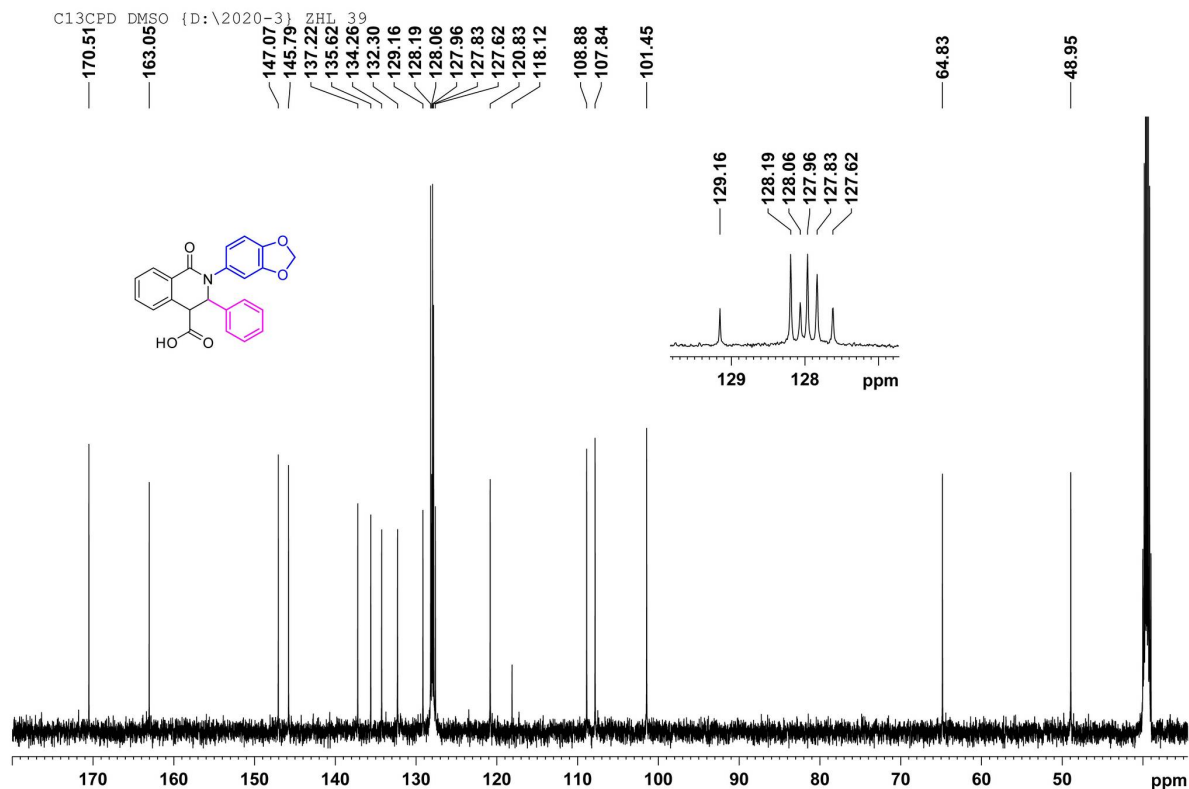


Figure S44. The ^{13}C NMR spectrum of compound I19

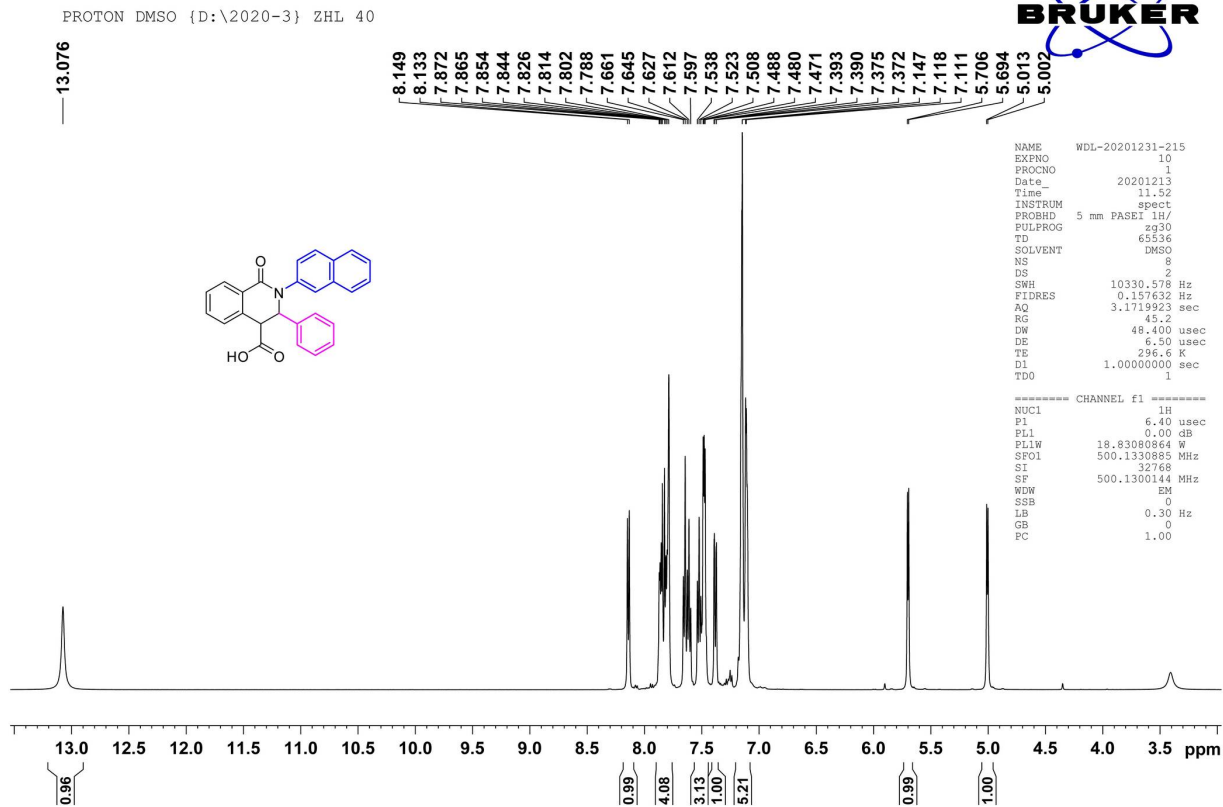


Figure S45. The ^1H NMR spectrum of compound I20

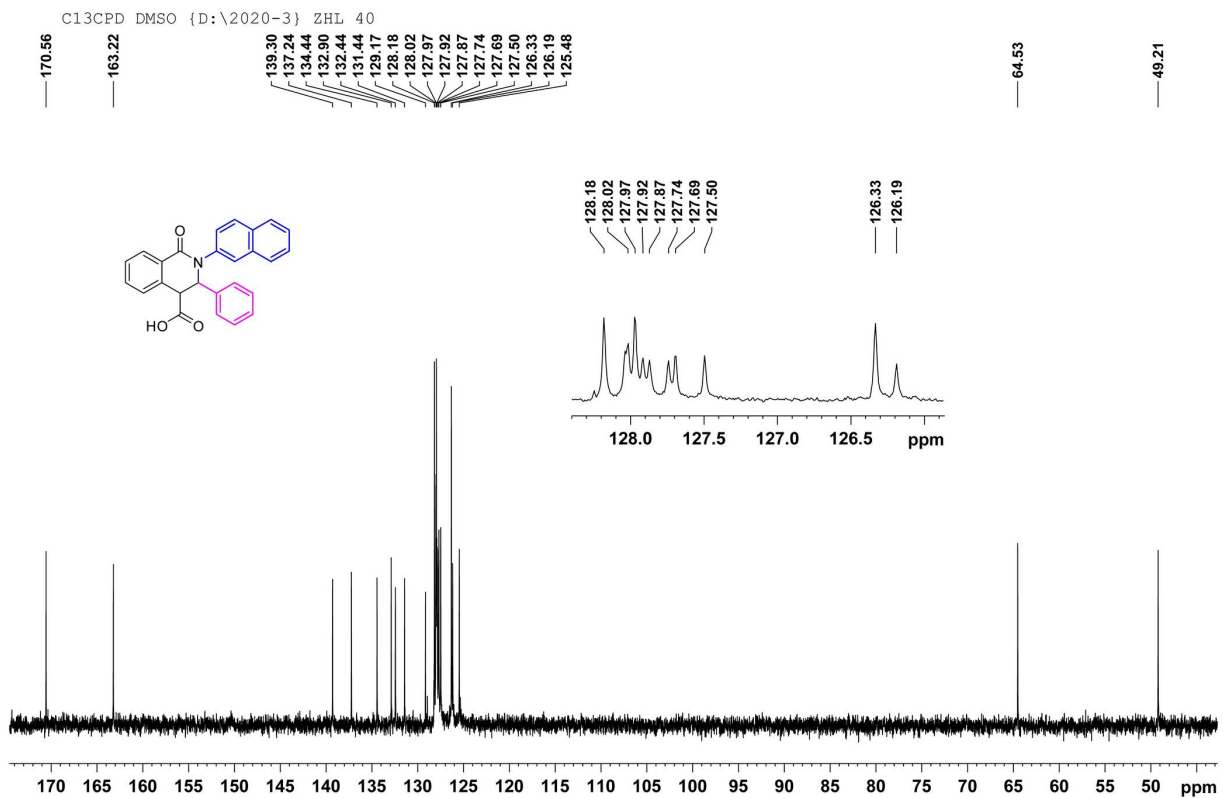


Figure S46. The ^{13}C NMR spectrum of compound I20

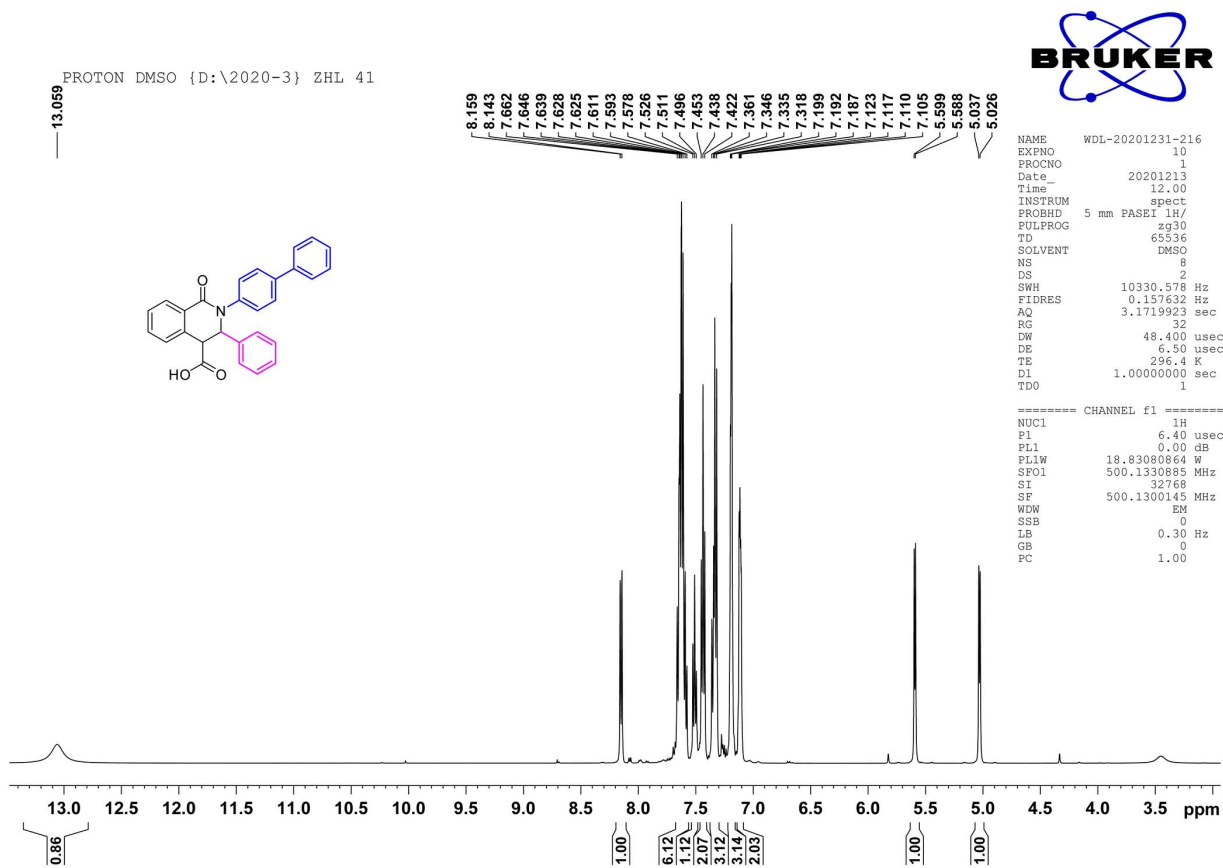


Figure S47. The ^1H NMR spectrum of compound I21

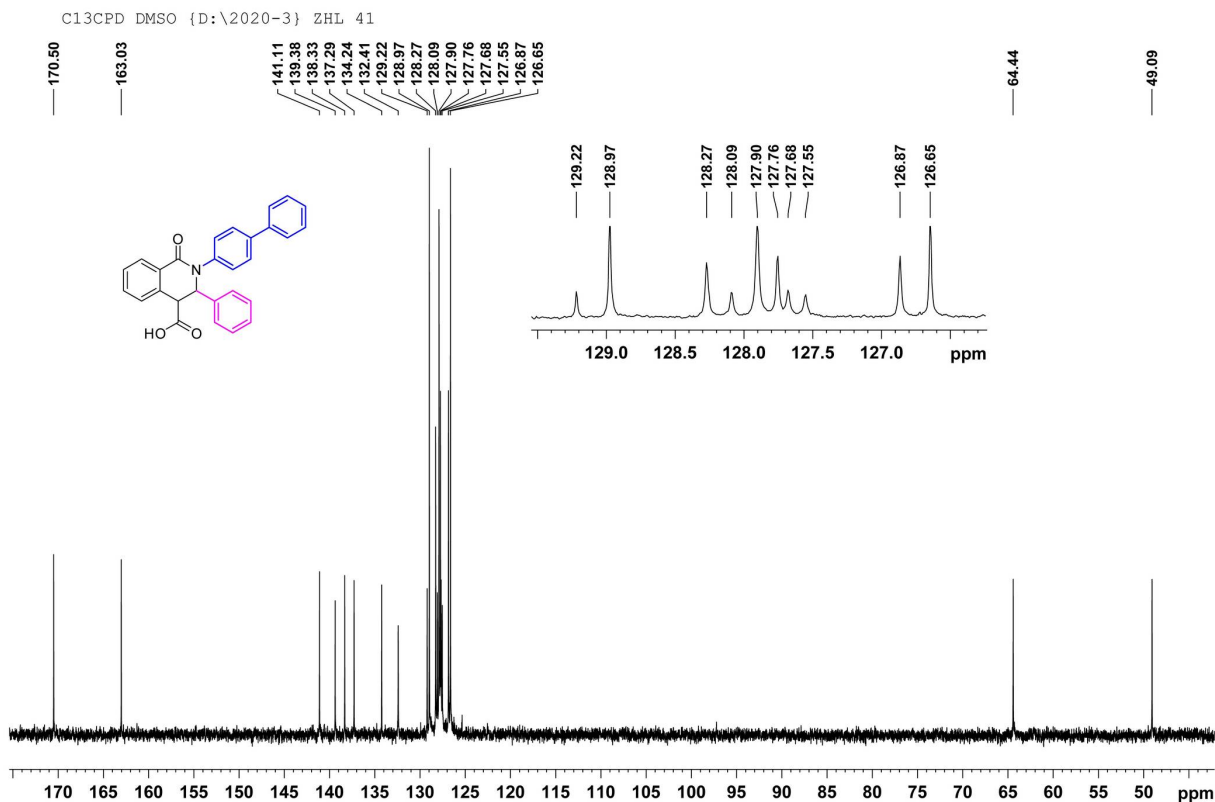


Figure S48. The ^{13}C NMR spectrum of compound I21

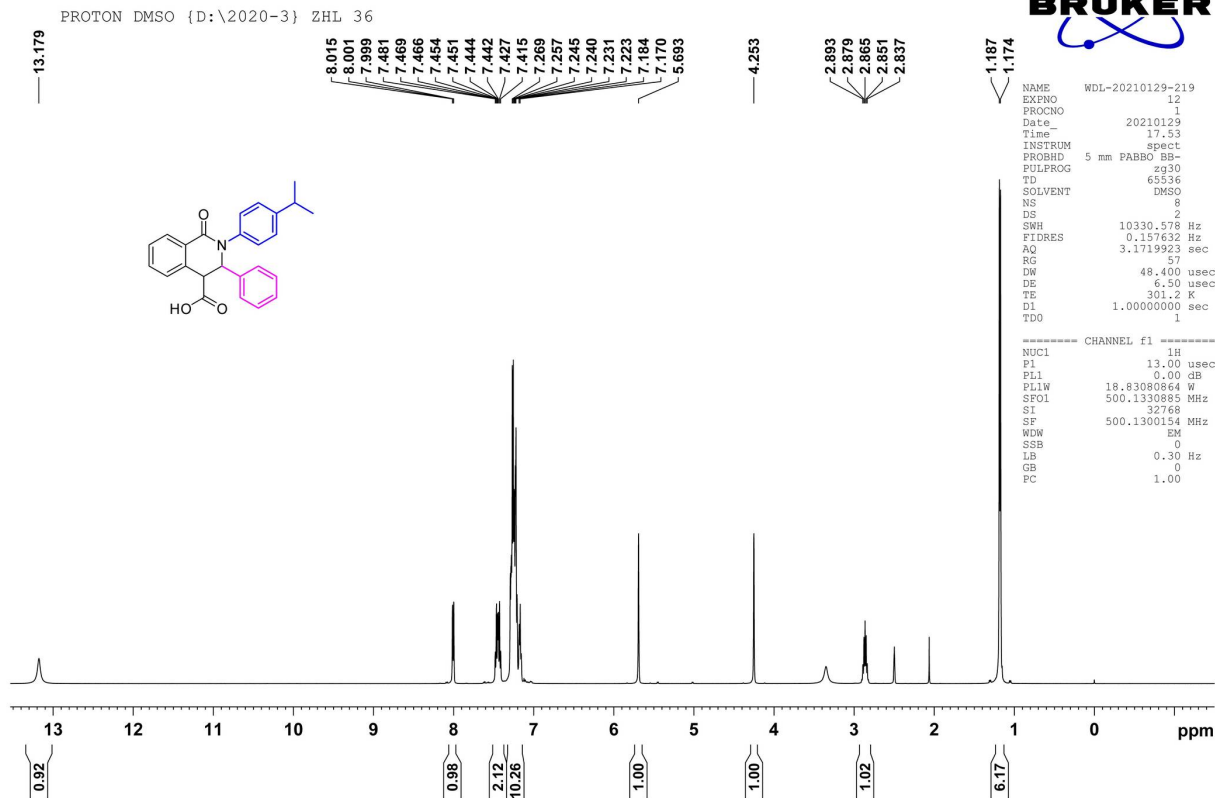


Figure S49. The ^1H NMR spectrum of compound I22

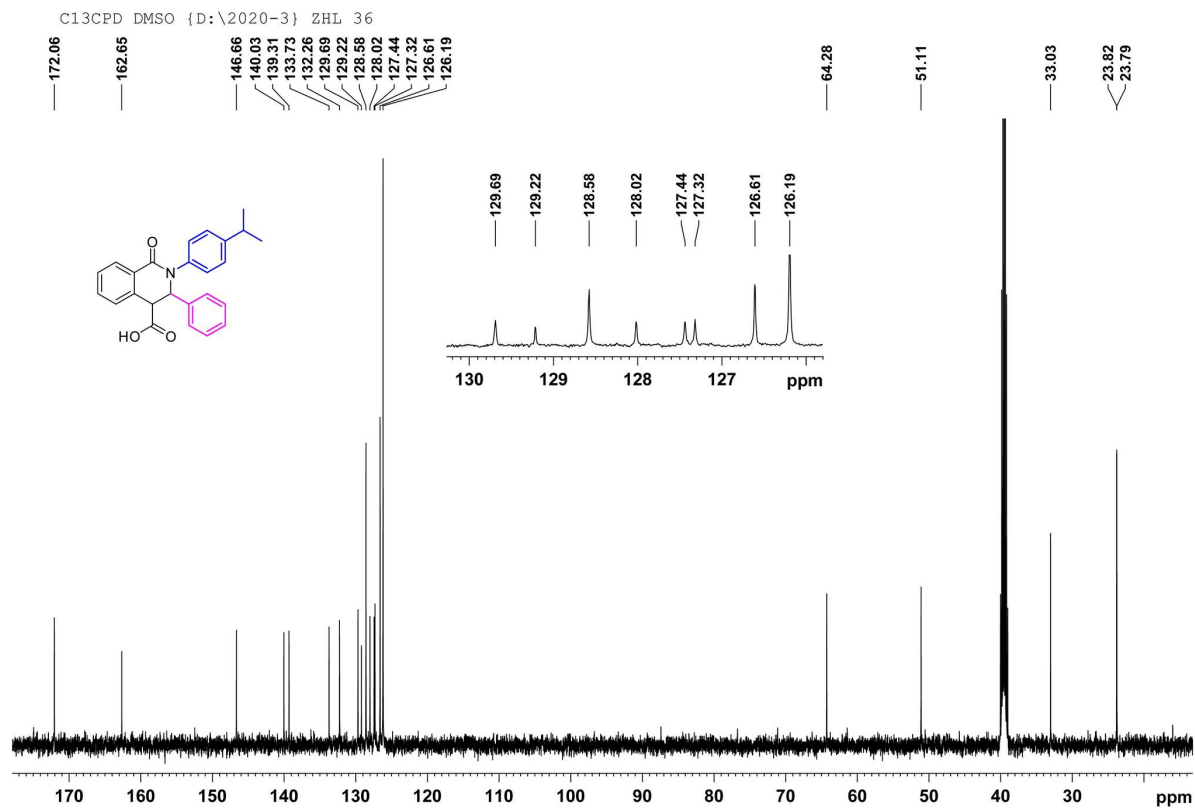


Figure S50. The ^{13}C NMR spectrum of compound I22

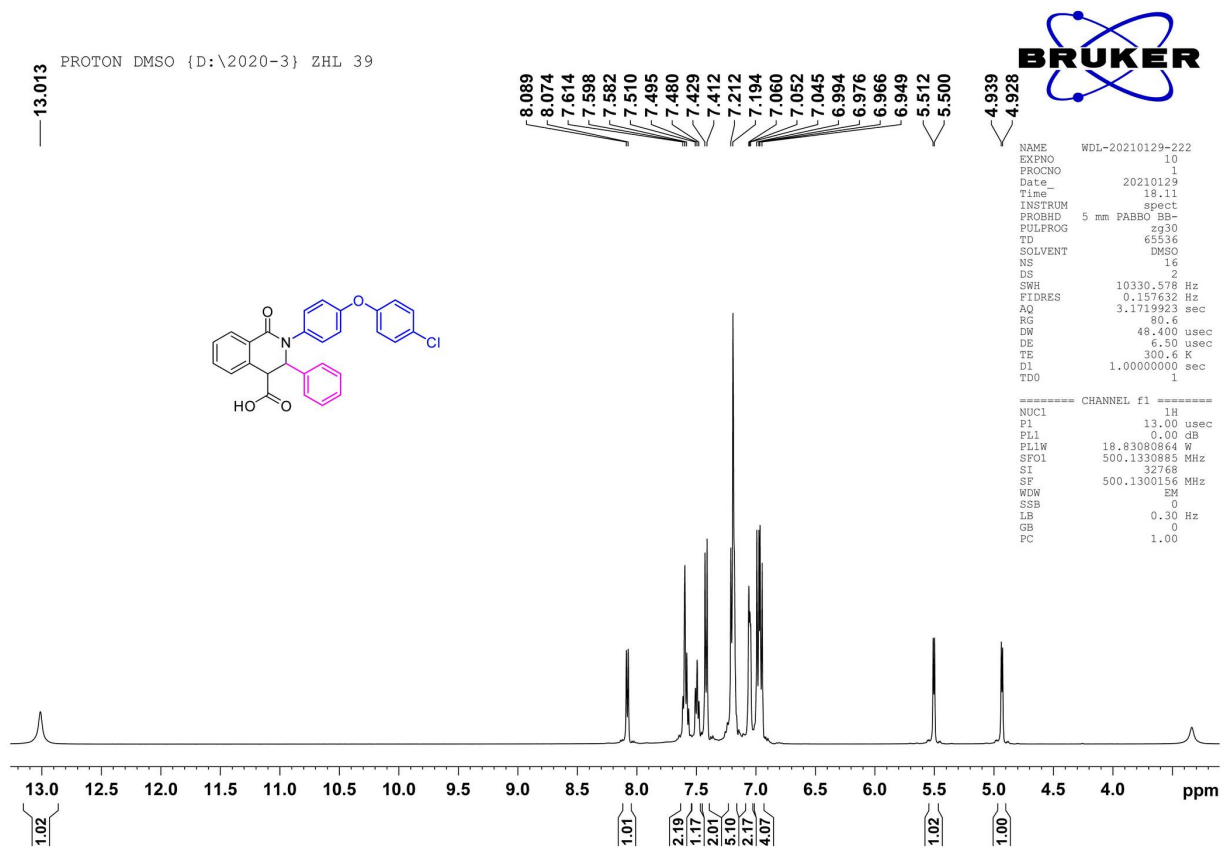


Figure S51. The ^1H NMR spectrum of compound I23

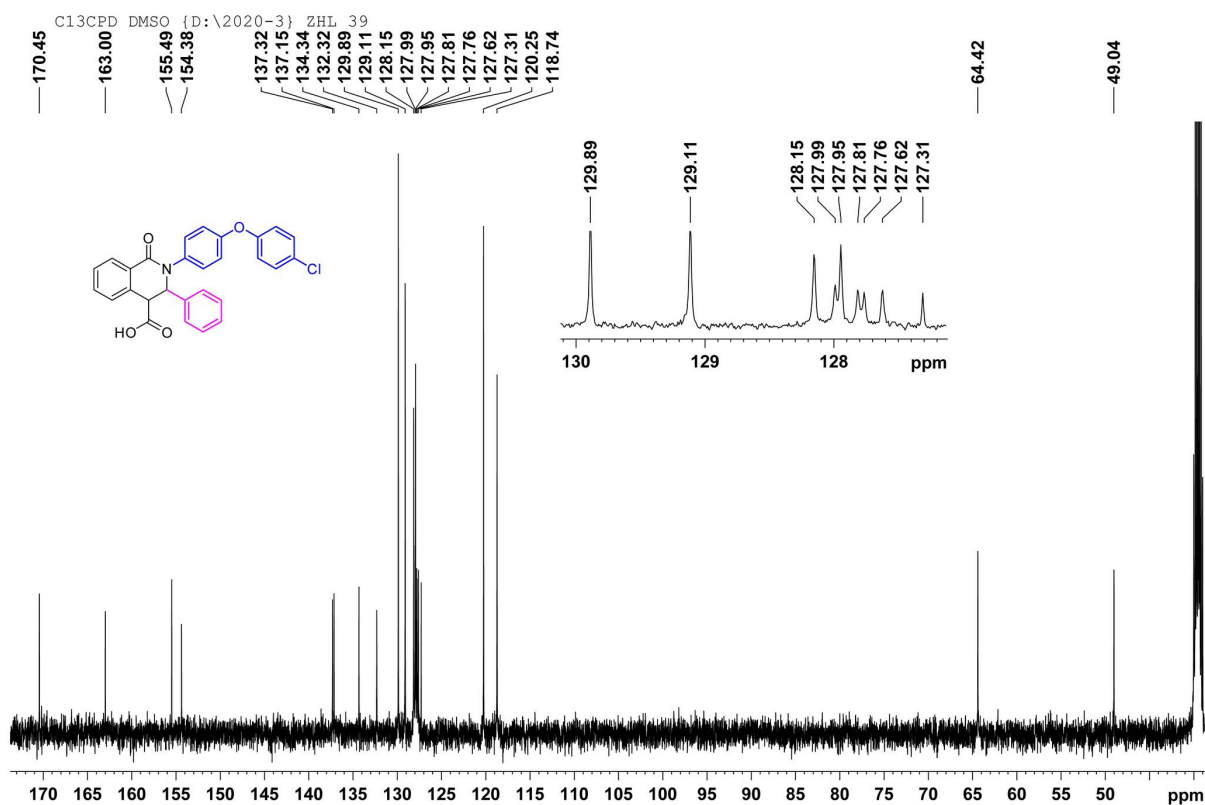


Figure S52. The ^{13}C NMR spectrum of compound I23

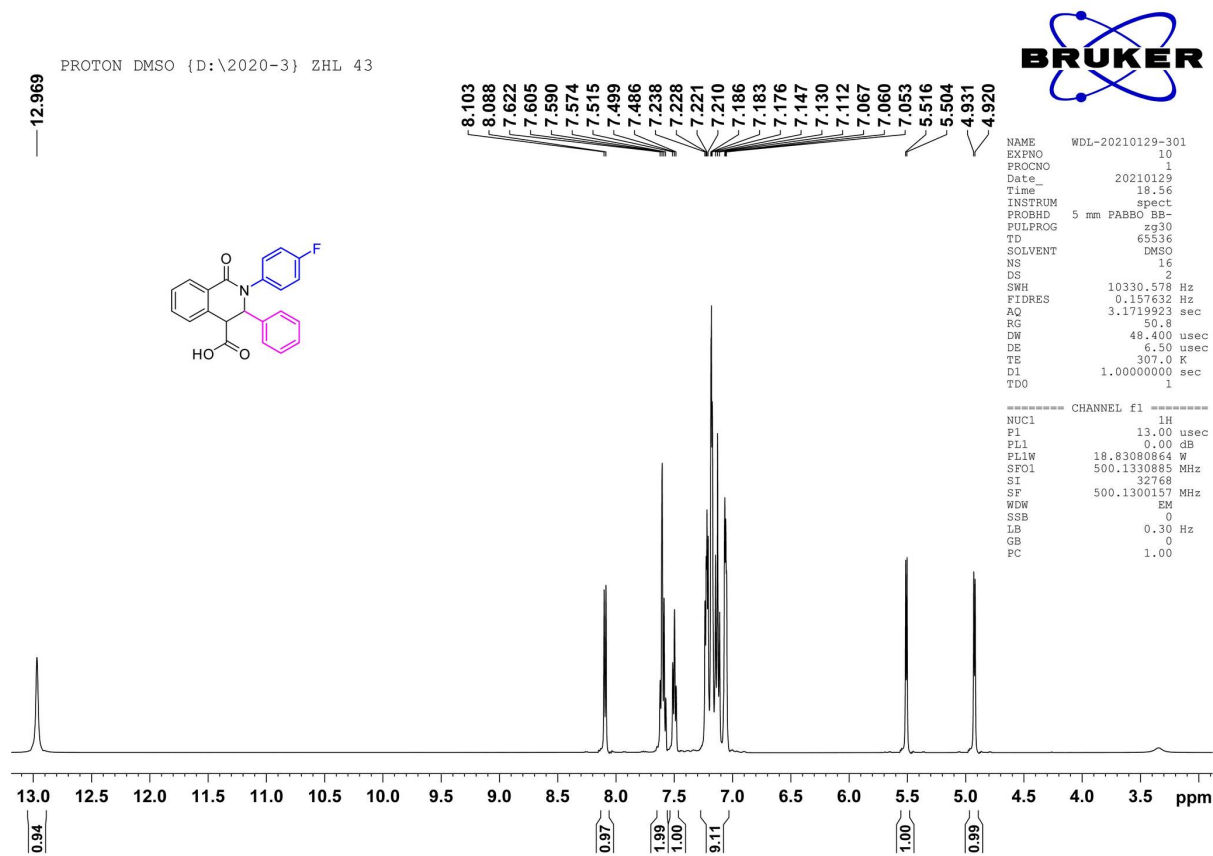


Figure S53. The ^1H NMR spectrum of compound I24

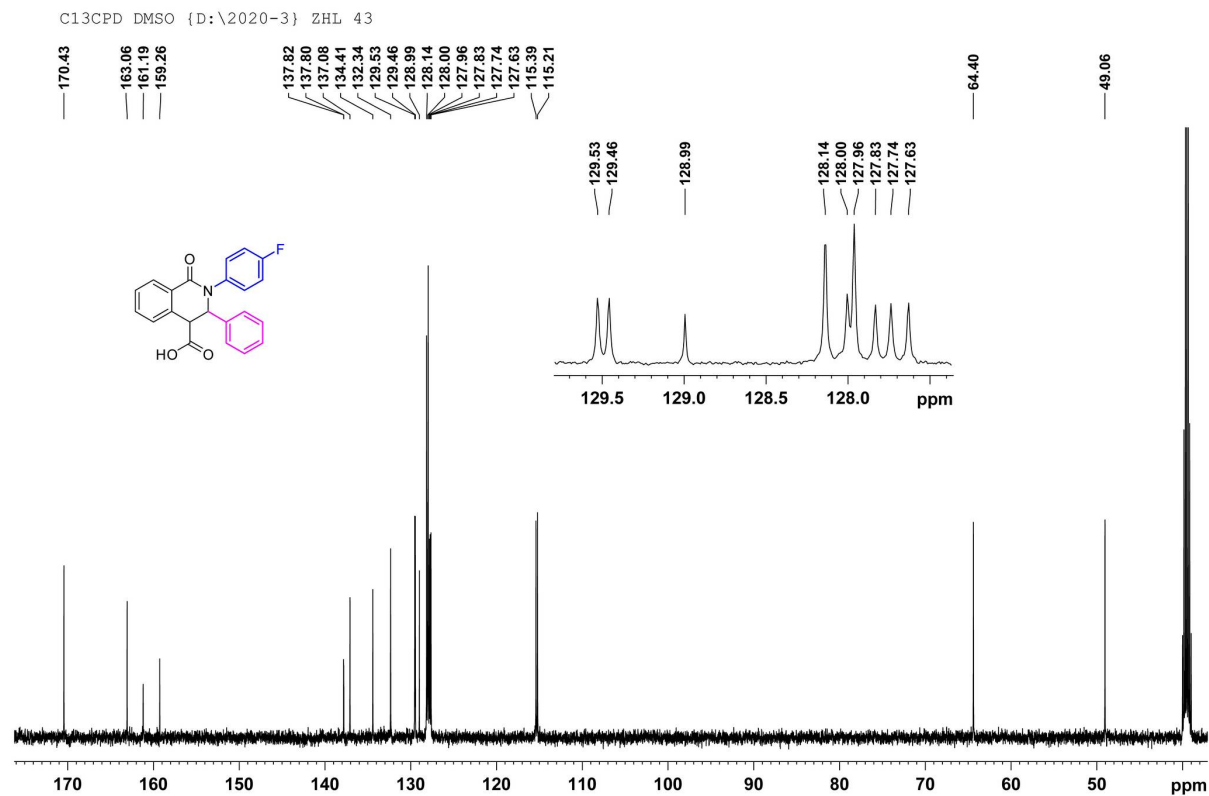


Figure S54. The ^{13}C NMR spectrum of compound I24

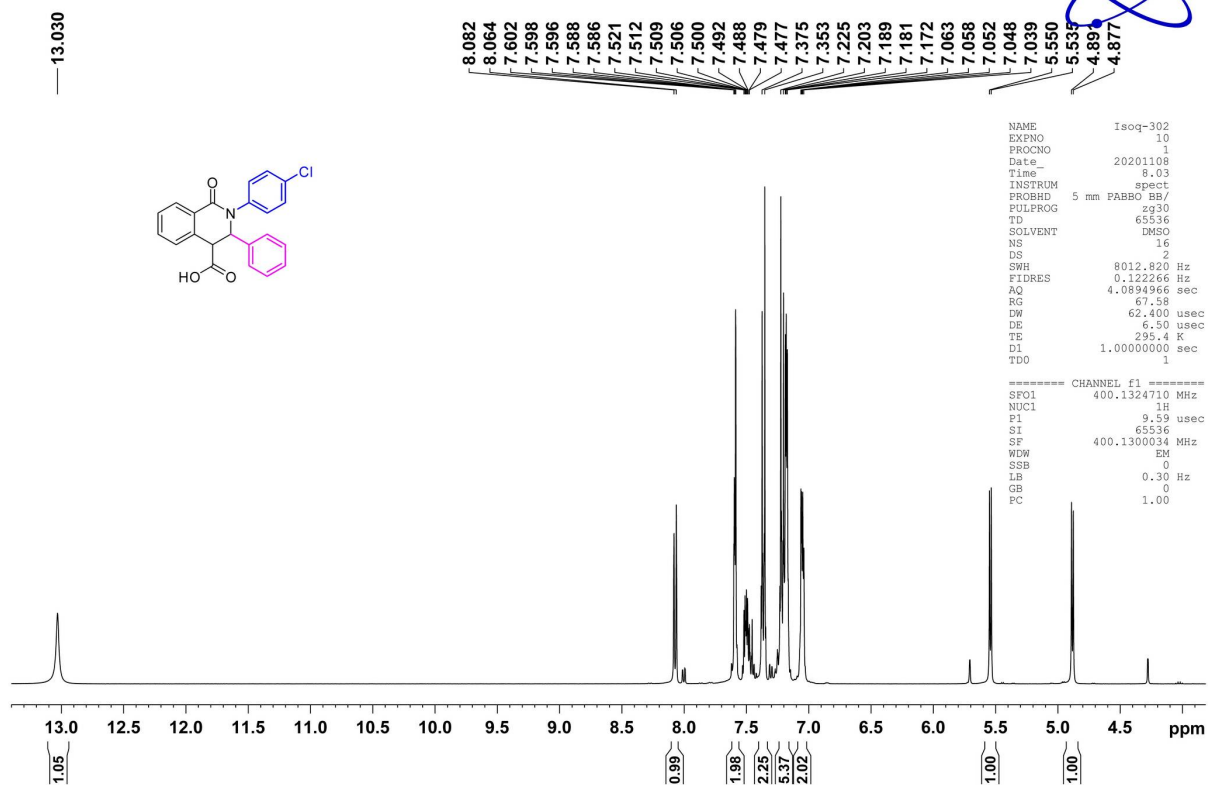


Figure S55. The ^1H NMR spectrum of compound I25

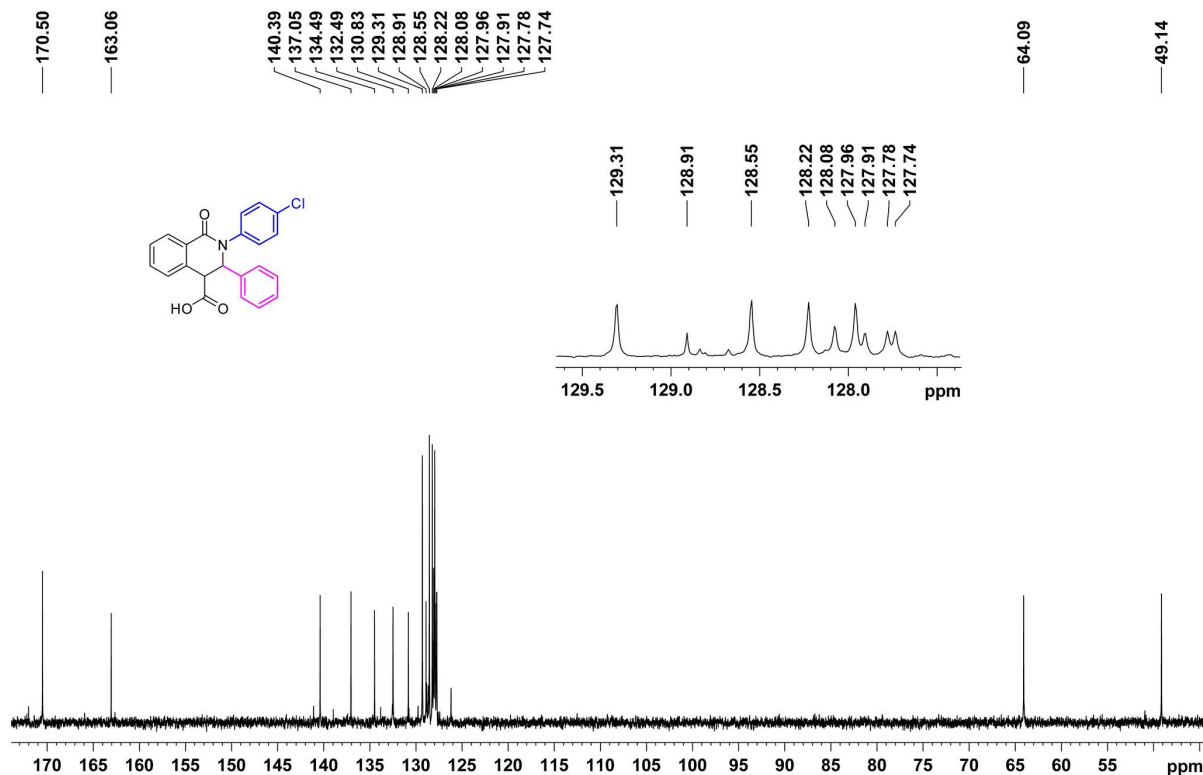


Figure S56. The ^{13}C NMR spectrum of compound I25

PROTON DMSO {D:\2020-3} ZHL 44

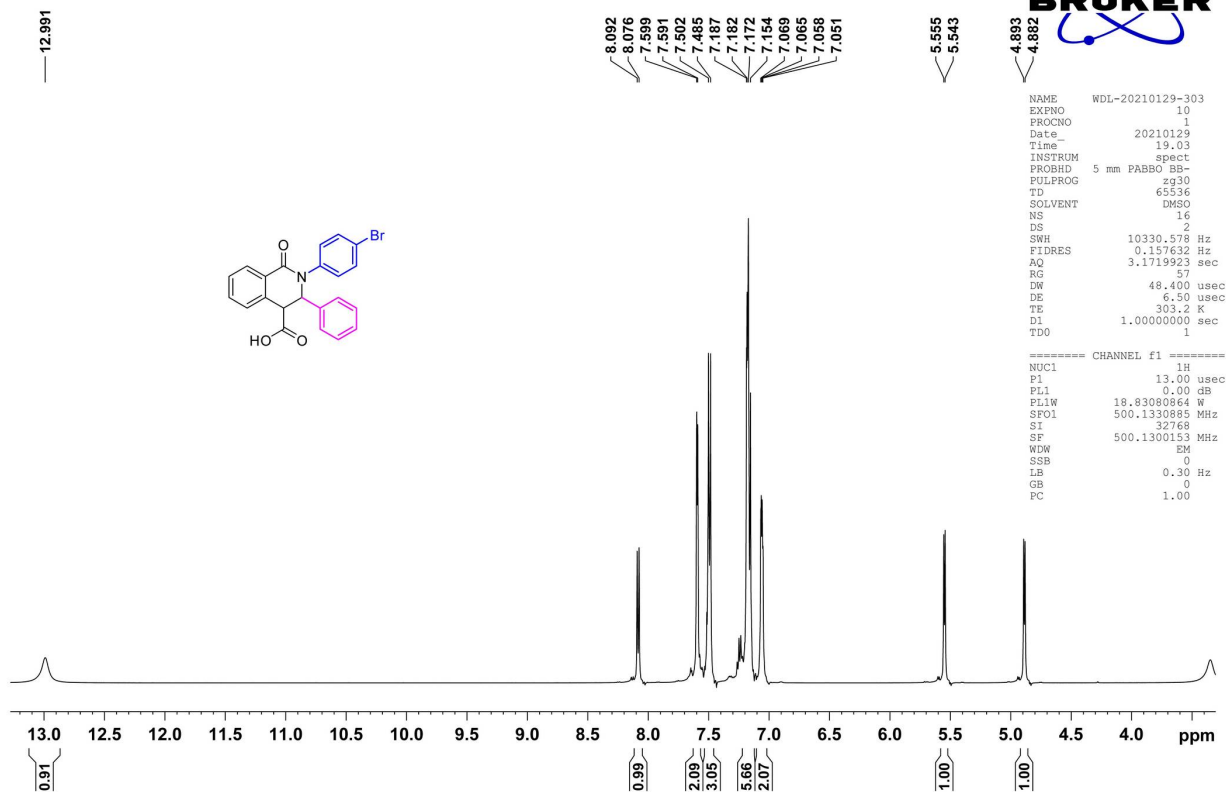


Figure S57. The ¹H NMR spectrum of compound I26

C13CPD DMSO {D:\2020-3} ZHL 44

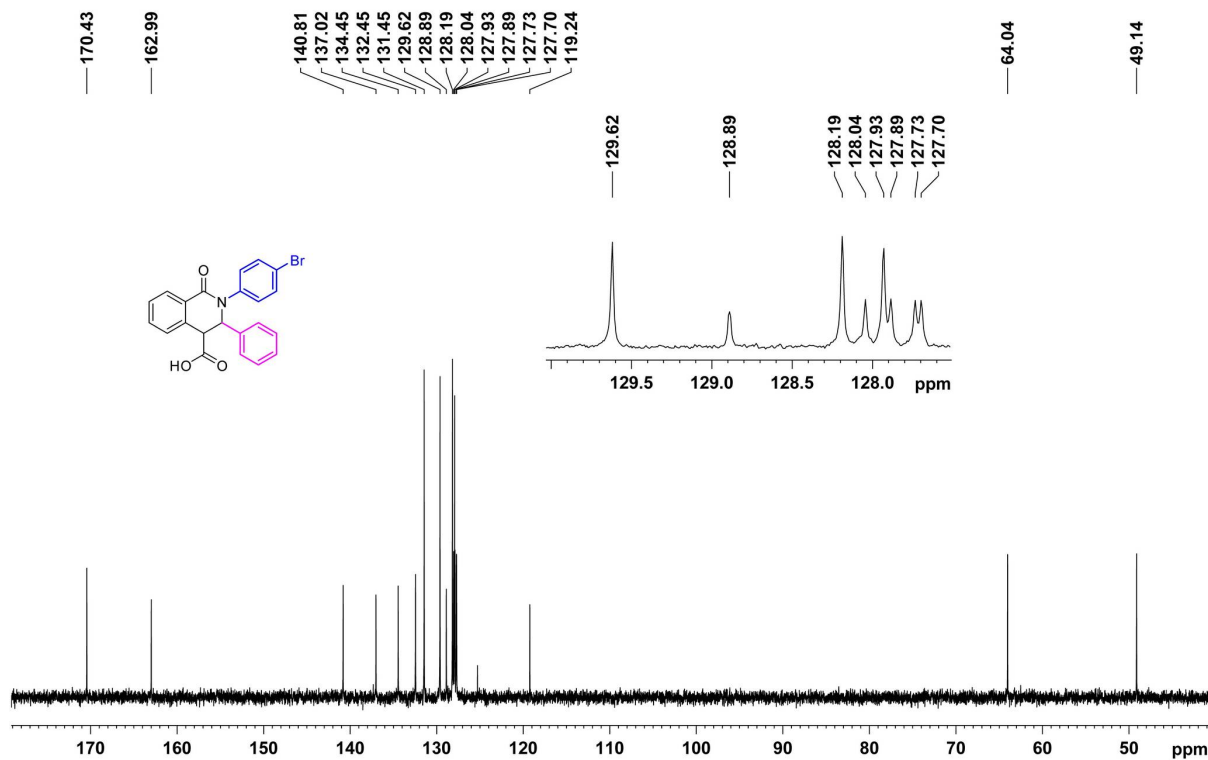


Figure S58. The ¹³C NMR spectrum of compound I26

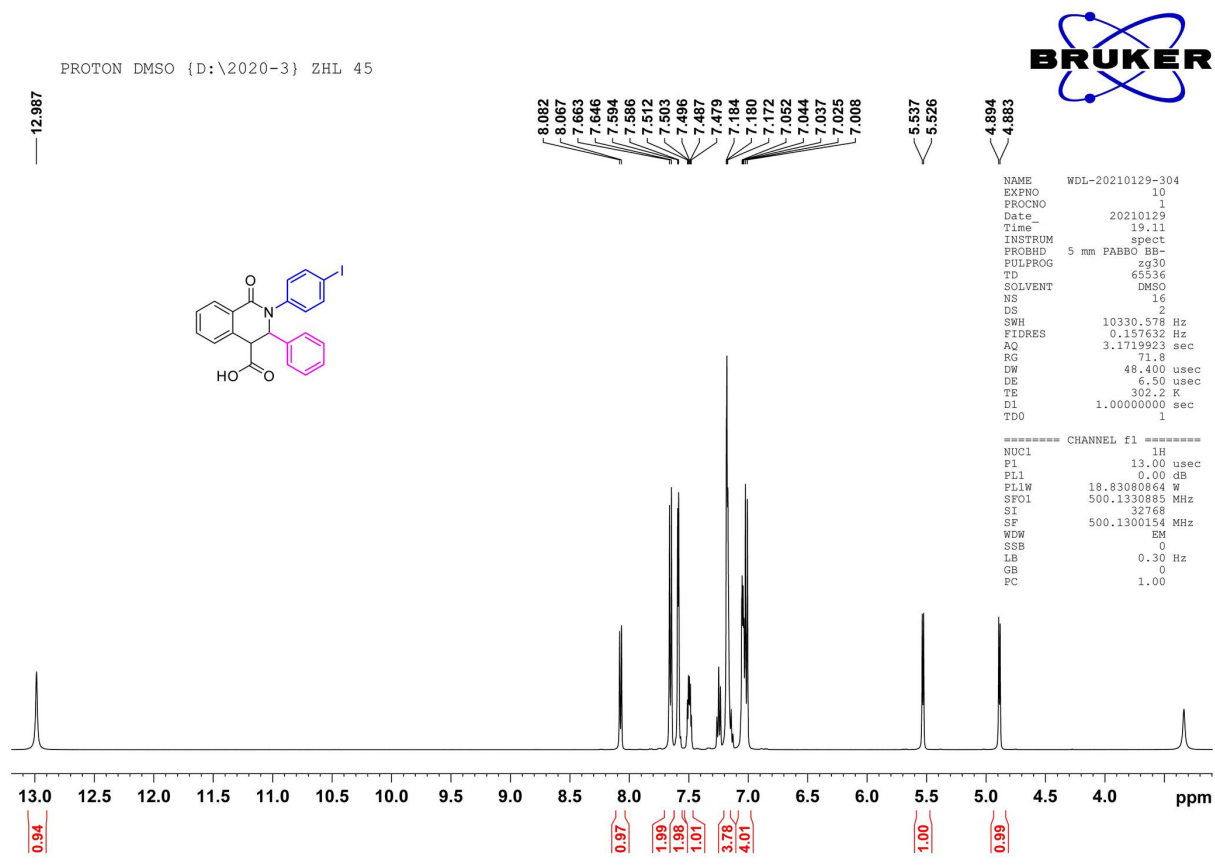


Figure S59. The ¹H NMR spectrum of compound I27

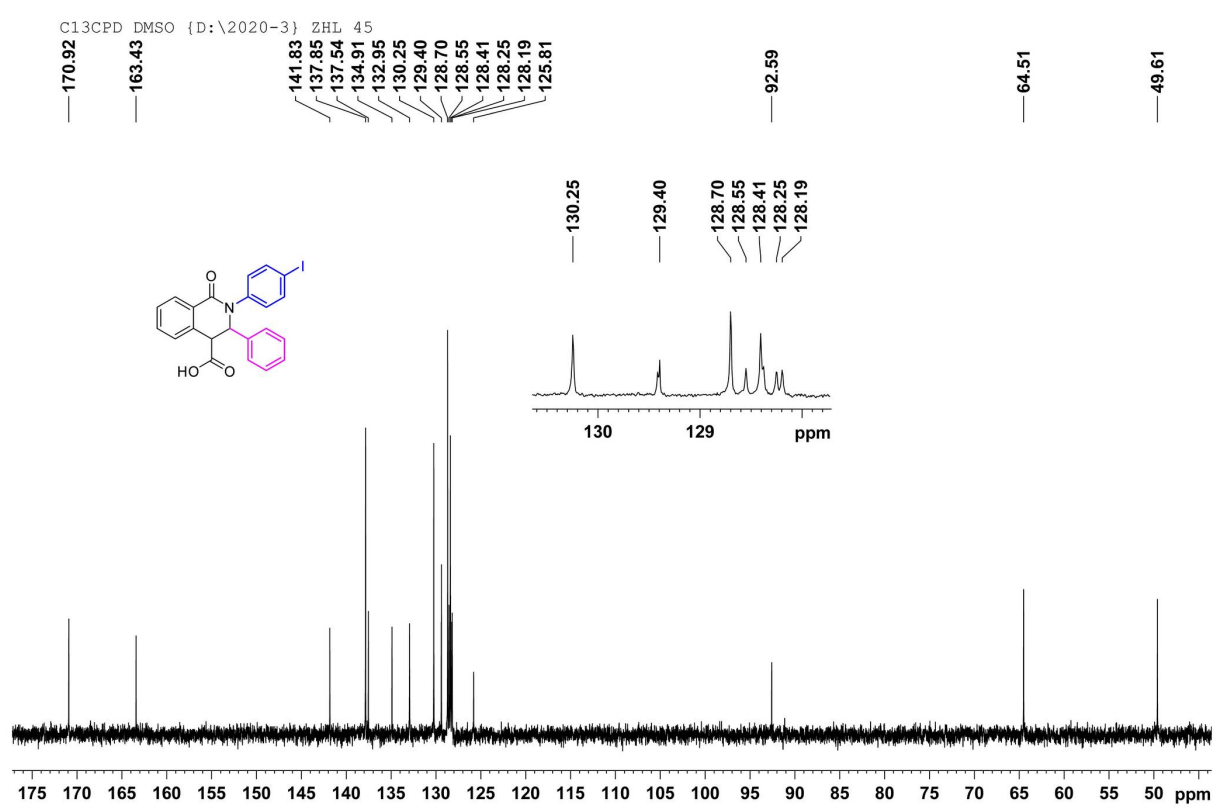


Figure S60. The ¹³C NMR spectrum of compound I27

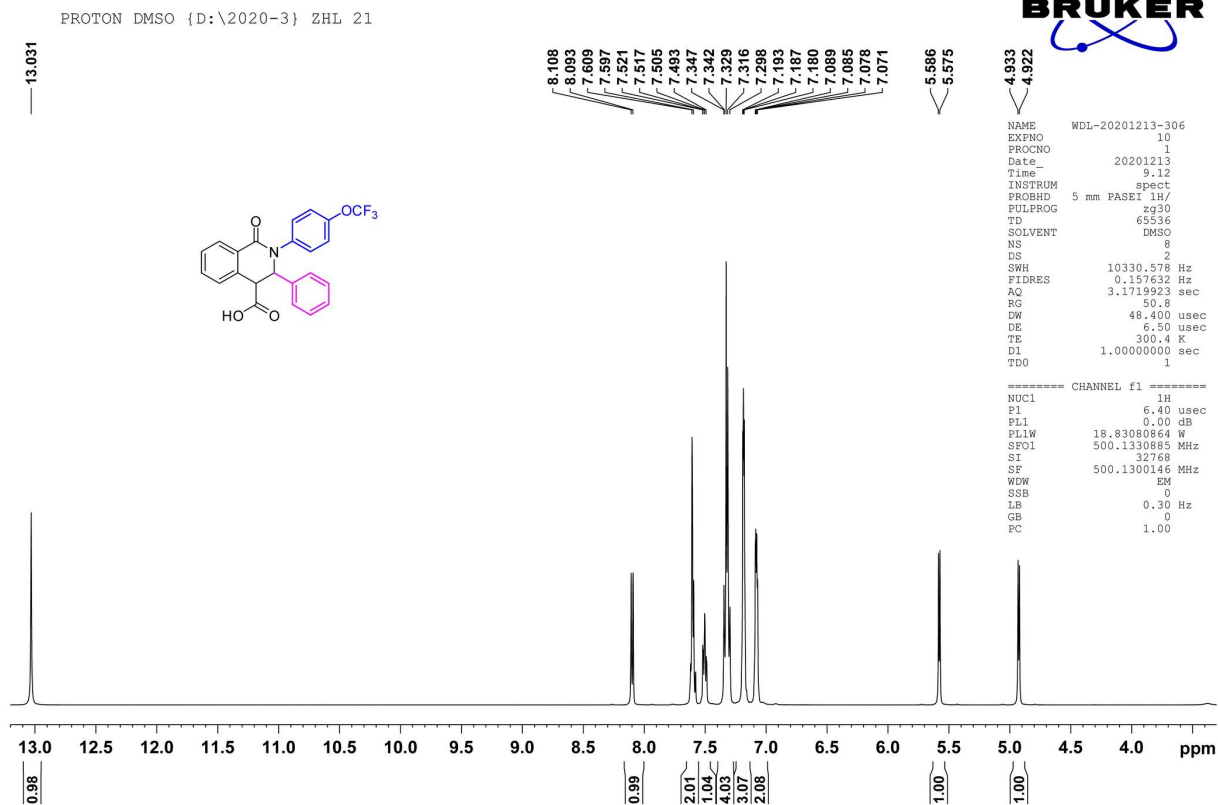


Figure S61. The ¹H NMR spectrum of compound I28

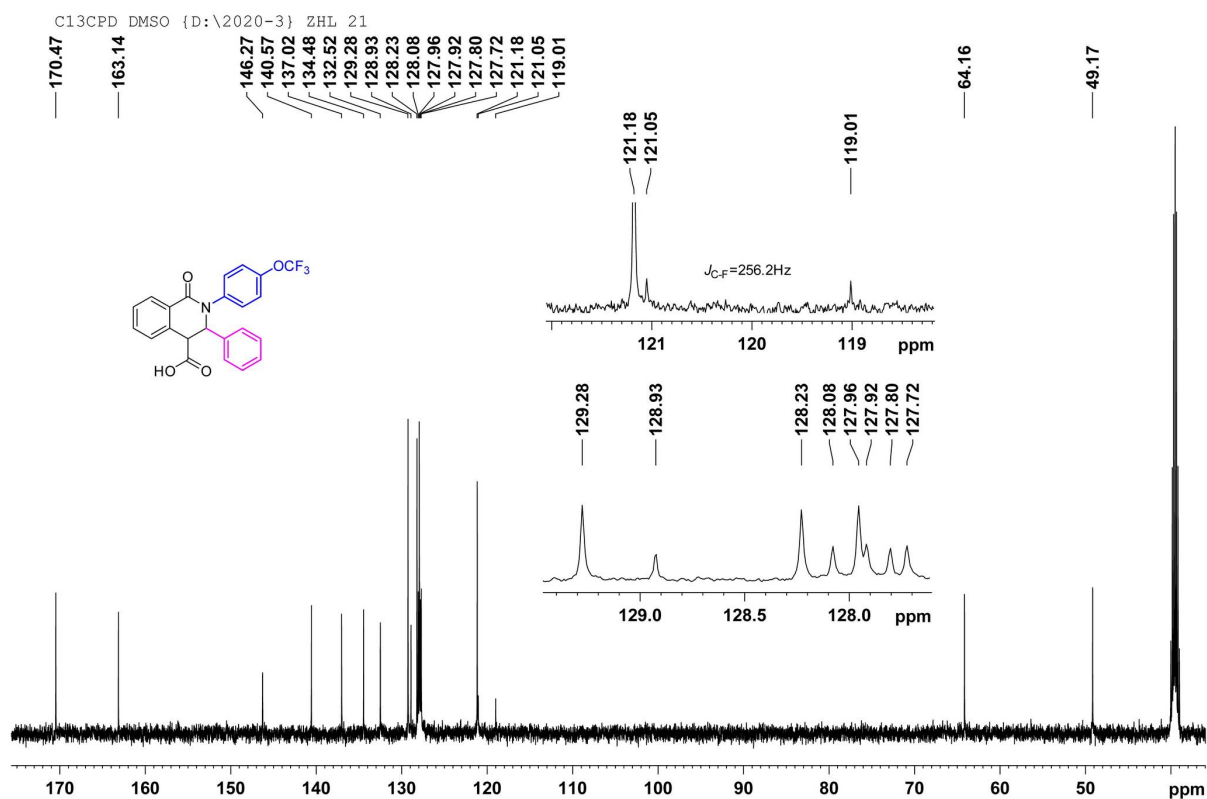


Figure S62. The ¹³C NMR spectrum of compound I28

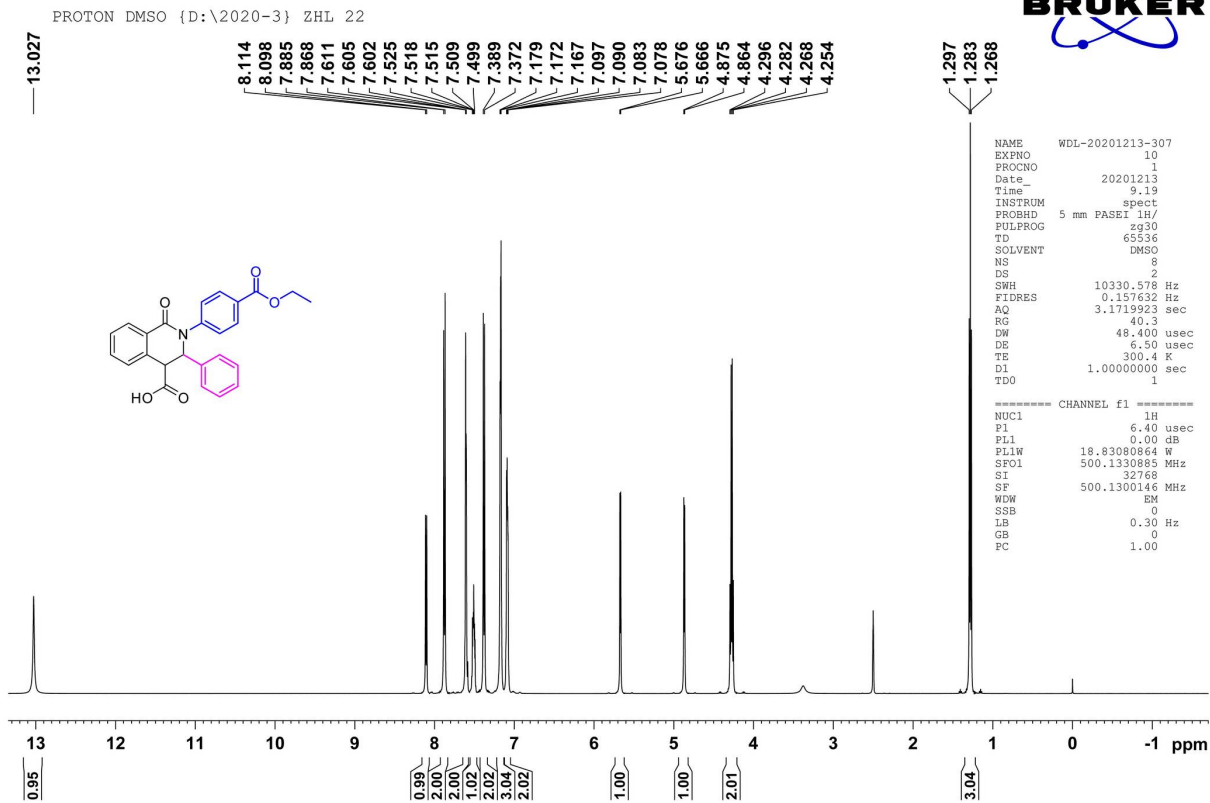


Figure S63. The ¹H NMR spectrum of compound I29

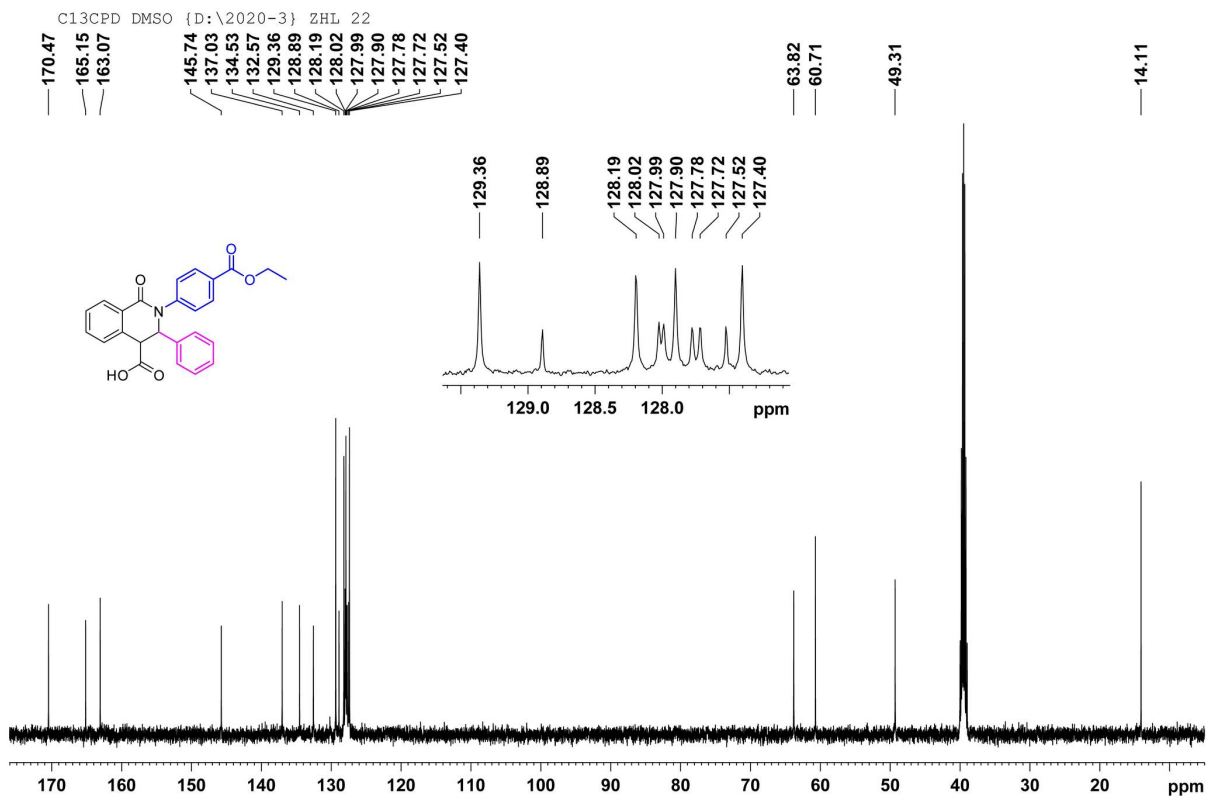


Figure S64. The ¹³C NMR spectrum of compound I29

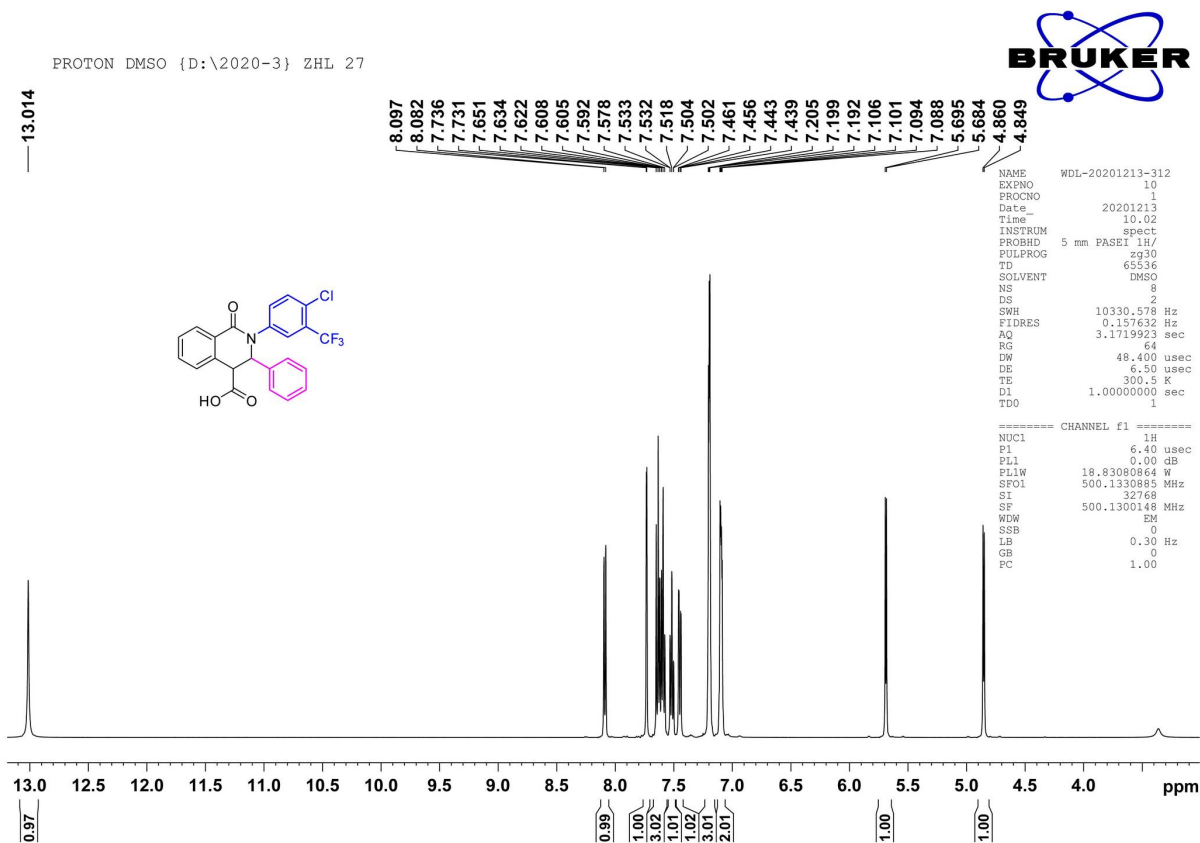


Figure S65. The ^1H NMR spectrum of compound I30

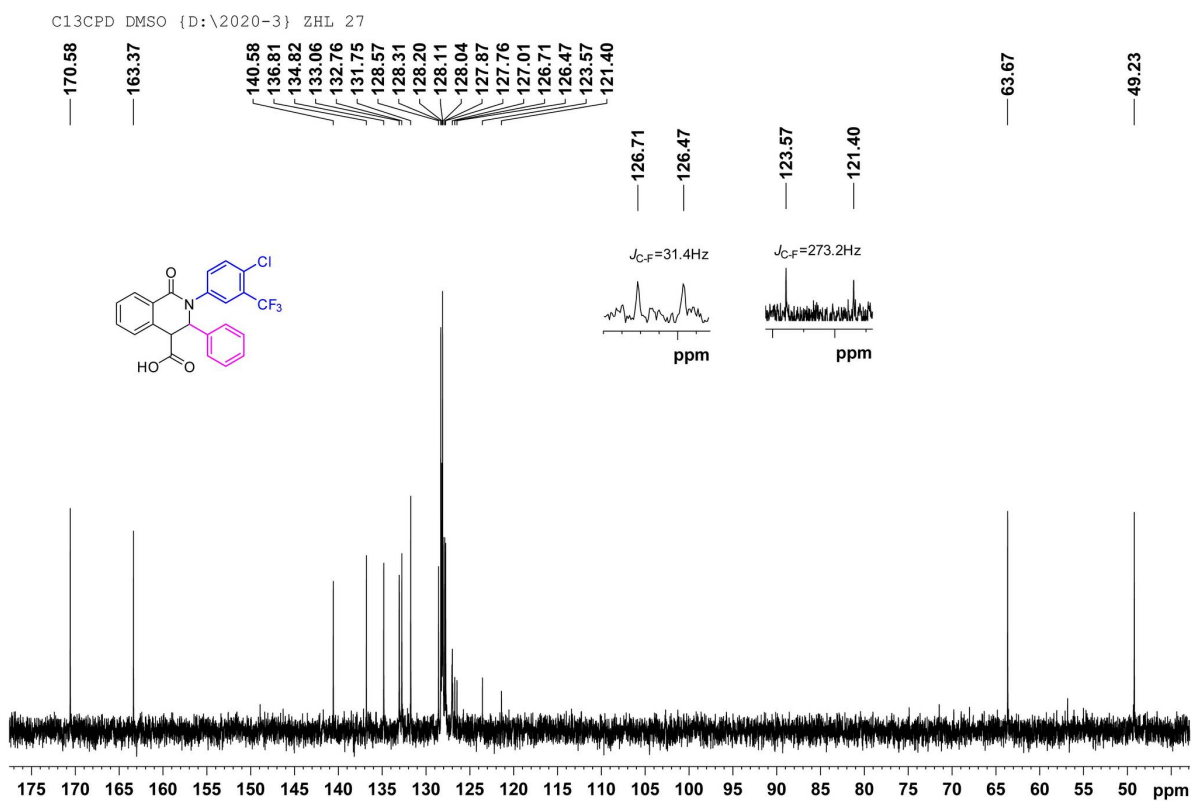
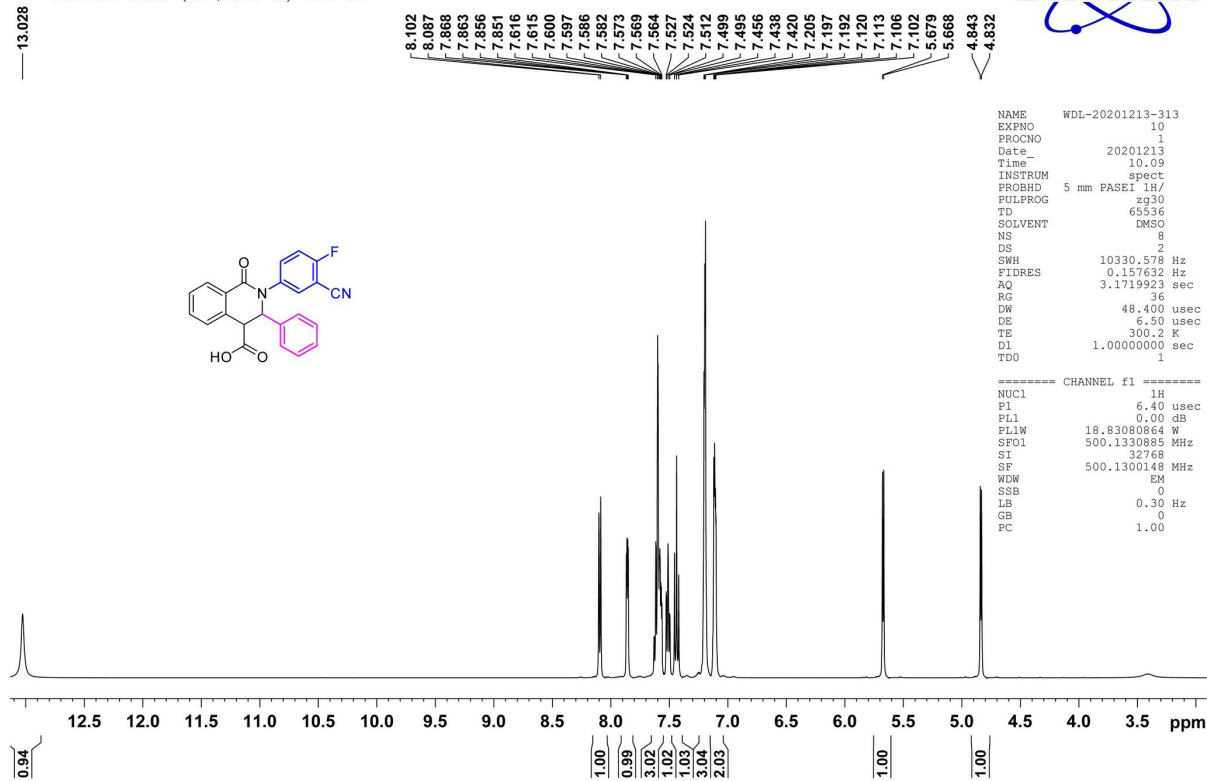
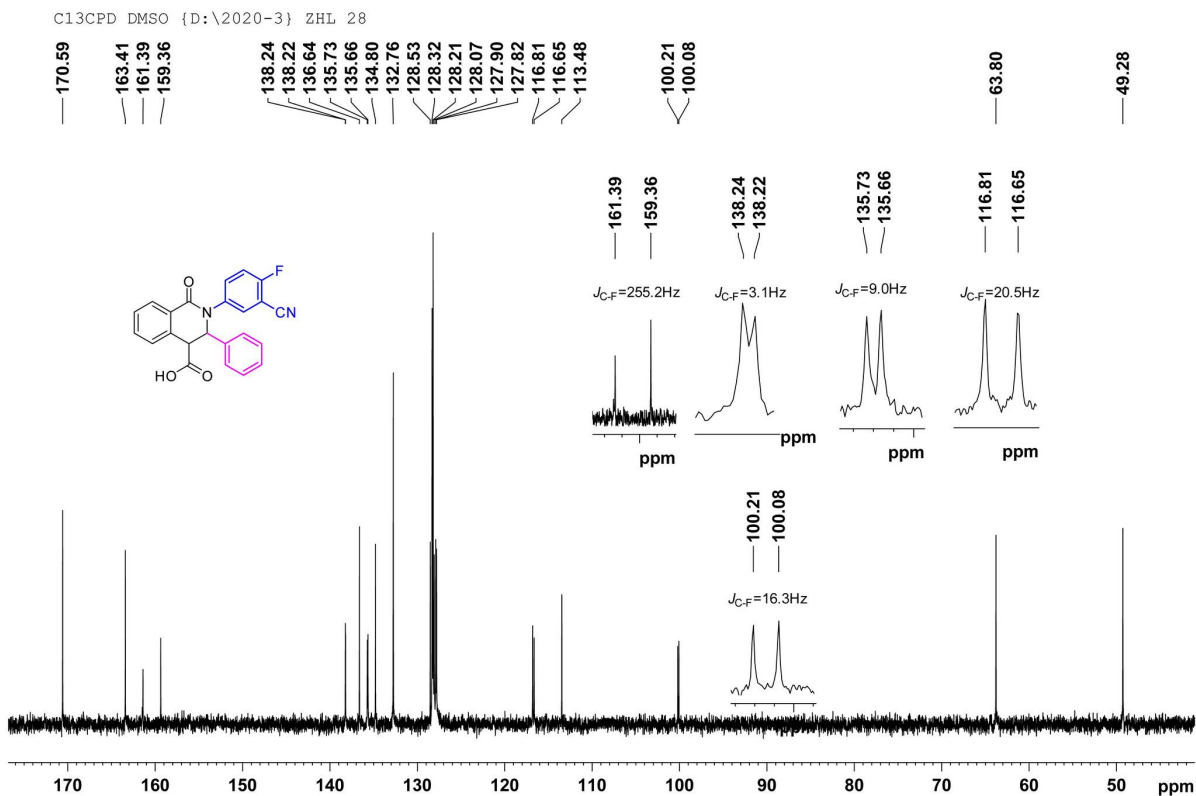


Figure S66. The ^{13}C NMR spectrum of compound I30

13.028

PROTON DMSO {D:\2020-3} ZHL 28

Figure S67. The ¹H NMR spectrum of compound I31Figure S68. The ¹³C NMR spectrum of compound I31

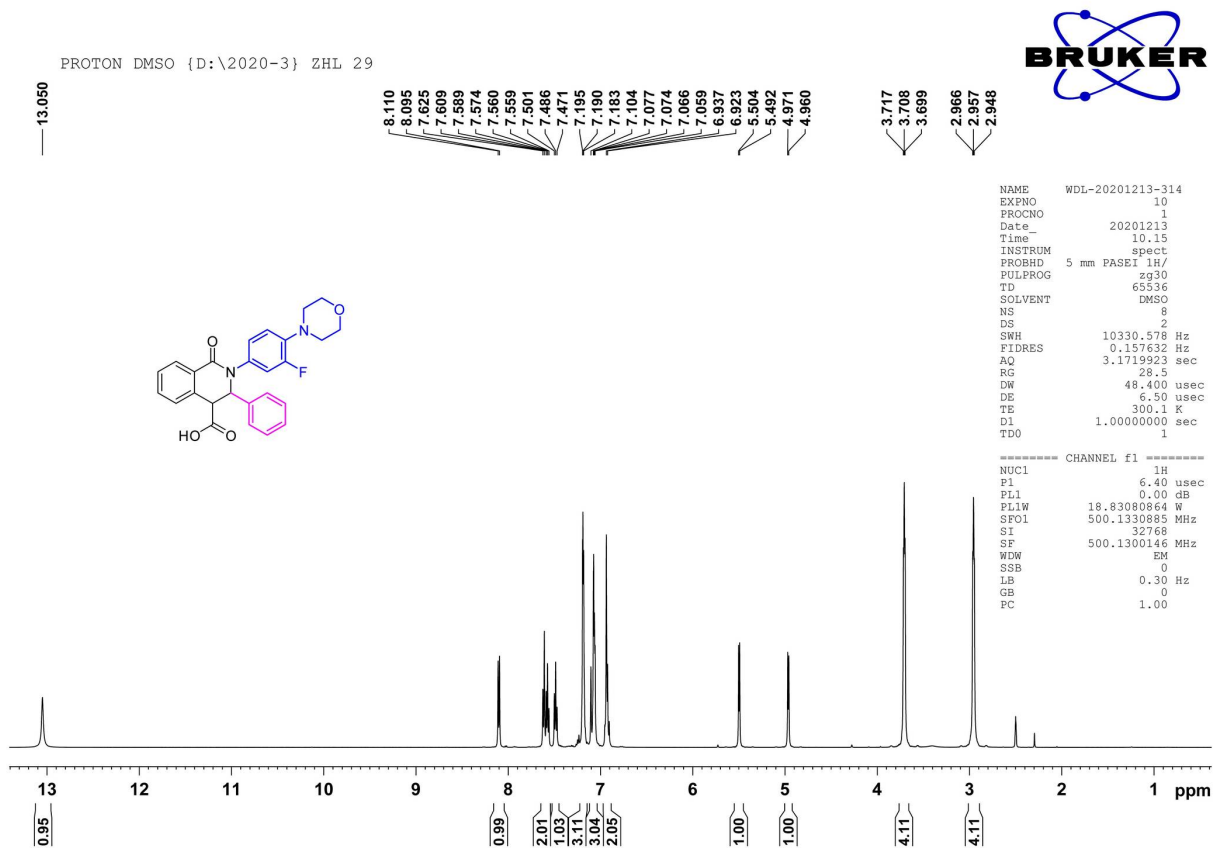


Figure S69. The ^1H NMR spectrum of compound I32

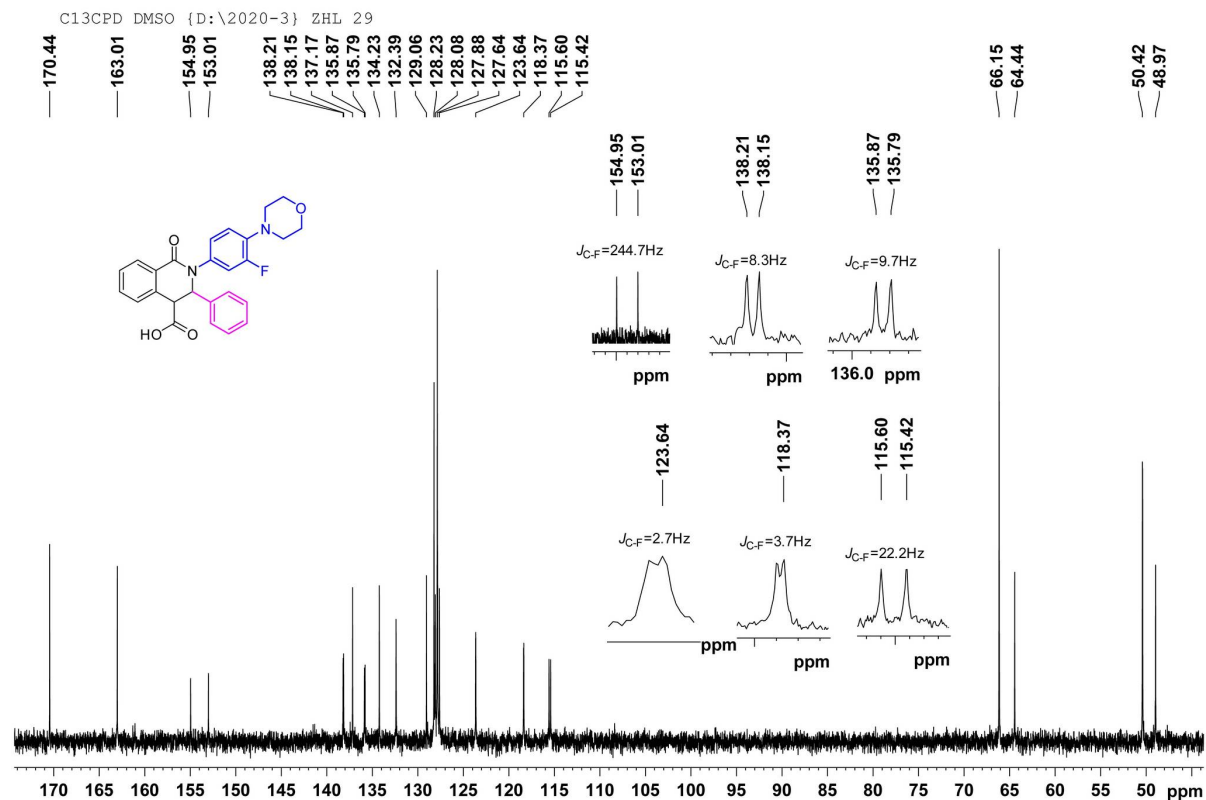


Figure S70. The ^{13}C NMR spectrum of compound I32

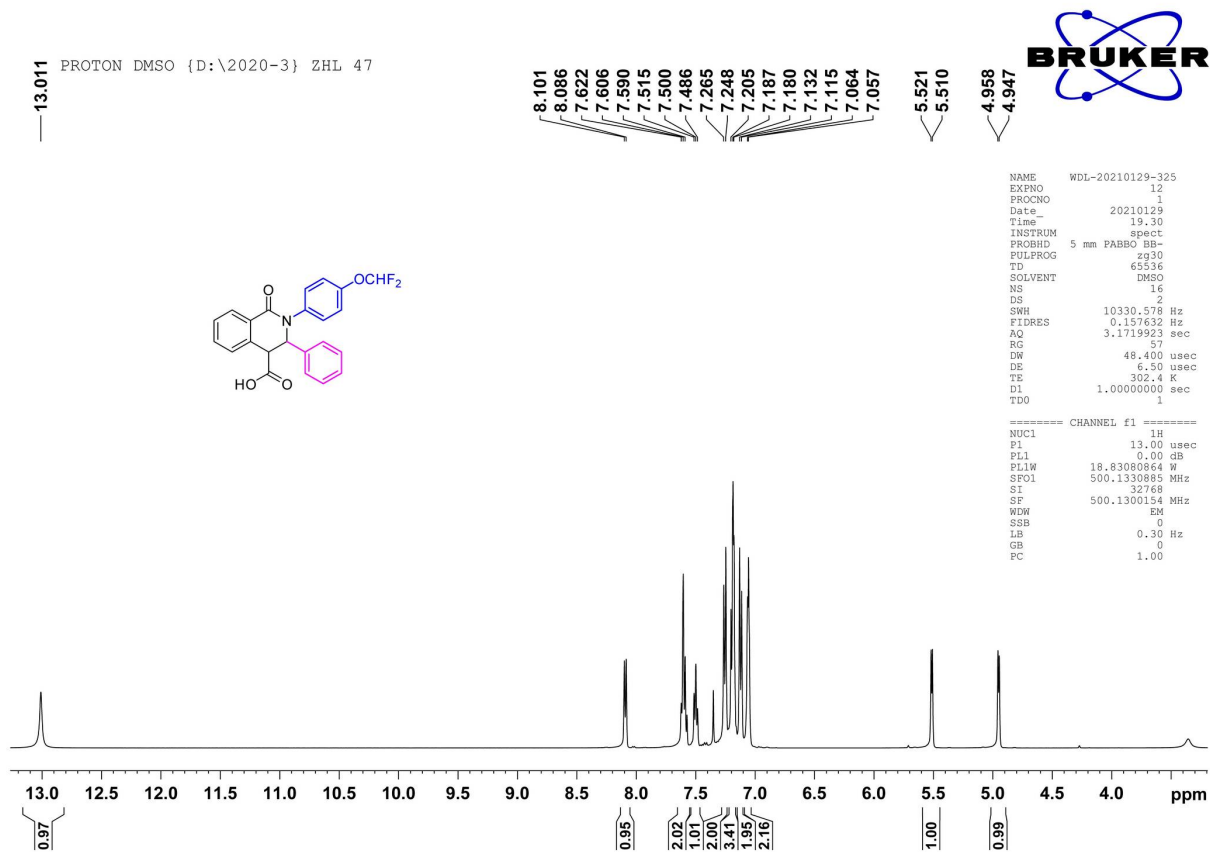


Figure S71. The ¹H NMR spectrum of compound I33

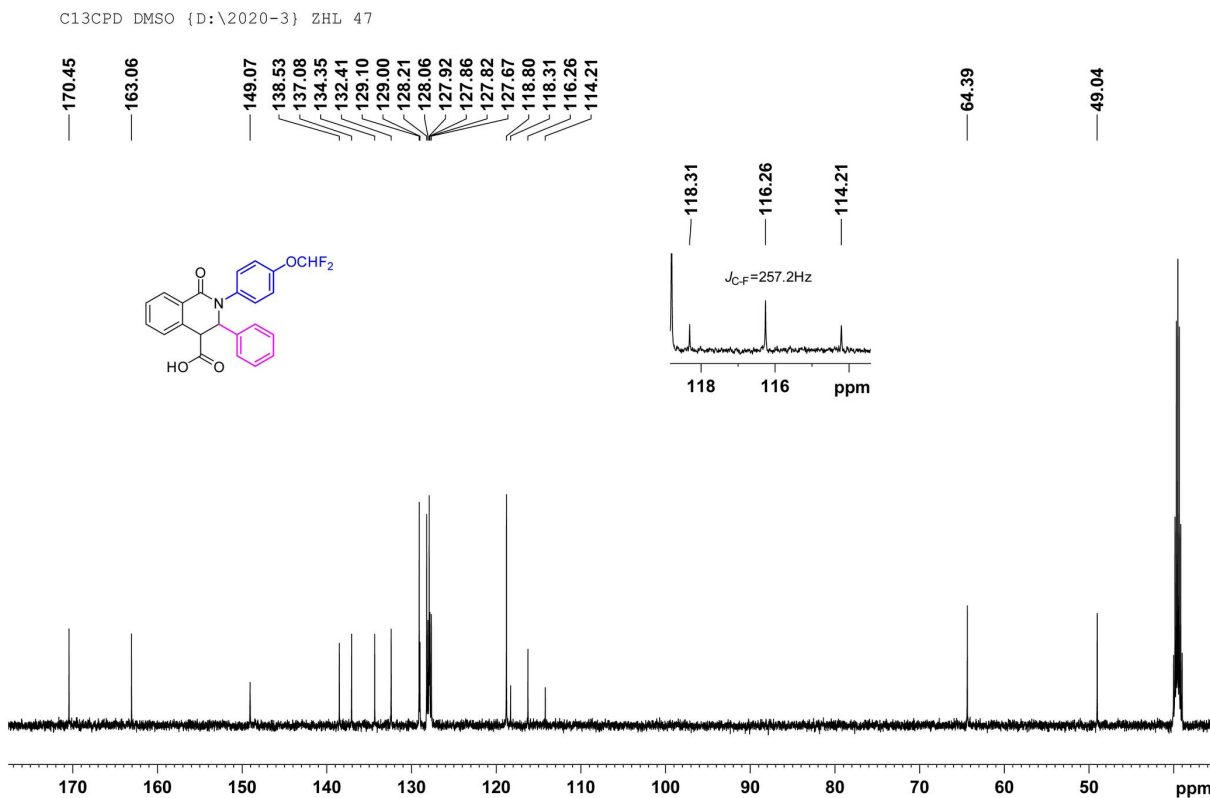


Figure S72. The ¹³C NMR spectrum of compound I33

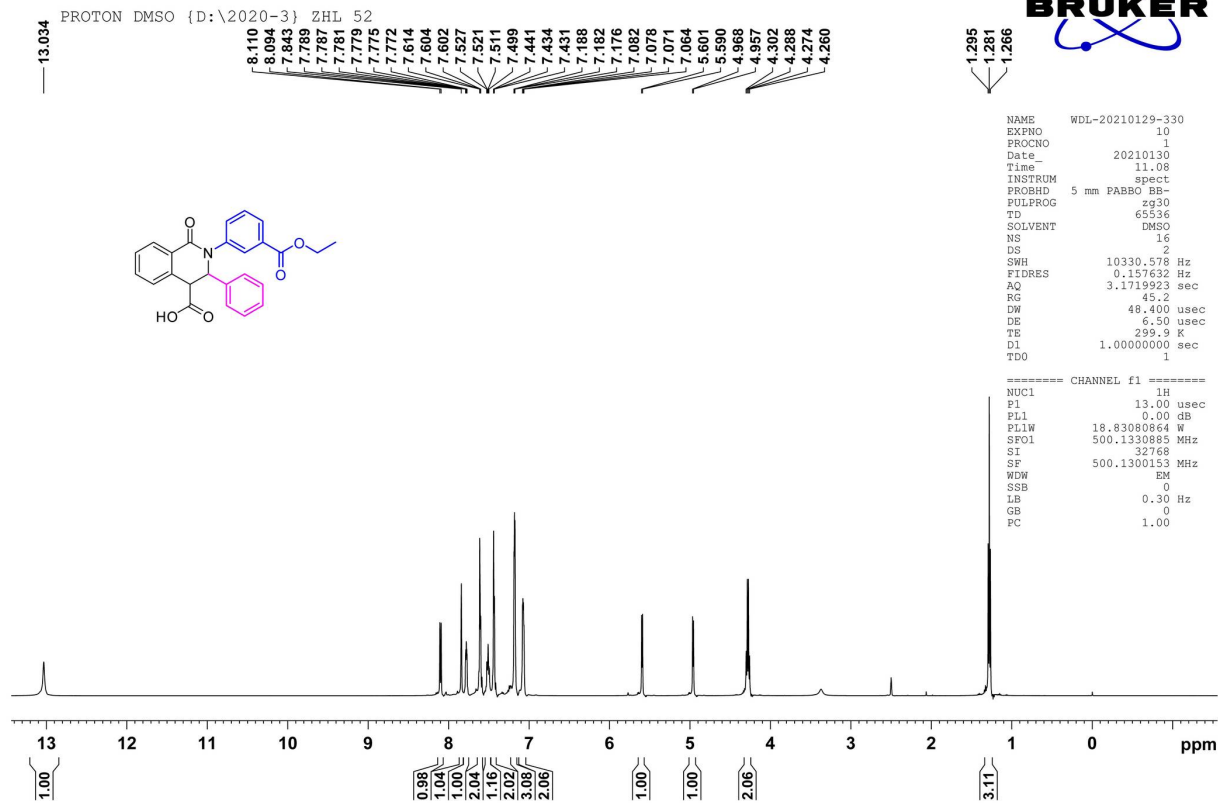


Figure S73. The ^1H NMR spectrum of compound I34

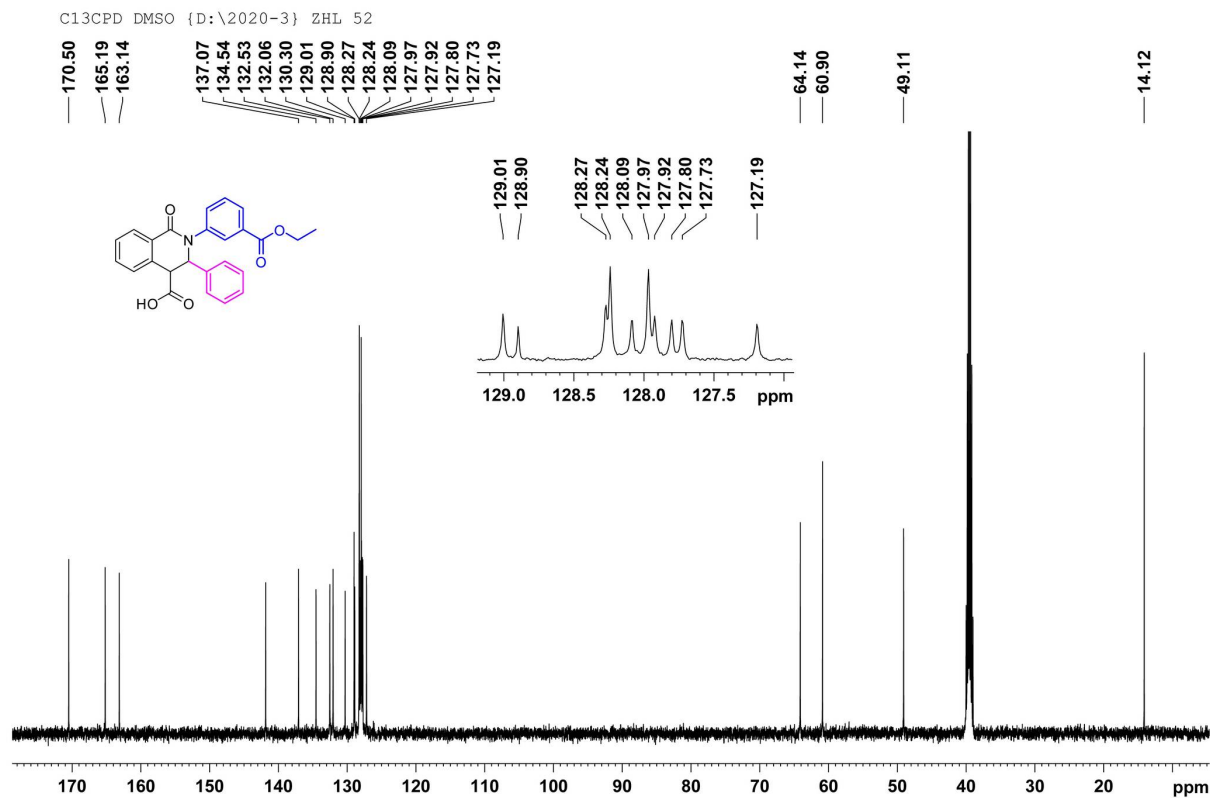


Figure S74. The ^{13}C NMR spectrum of compound I34

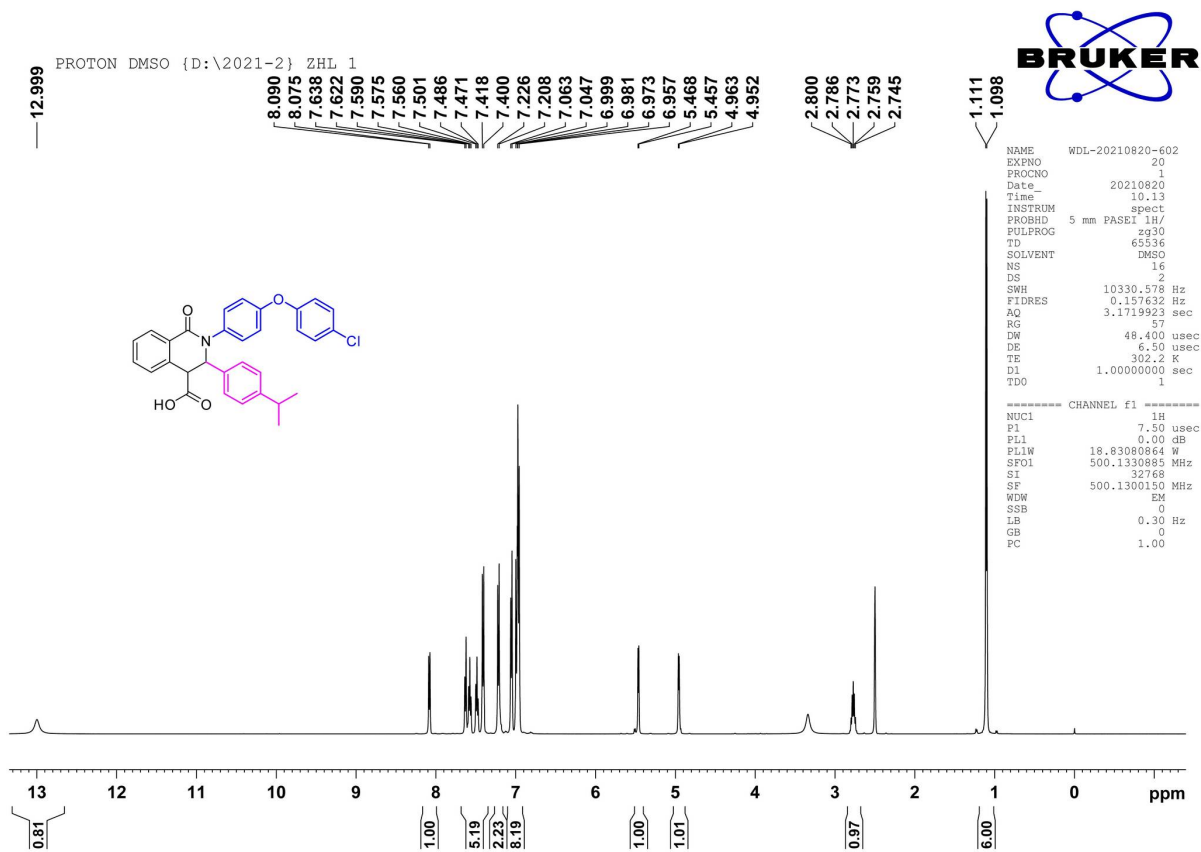


Figure S75. The ^1H NMR spectrum of compound III1

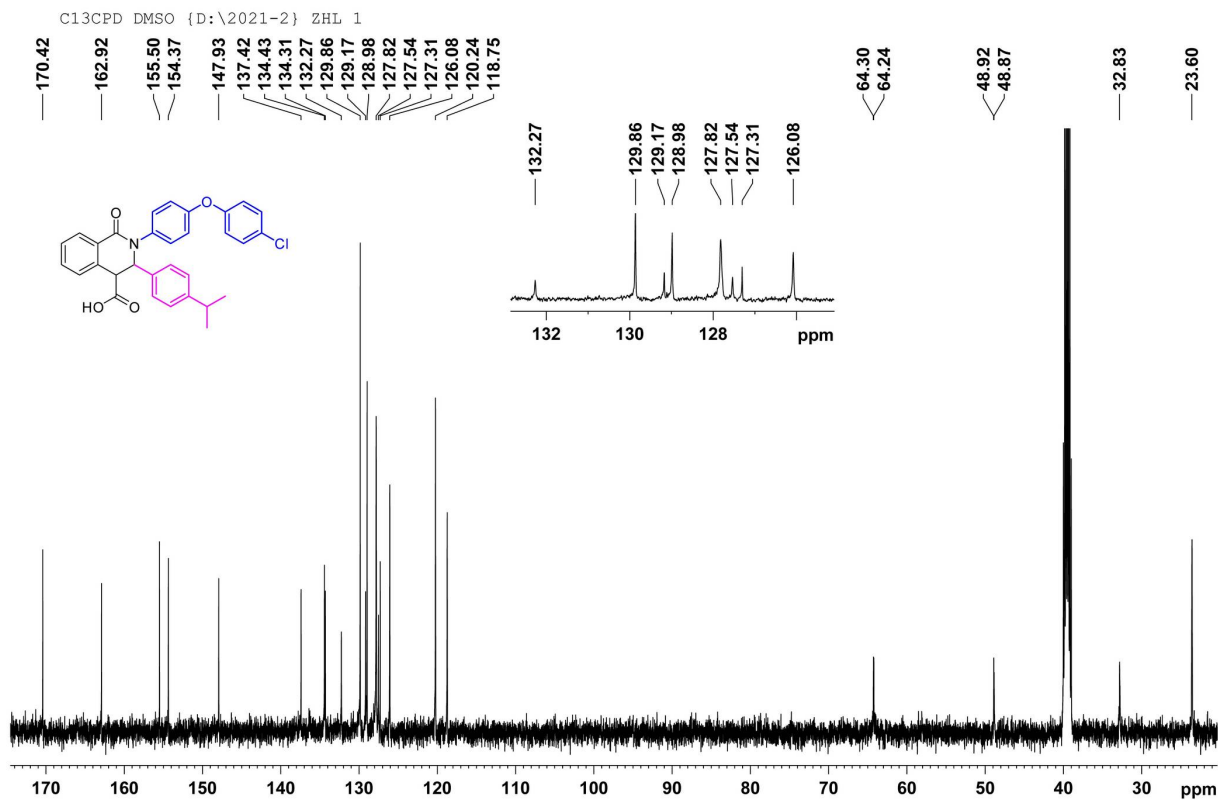


Figure S76. The ^{13}C NMR spectrum of compound III1

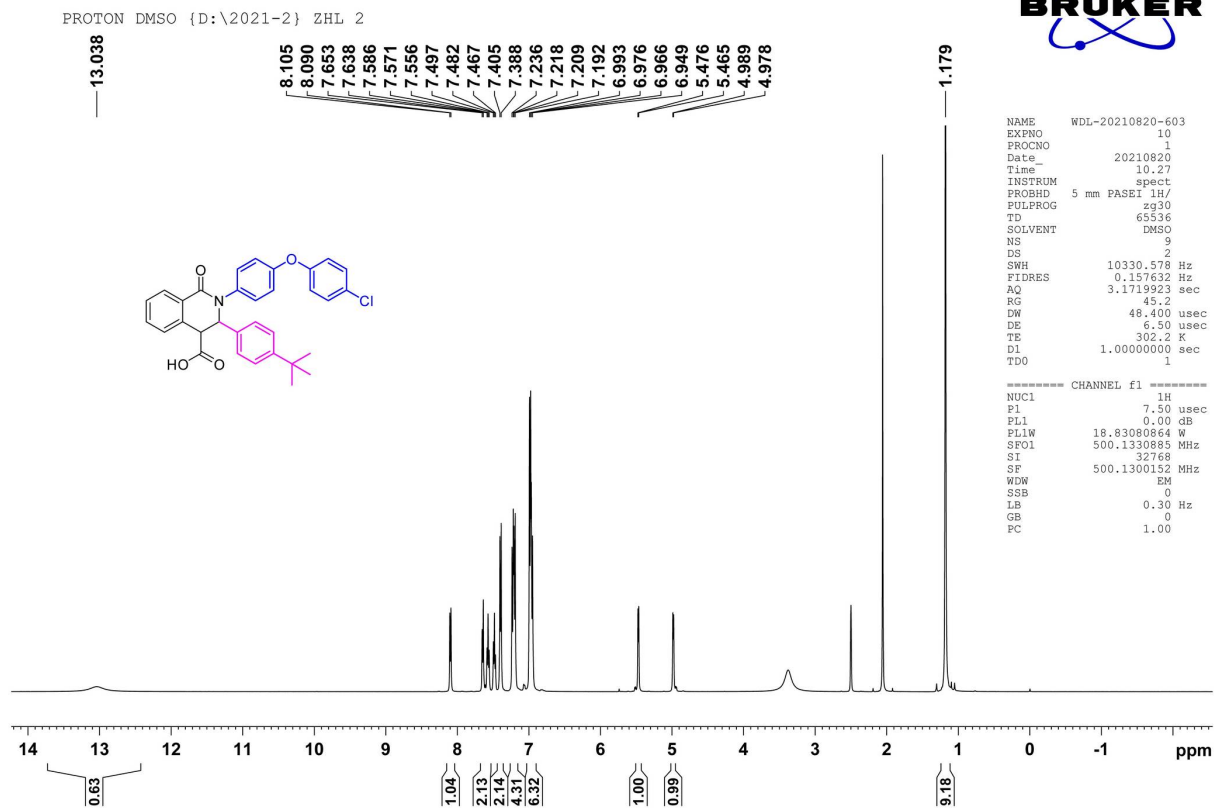


Figure S77. The ^1H NMR spectrum of compound II2

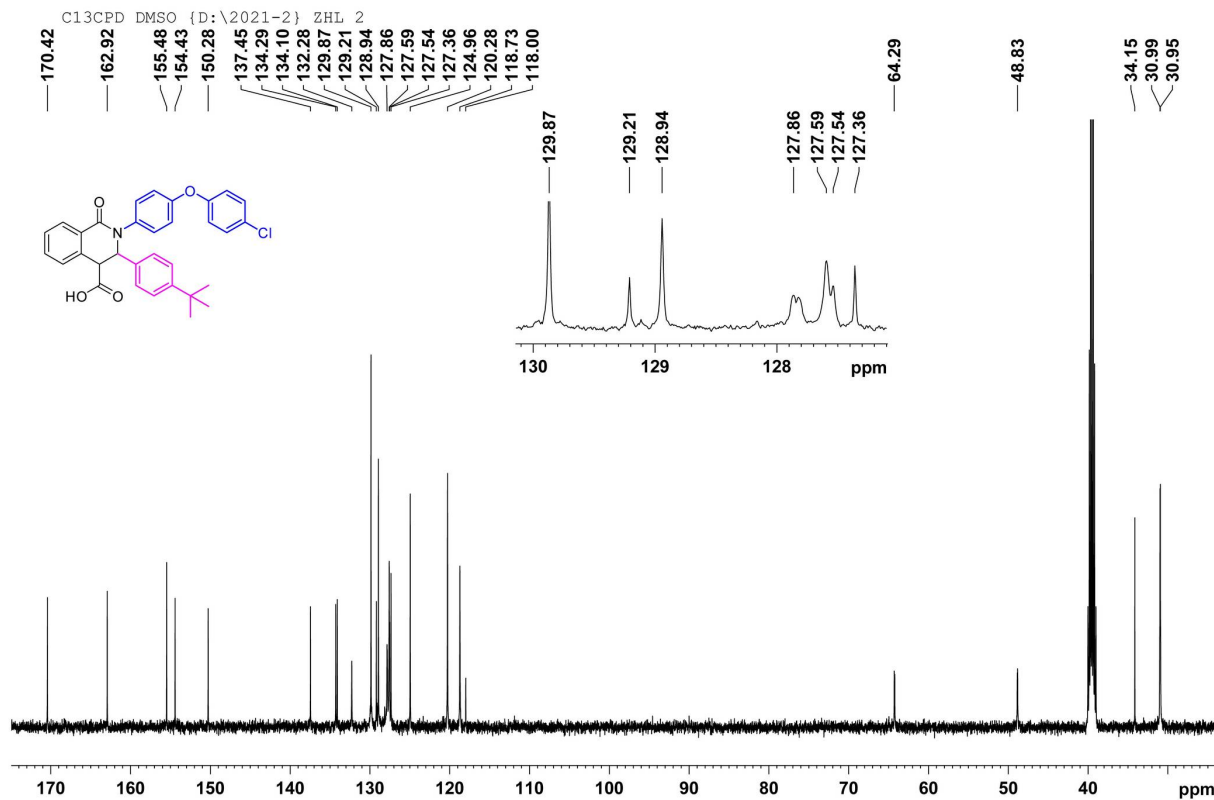


Figure S78. The ^{13}C NMR spectrum of compound II2

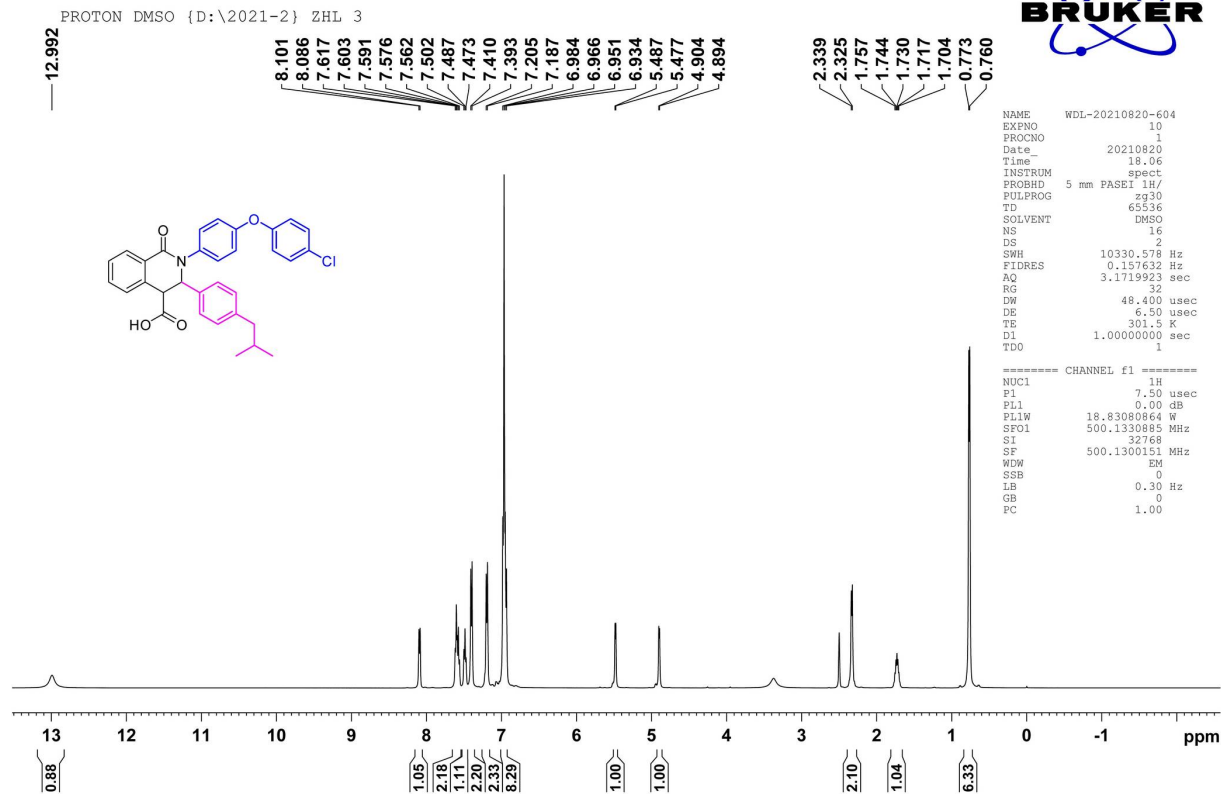


Figure S79. The ^1H NMR spectrum of compound II3

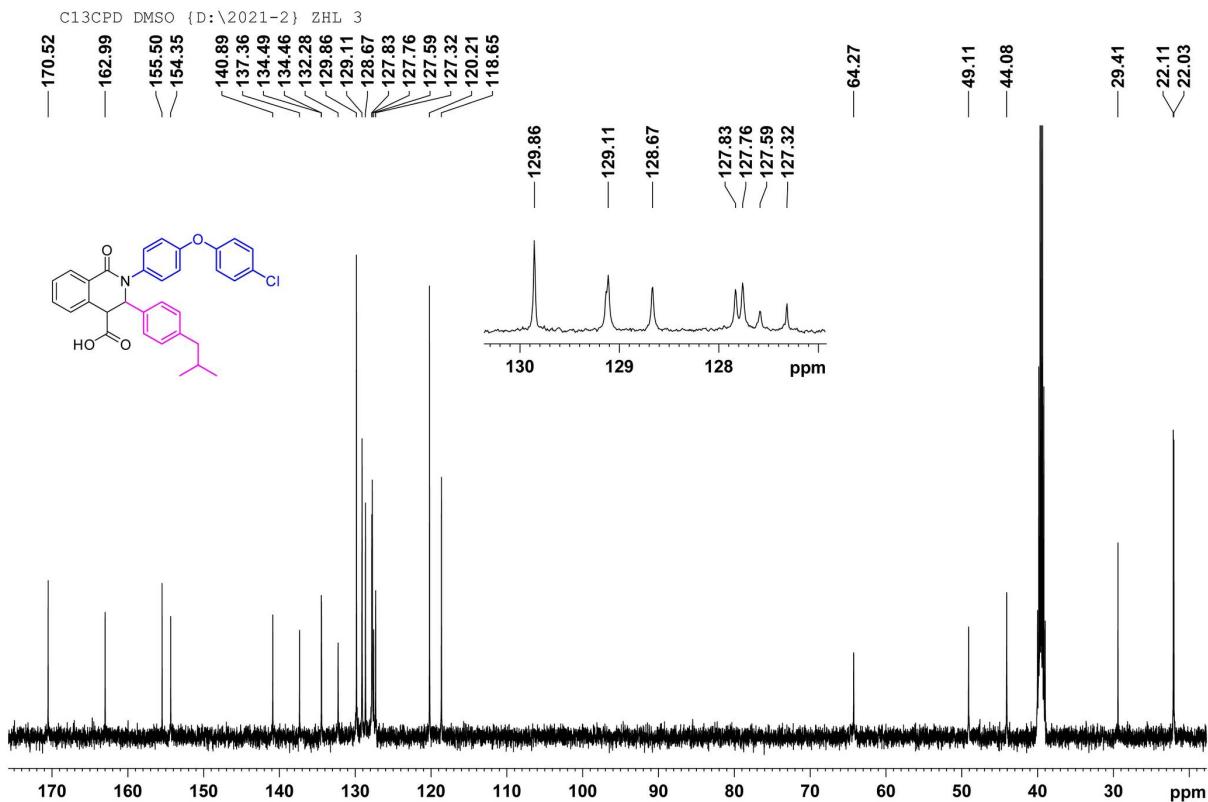


Figure S80. The ^{13}C NMR spectrum of compound II3

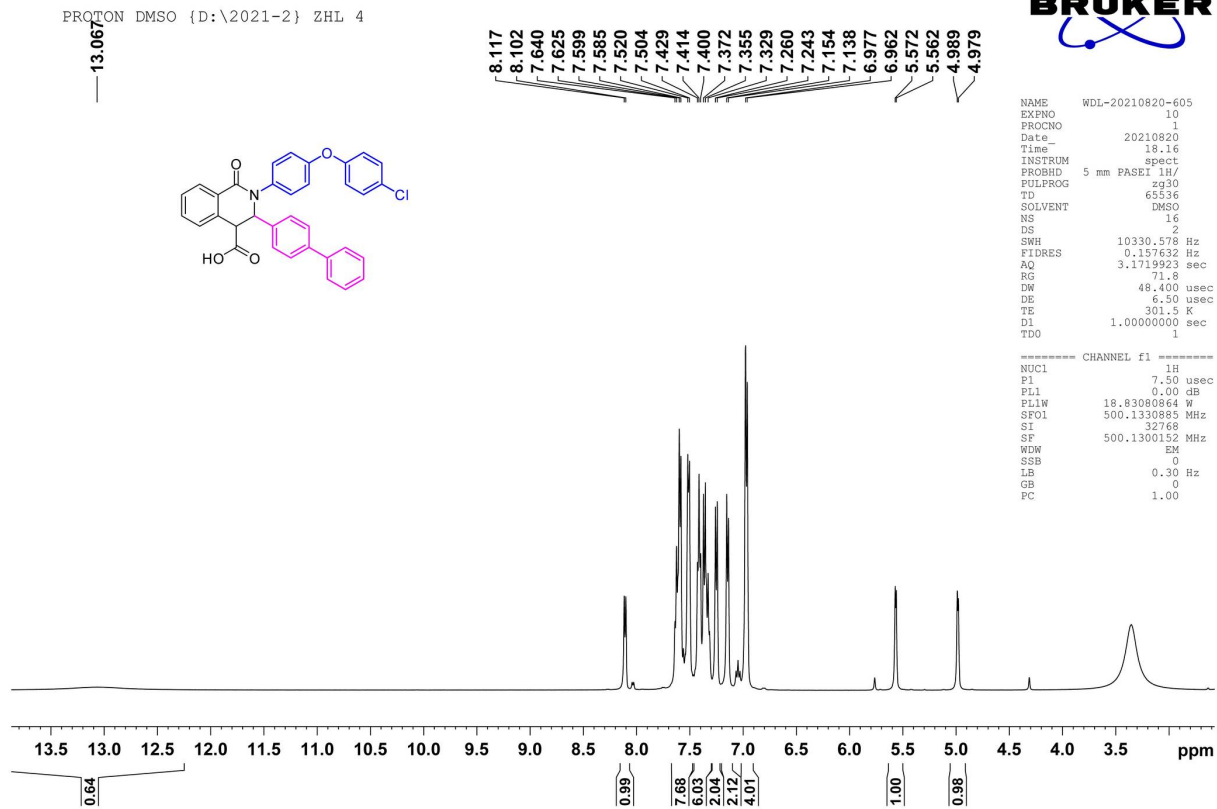


Figure S81. The ^1H NMR spectrum of compound II4

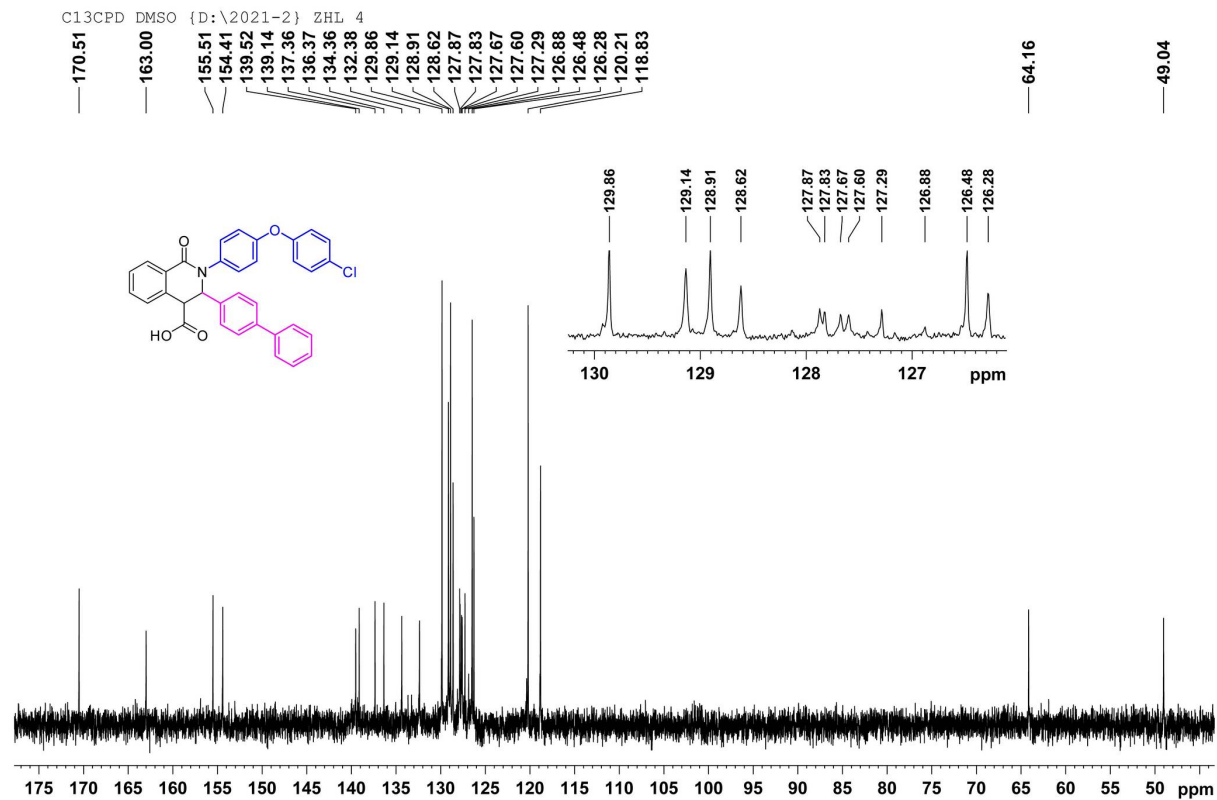


Figure S82. The ^{13}C NMR spectrum of compound II4

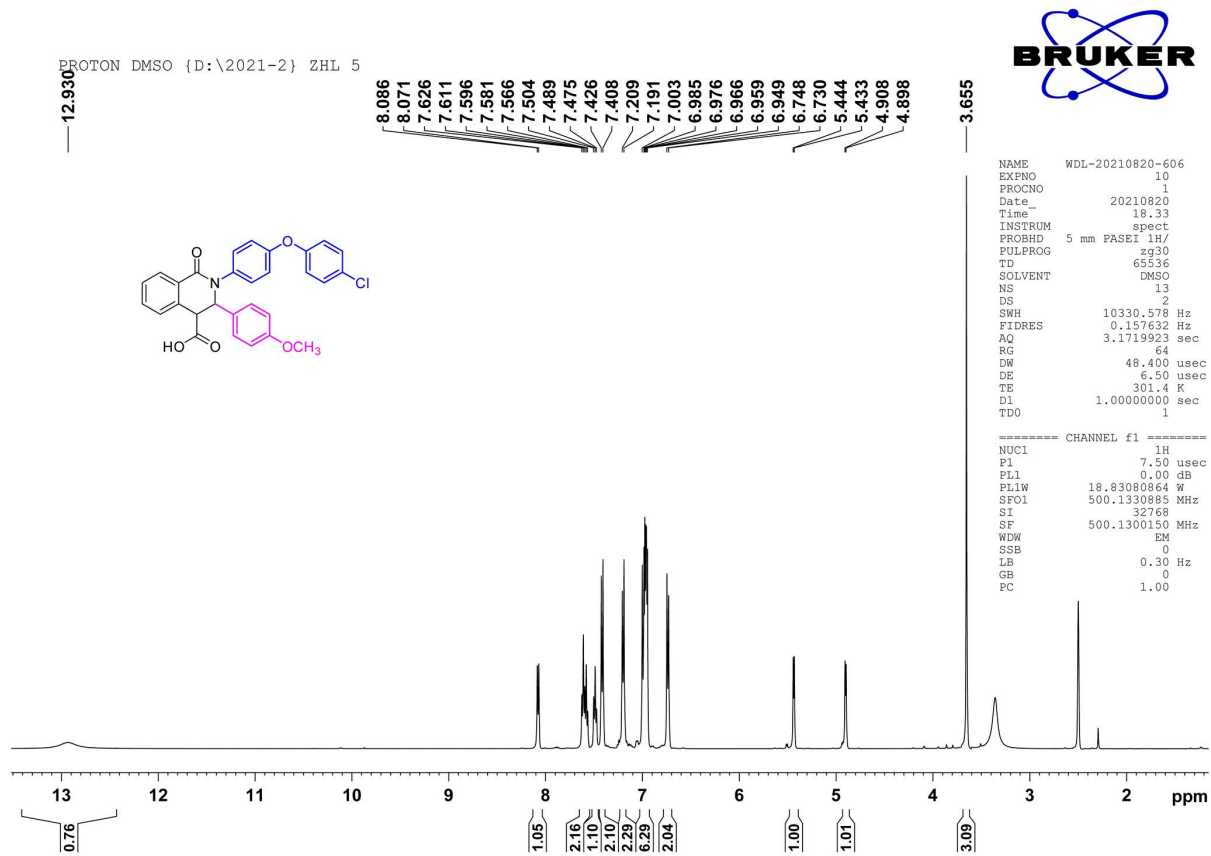


Figure S83. The ^1H NMR spectrum of compound II5

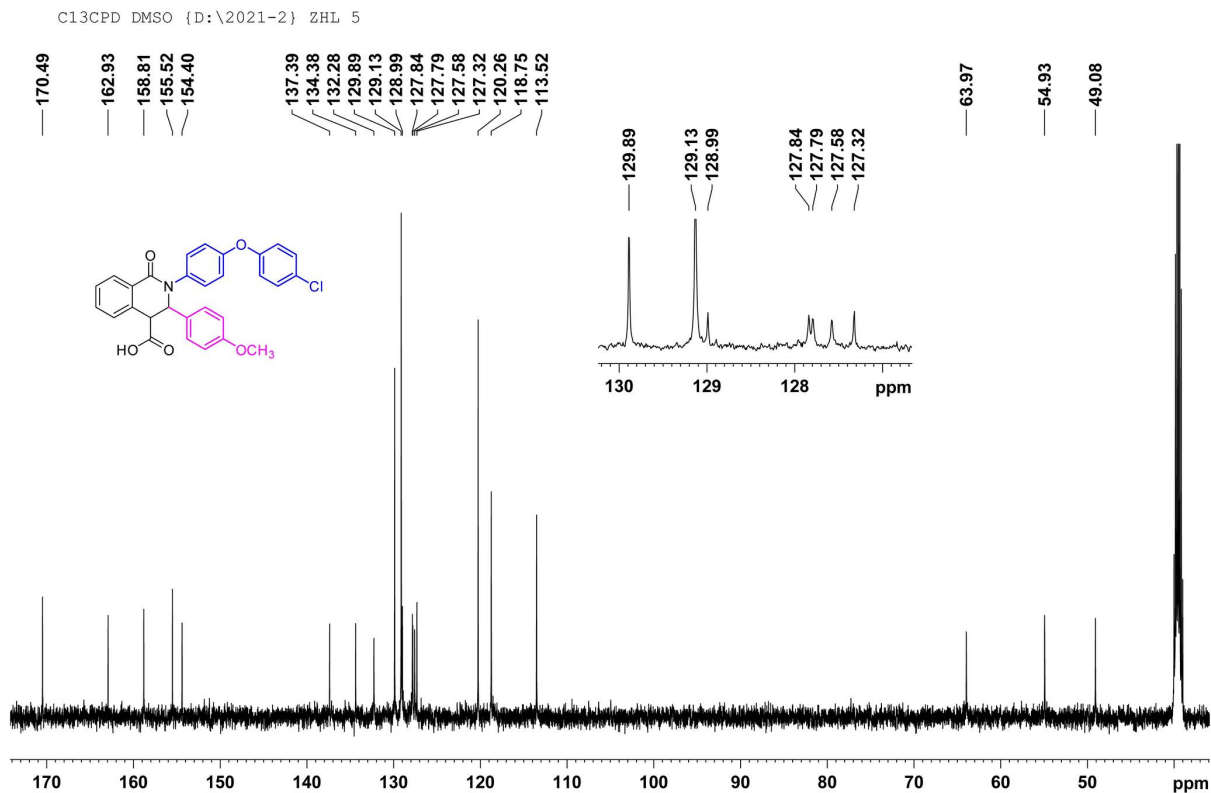


Figure S84. The ^{13}C NMR spectrum of compound II5

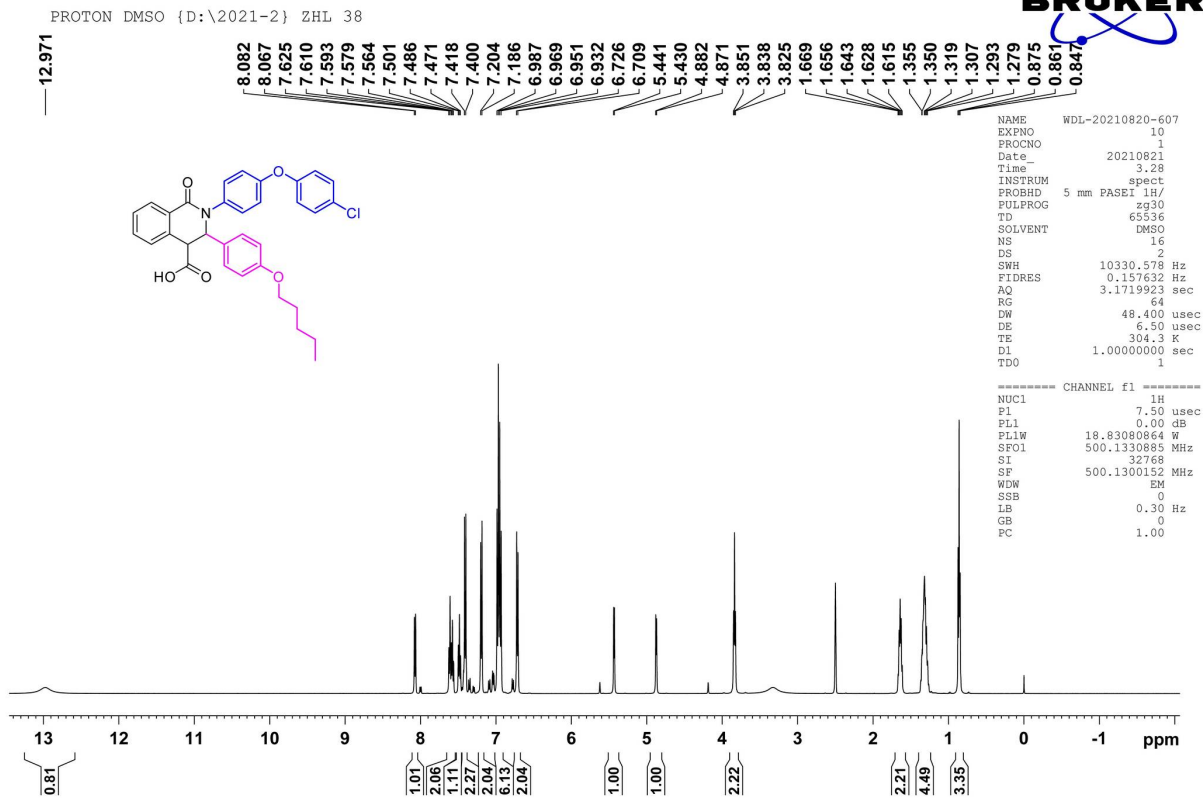


Figure S85. The ^1H NMR spectrum of compound II6

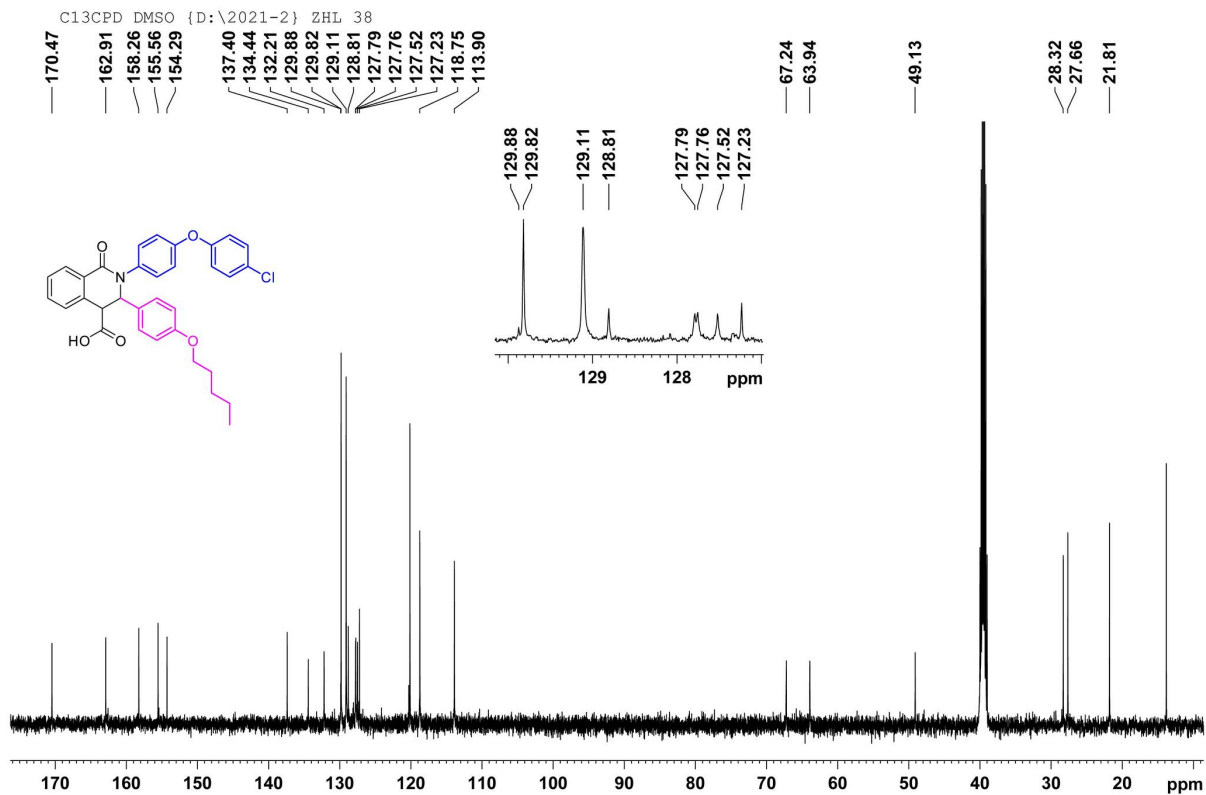


Figure S86. The ^{13}C NMR spectrum of compound II6

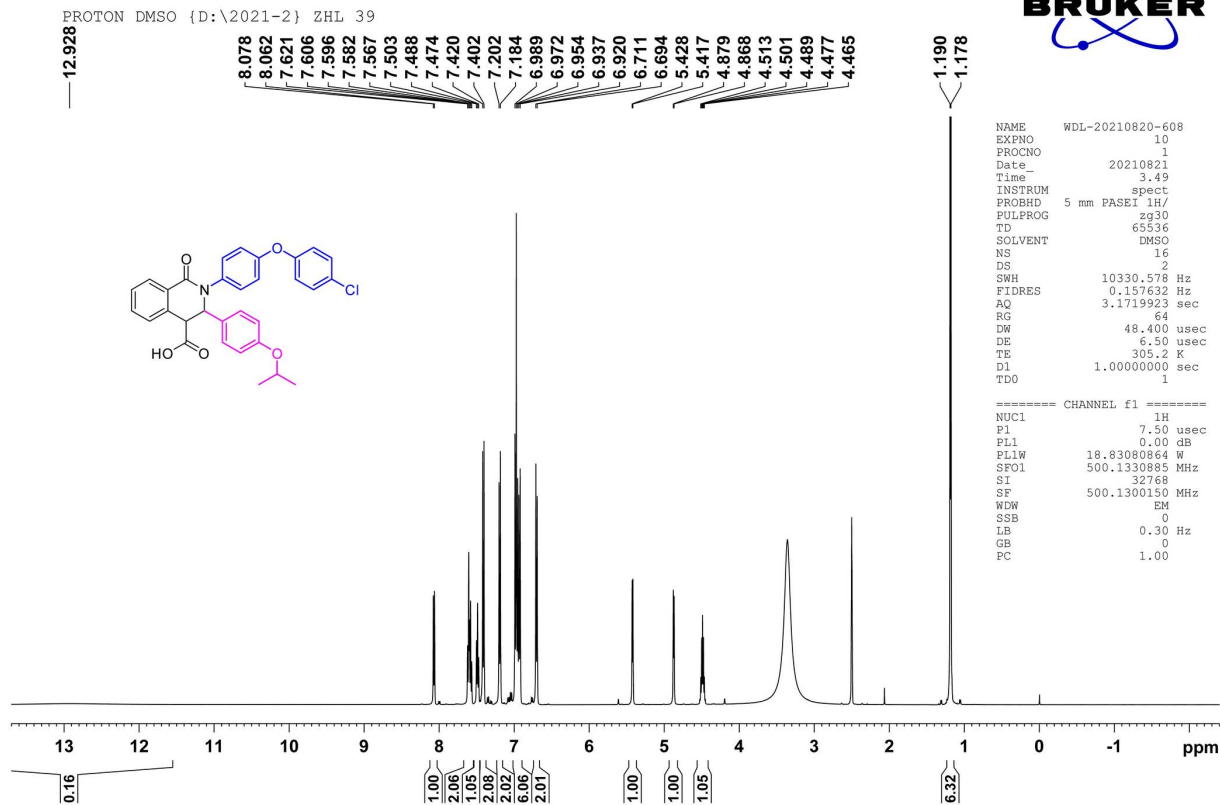


Figure S87. The ^1H NMR spectrum of compound II7

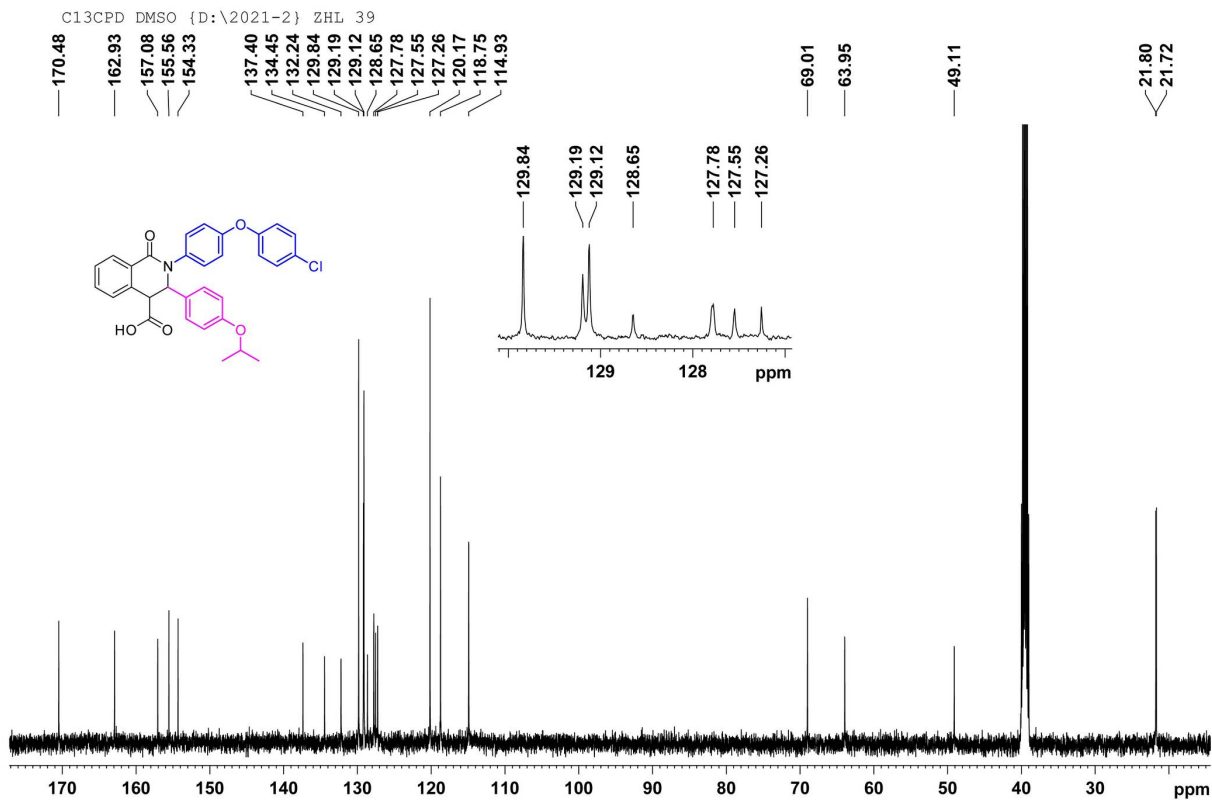


Figure S88. The ^{13}C NMR spectrum of compound II7

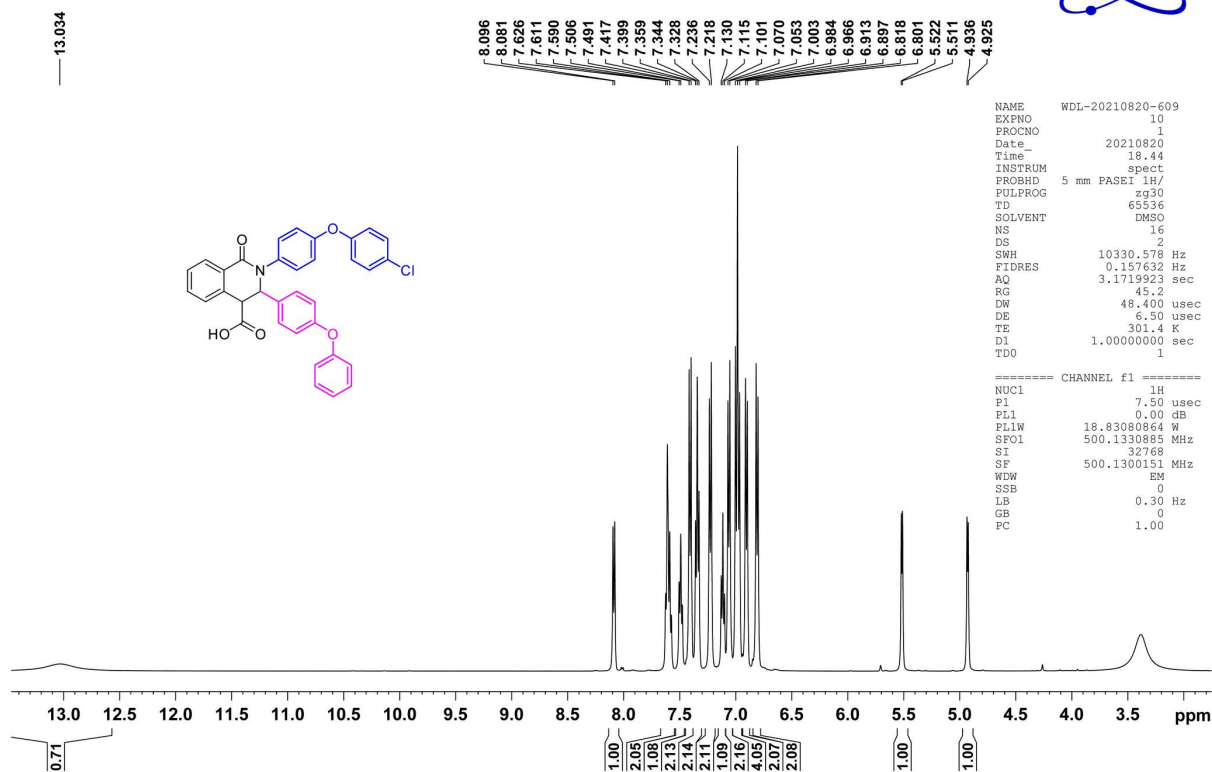


Figure S89. The ¹H NMR spectrum of compound II8

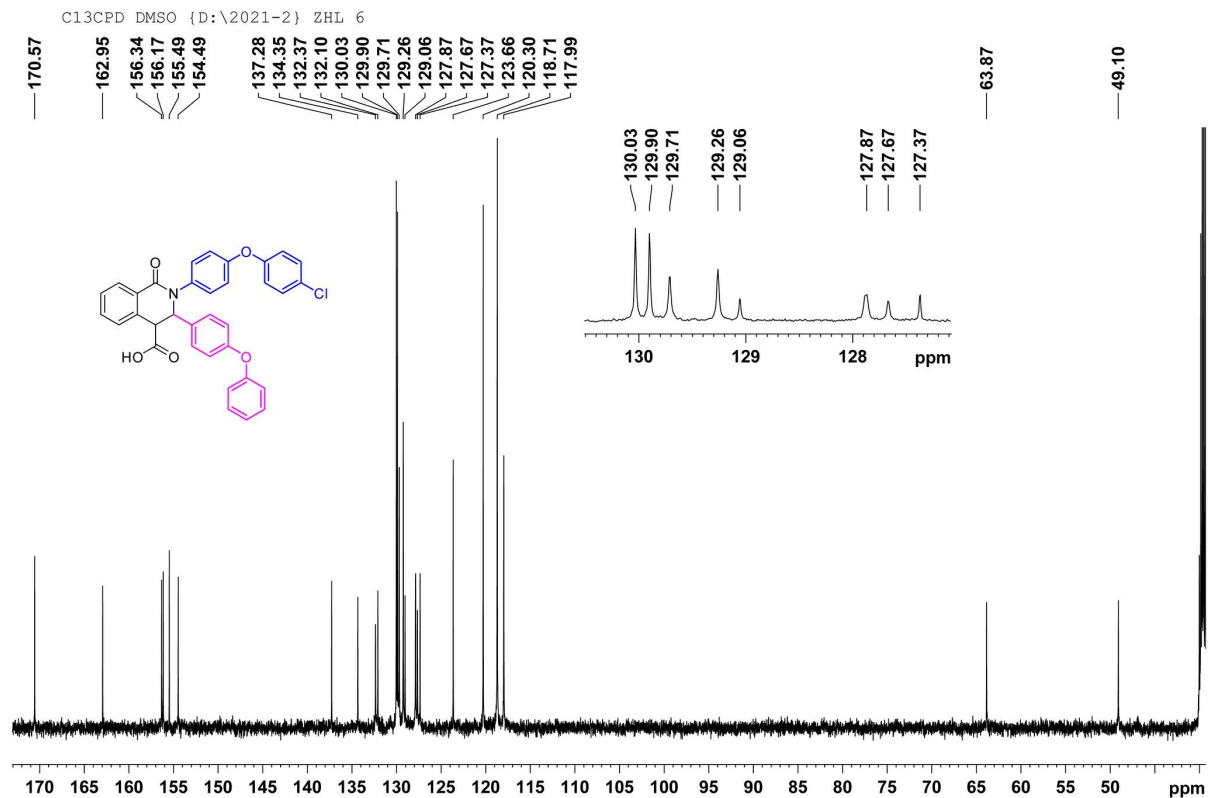


Figure S90. The ¹³C NMR spectrum of compound II8

PROTON DMSO {D:\2021-2} ZHL 41

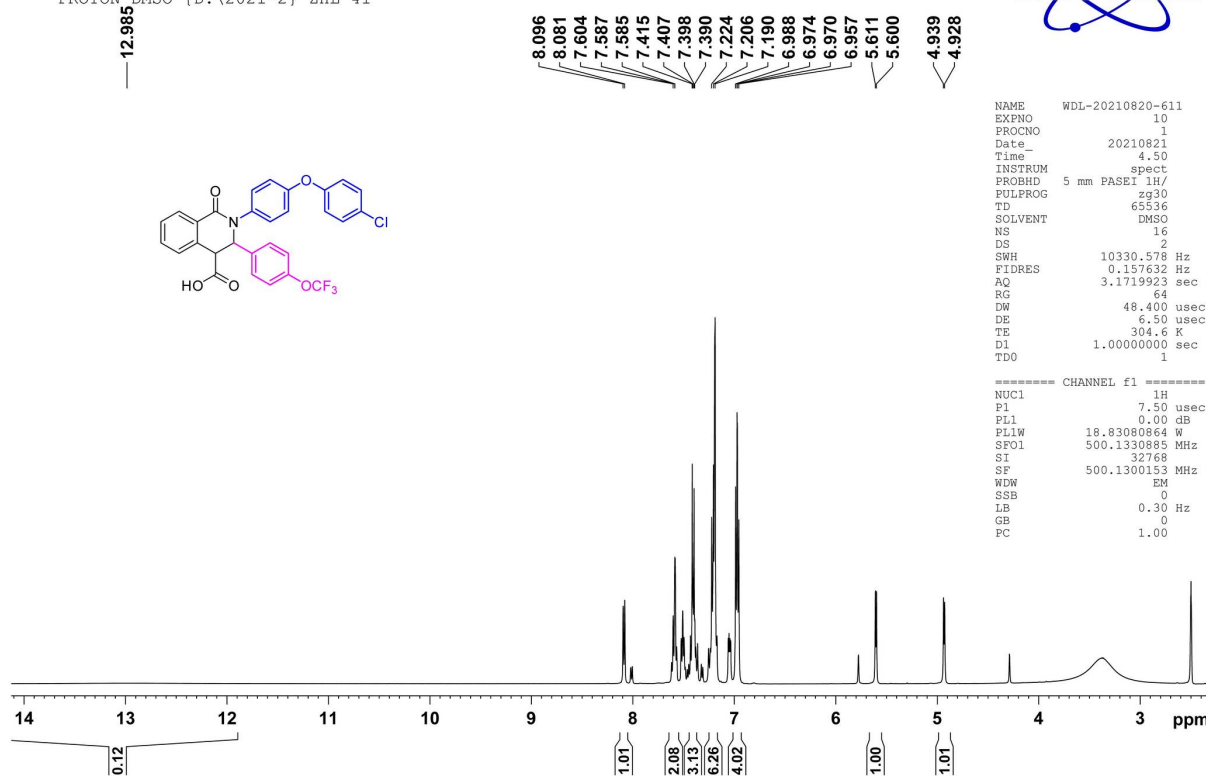


Figure S91. The ¹H NMR spectrum of compound II9

C13CPD DMSO {D:\2021-2} ZHL 41

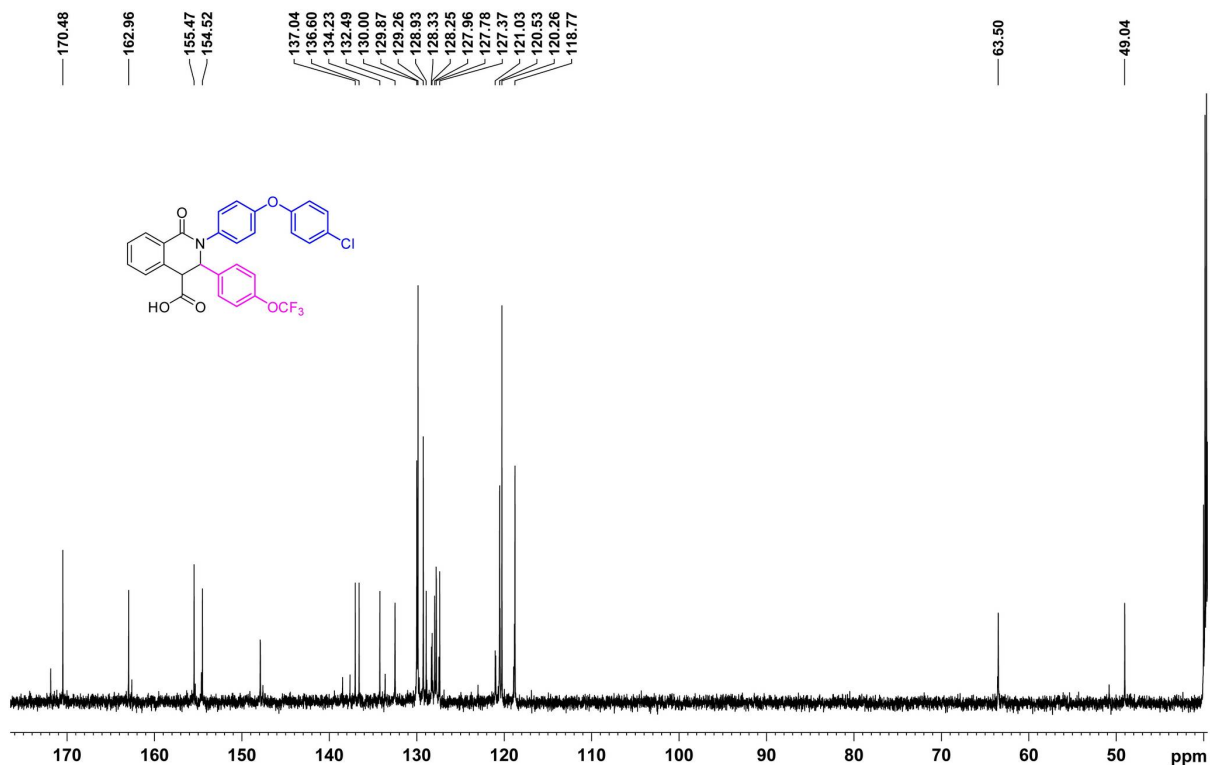


Figure S92. The ¹³C NMR spectrum of compound II9

PROTON DMSO {D:\2021-2} ZHL 7

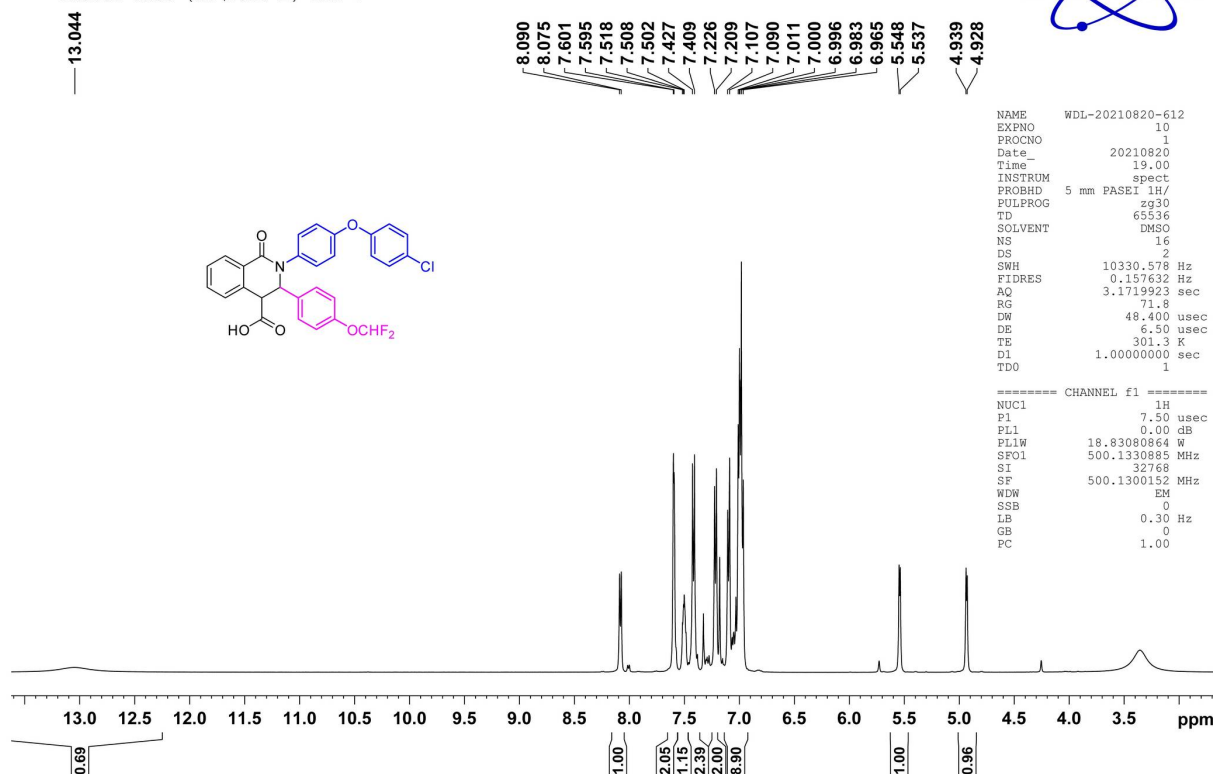


Figure S93. The ^1H NMR spectrum of compound III10

C13CPD DMSO {D:\2021-2} ZHL 7

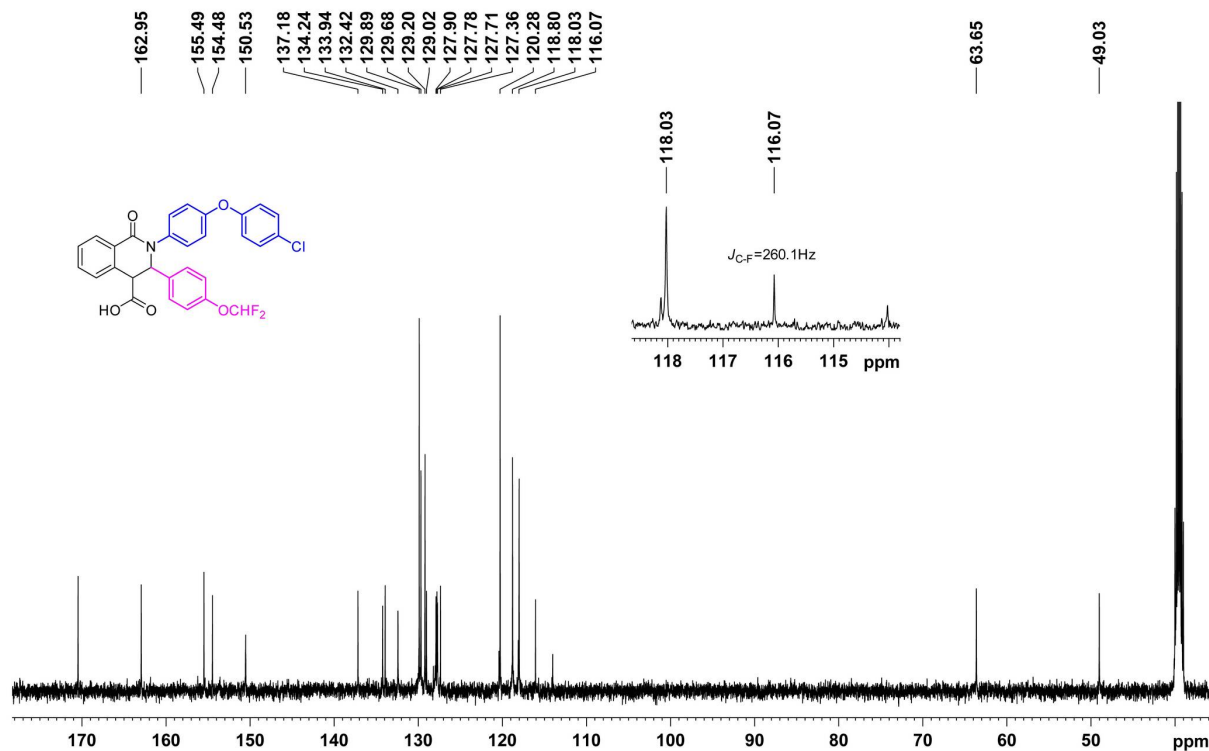


Figure S94. The ^{13}C NMR spectrum of compound III10

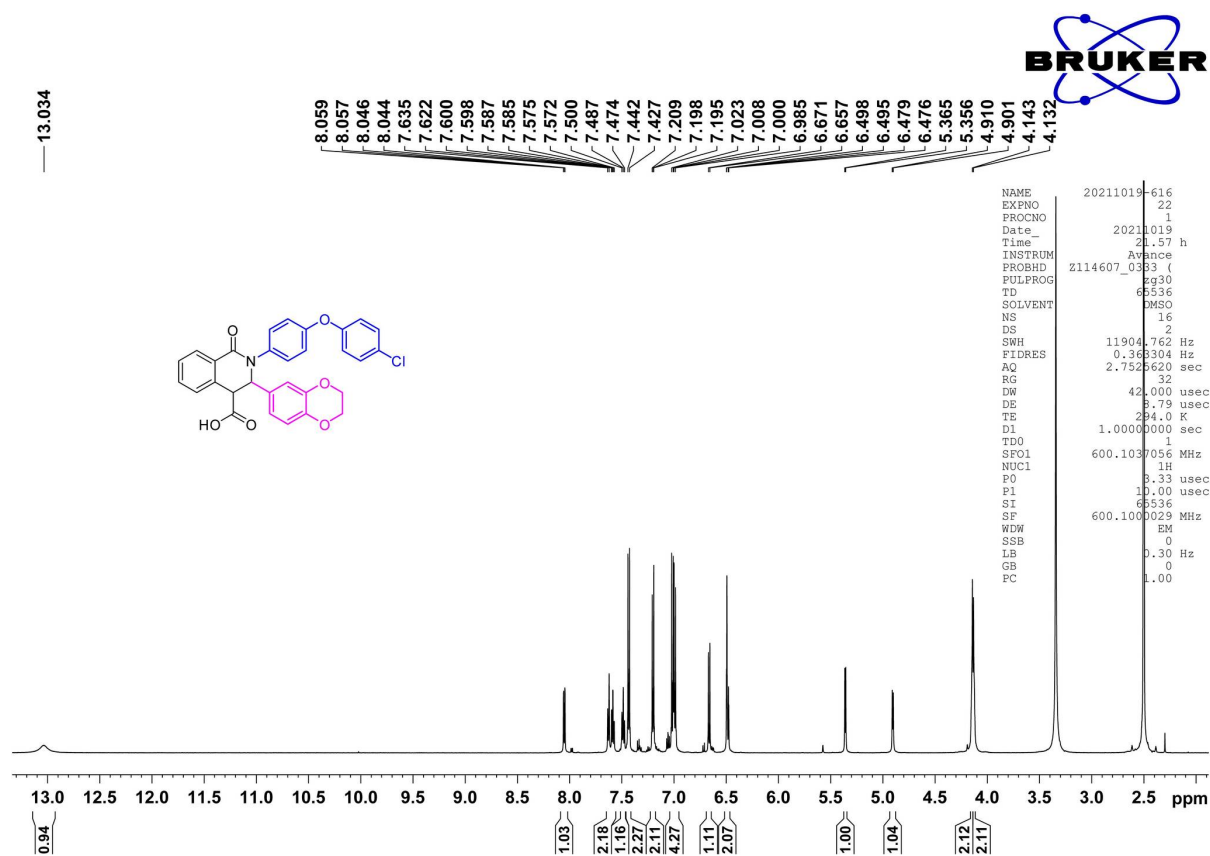


Figure S95. The ^1H NMR spectrum of compound III1

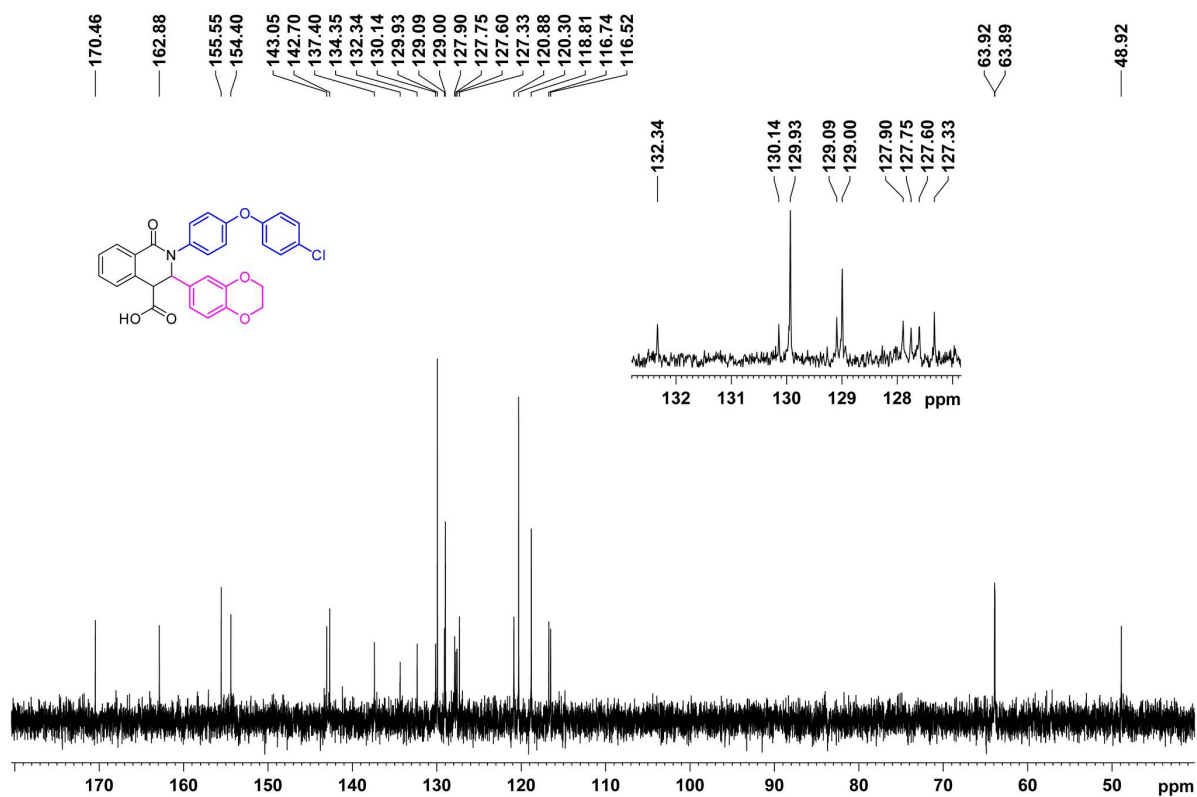


Figure S96. The ^{13}C NMR spectrum of compound III1

PROTON DMSO {D:\2021-2} ZHL 8

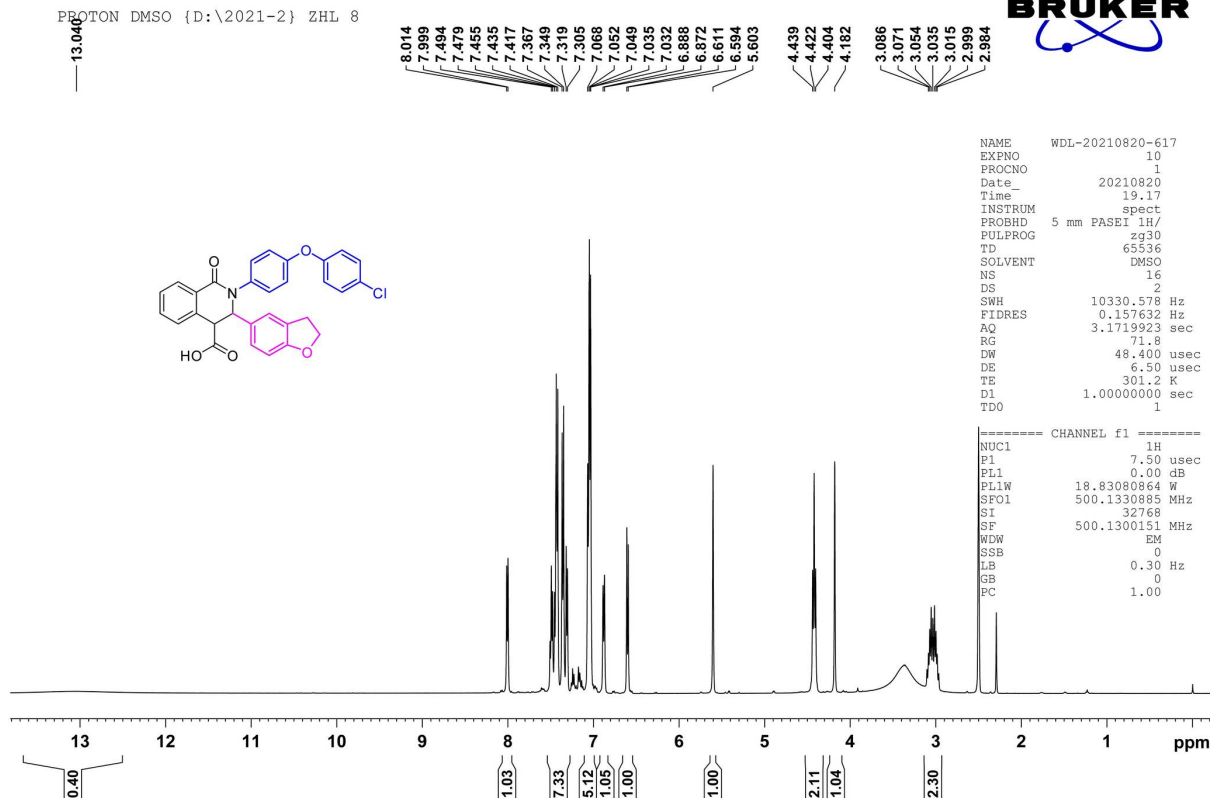


Figure S97. The ^1H NMR spectrum of compound III2

C13CPD DMSO {D:\2021-2} ZHL 8

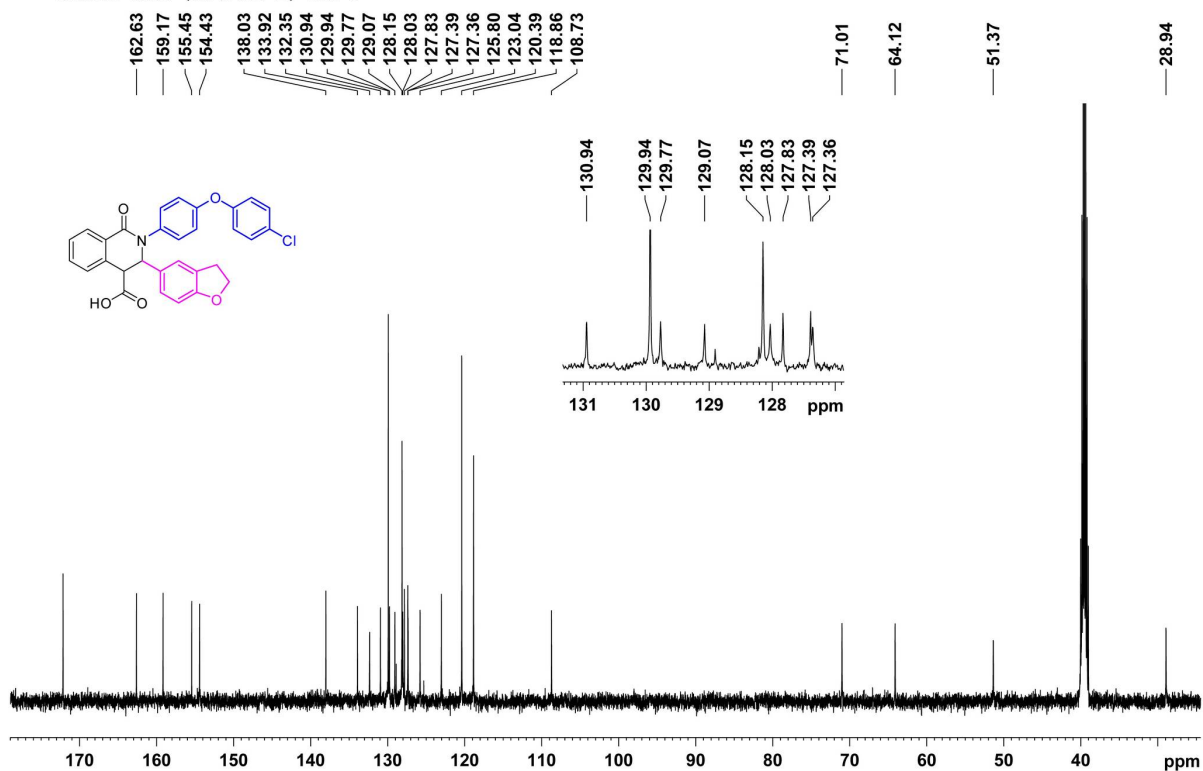


Figure S98. The ^{13}C NMR spectrum of compound III2

PROTON DMSO {D:\2021-2} ZHL 9

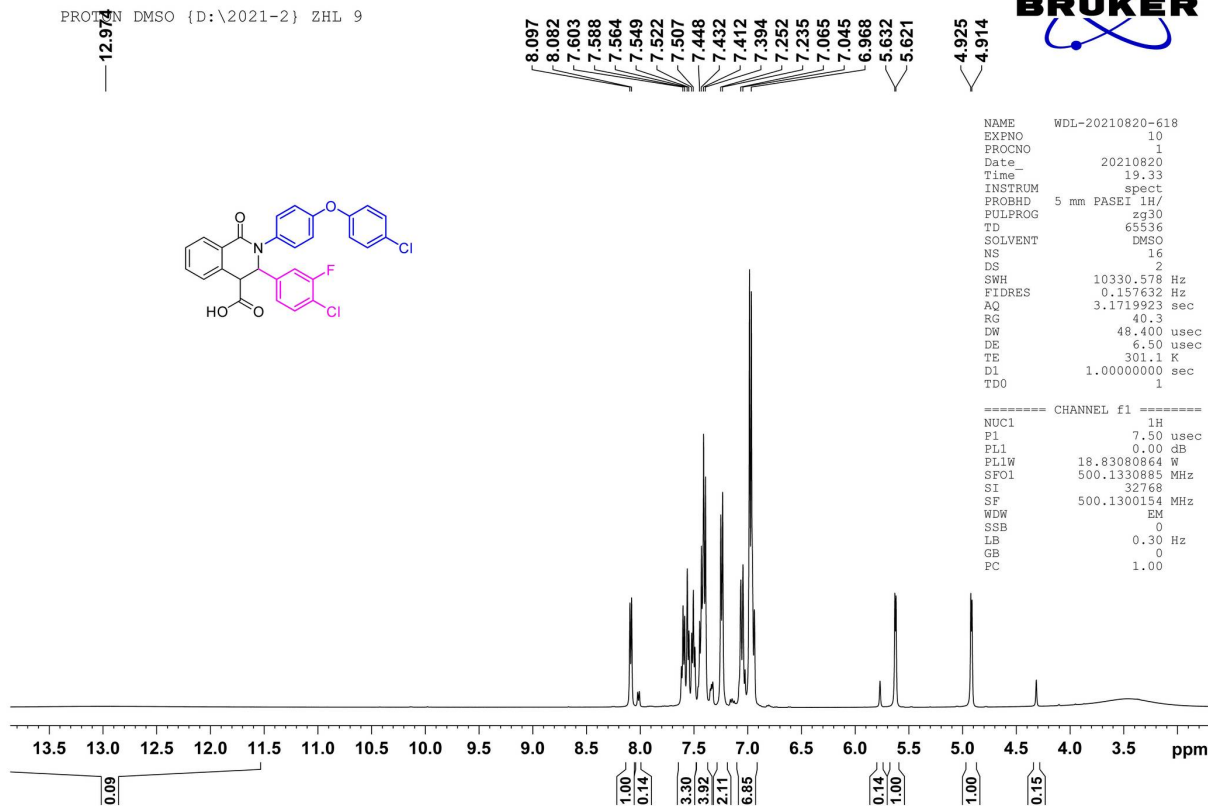


Figure S99. The ¹H NMR spectrum of compound III3

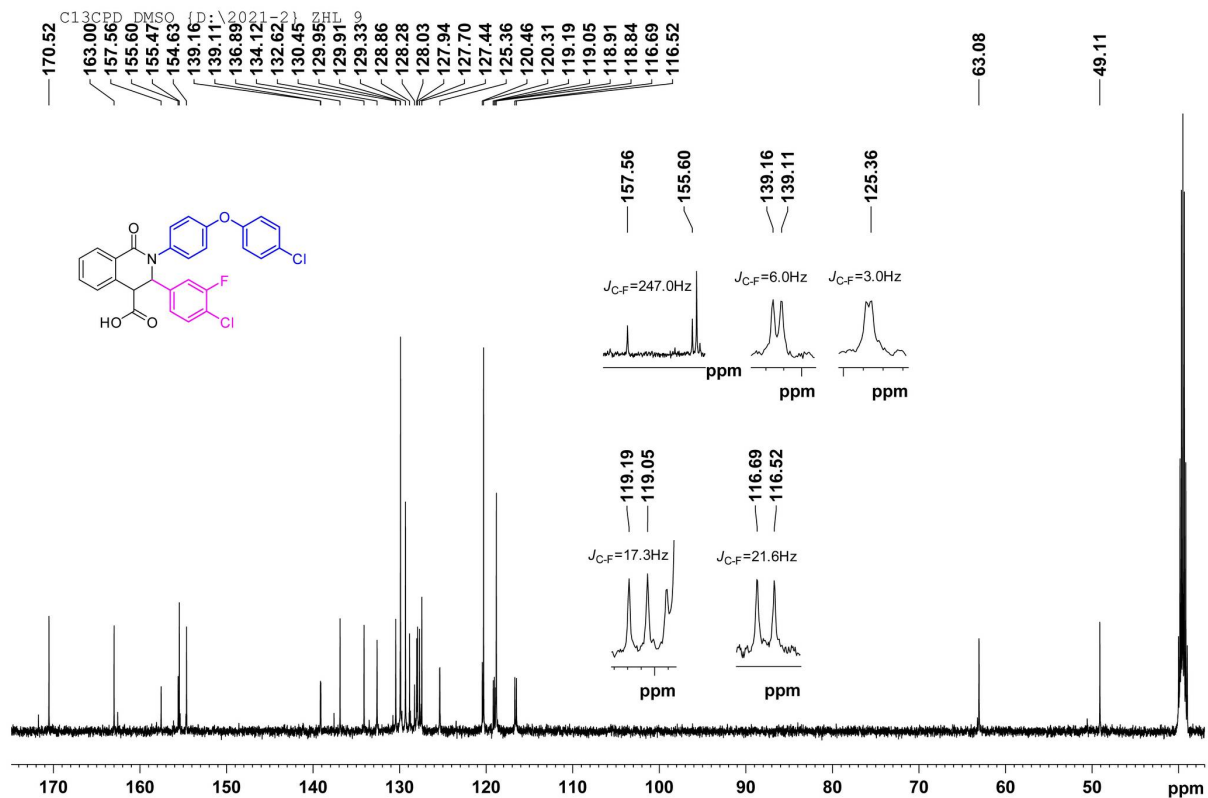


Figure S100. The ¹³C NMR spectrum of compound III3

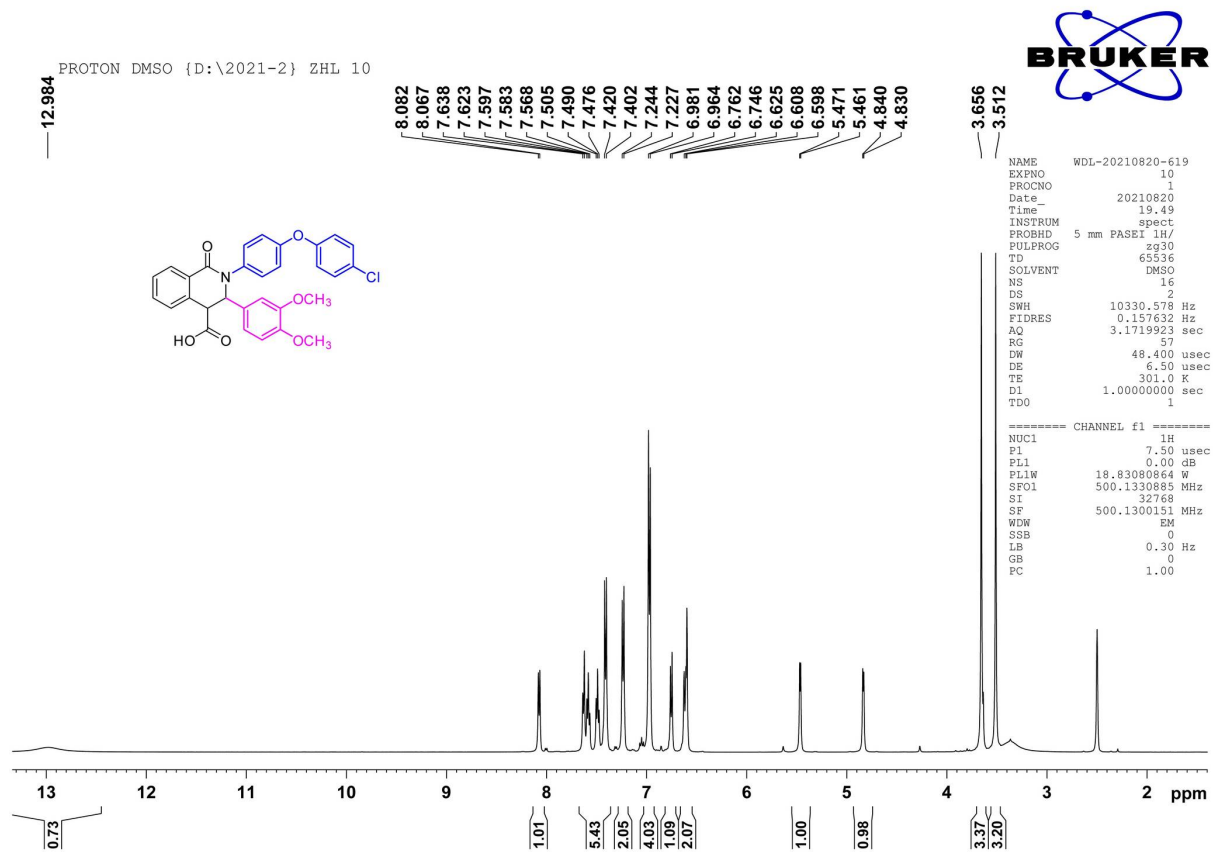


Figure S101. The ^1H NMR spectrum of compound II14

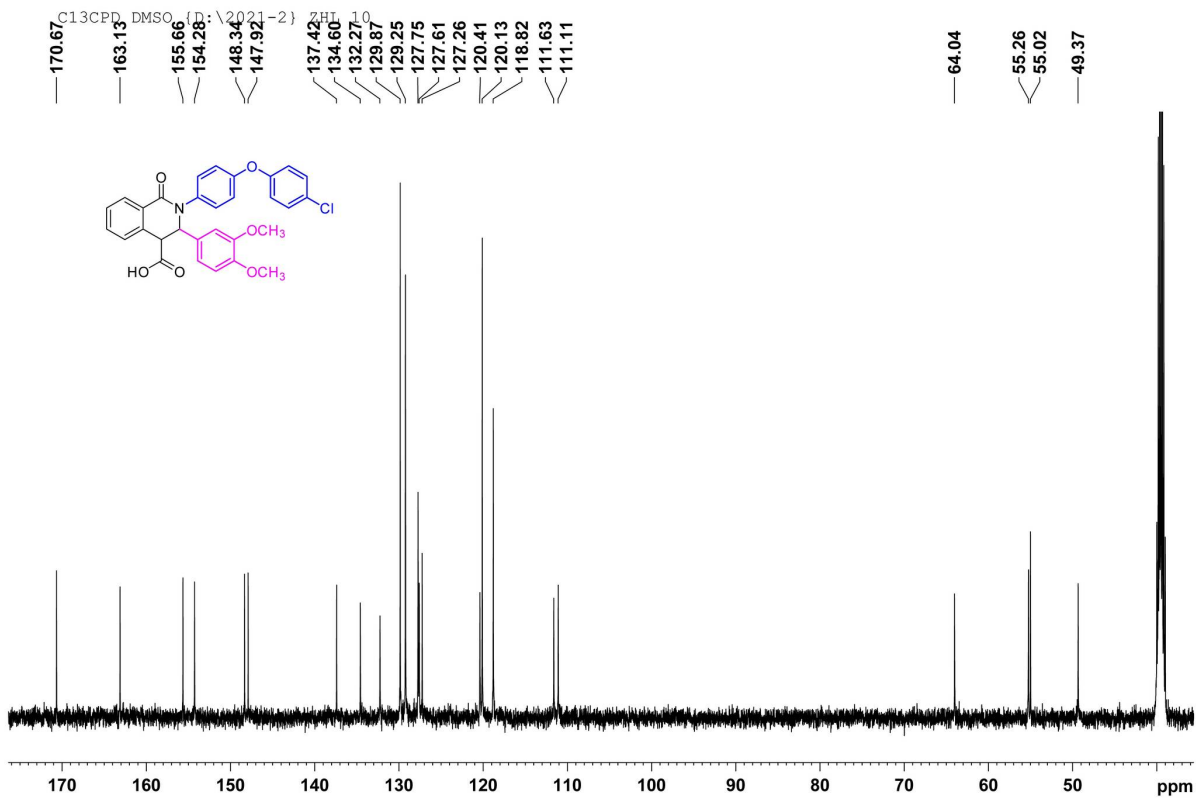


Figure S102. The ^{13}C NMR spectrum of compound II14

PROTON DMSO {D:\2021-2} ZHL 11

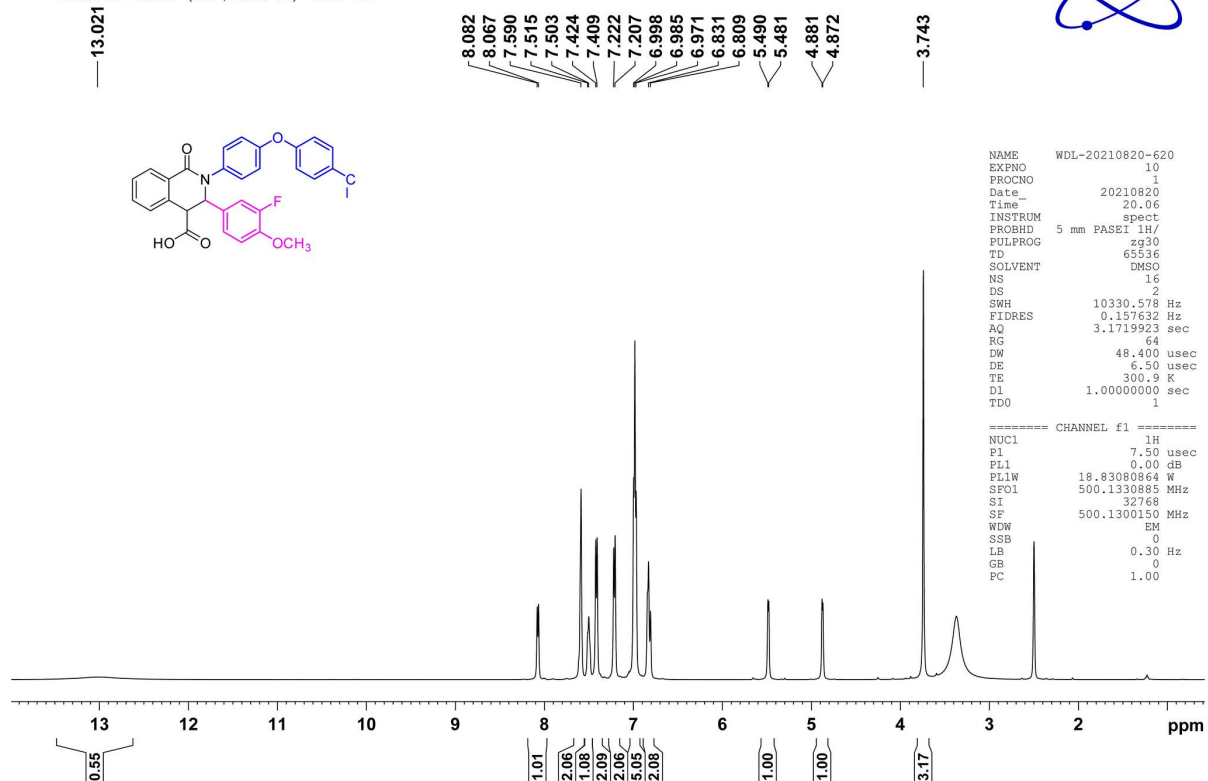


Figure S103. The ¹H NMR spectrum of compound II15

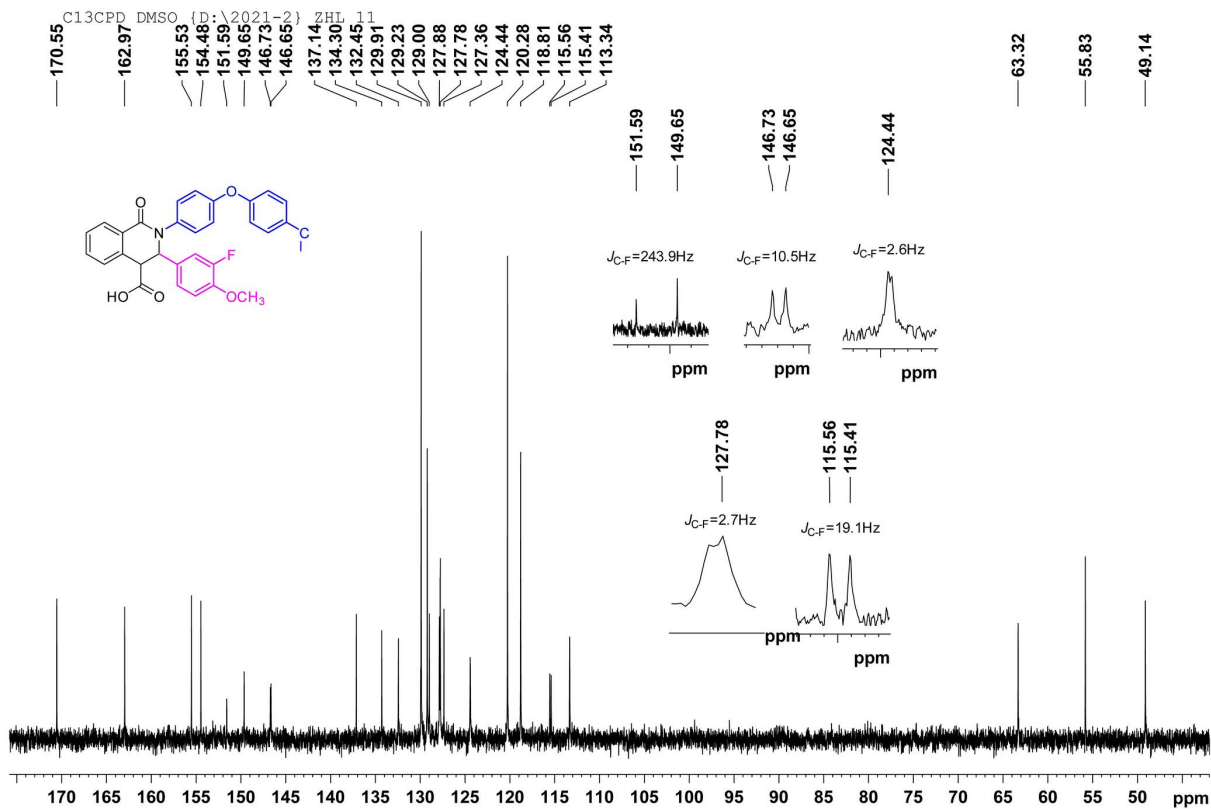


Figure S104. The ¹³C NMR spectrum of compound II15

PROTON DMSO {D:\2021-2} ZHL 12

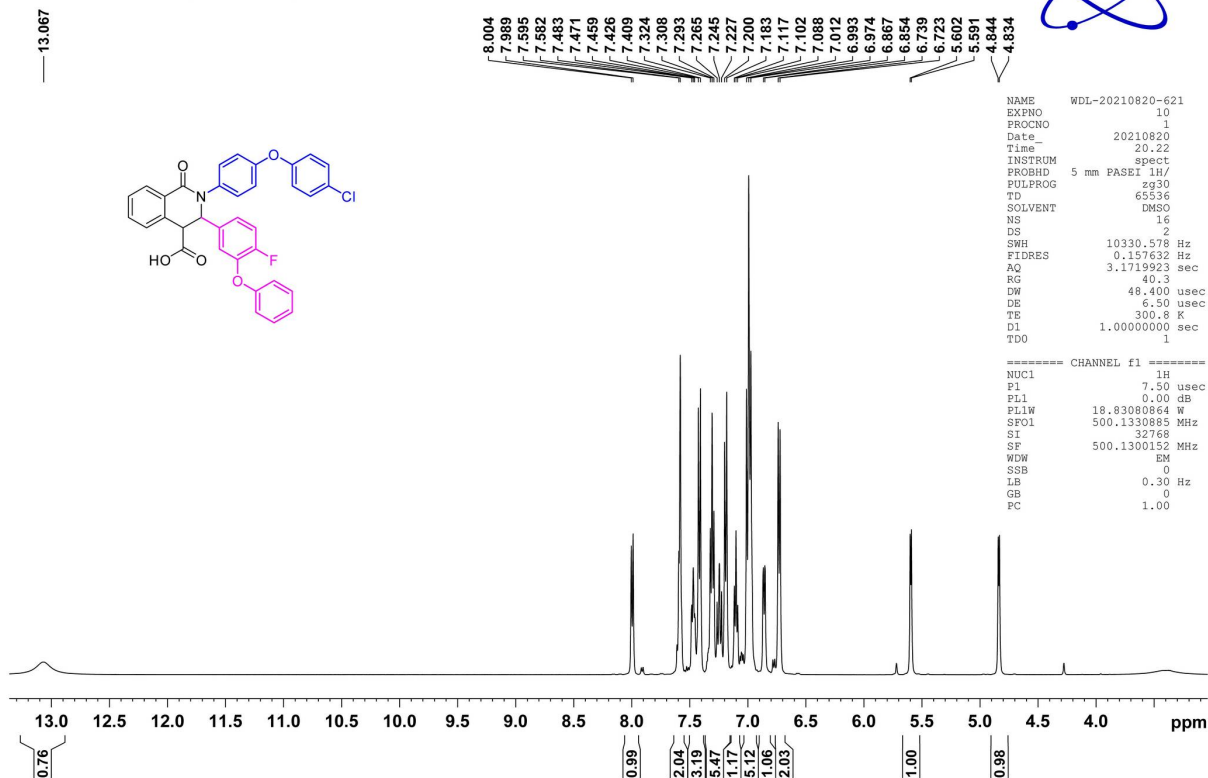


Figure S105. The ^1H NMR spectrum of compound II16

C13CPD DMSO {D:\2021-2} ZHL 12

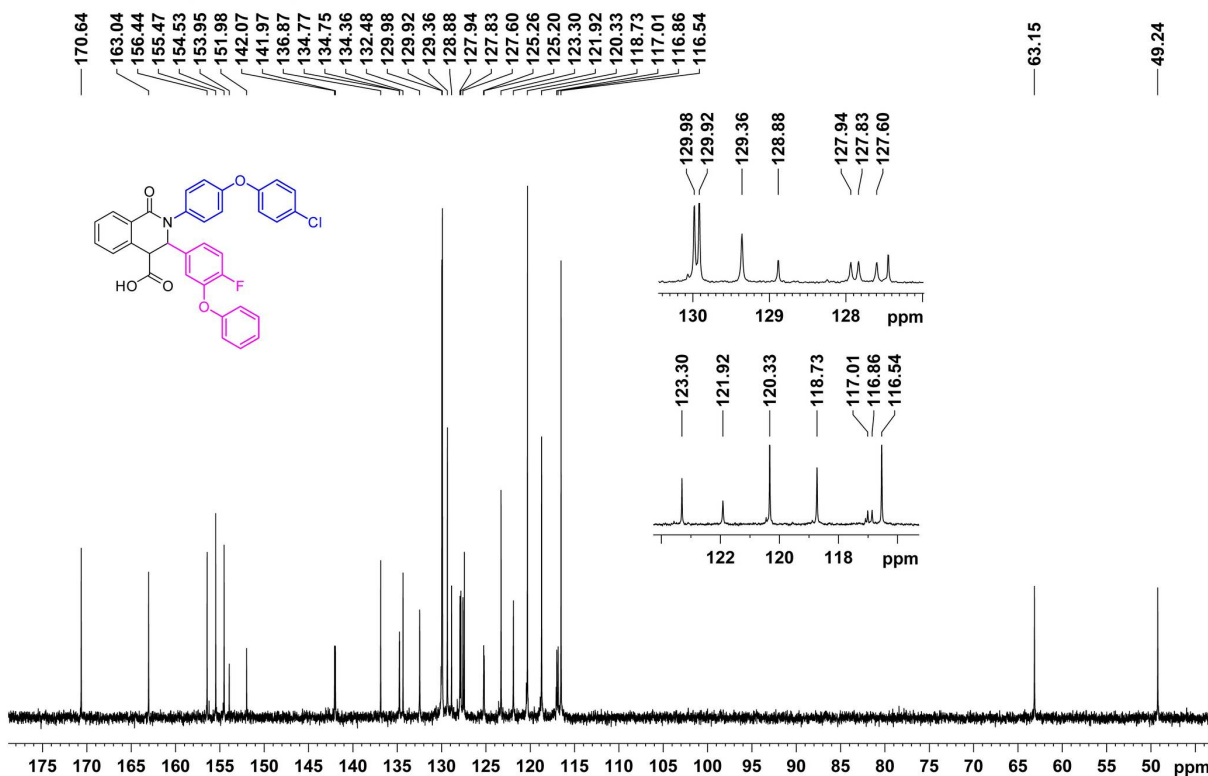


Figure S106. The ^{13}C NMR spectrum of compound II16

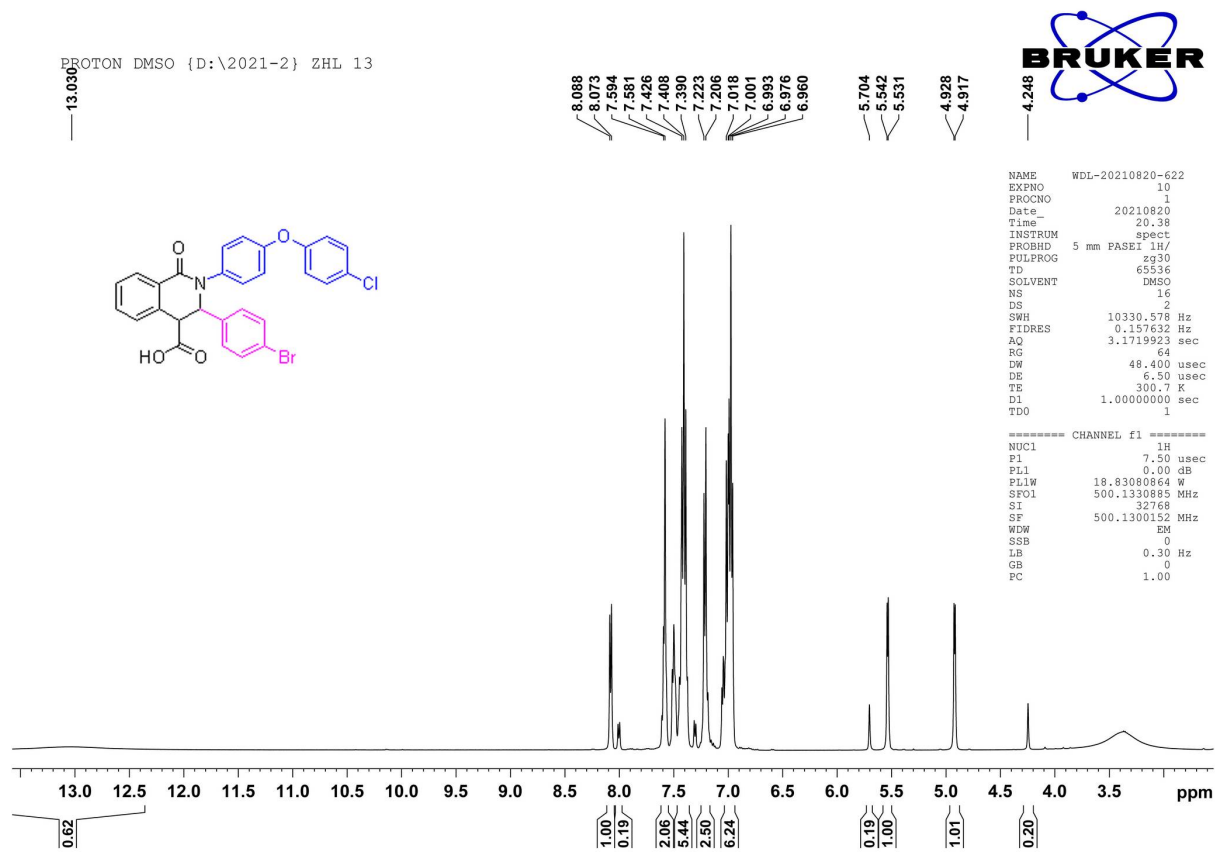


Figure S107. The ^1H NMR spectrum of compound II17

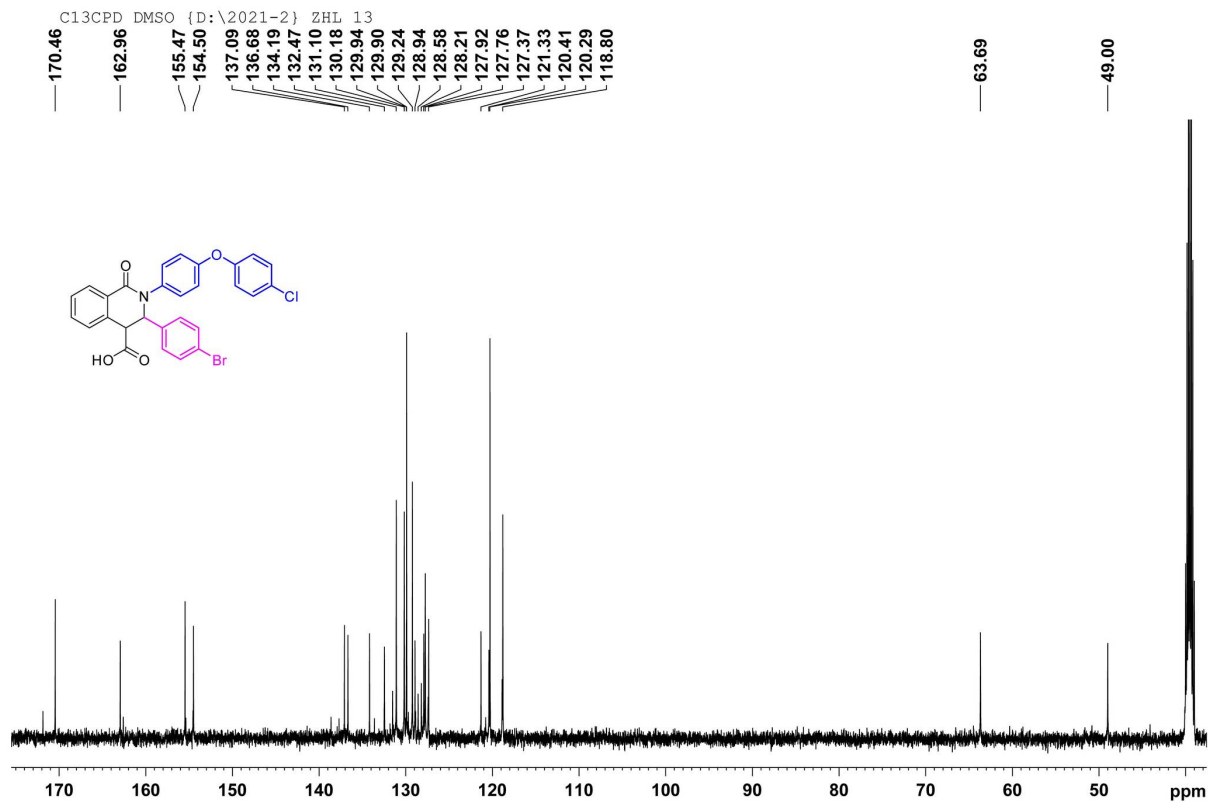


Figure S108. The ^{13}C NMR spectrum of compound II17

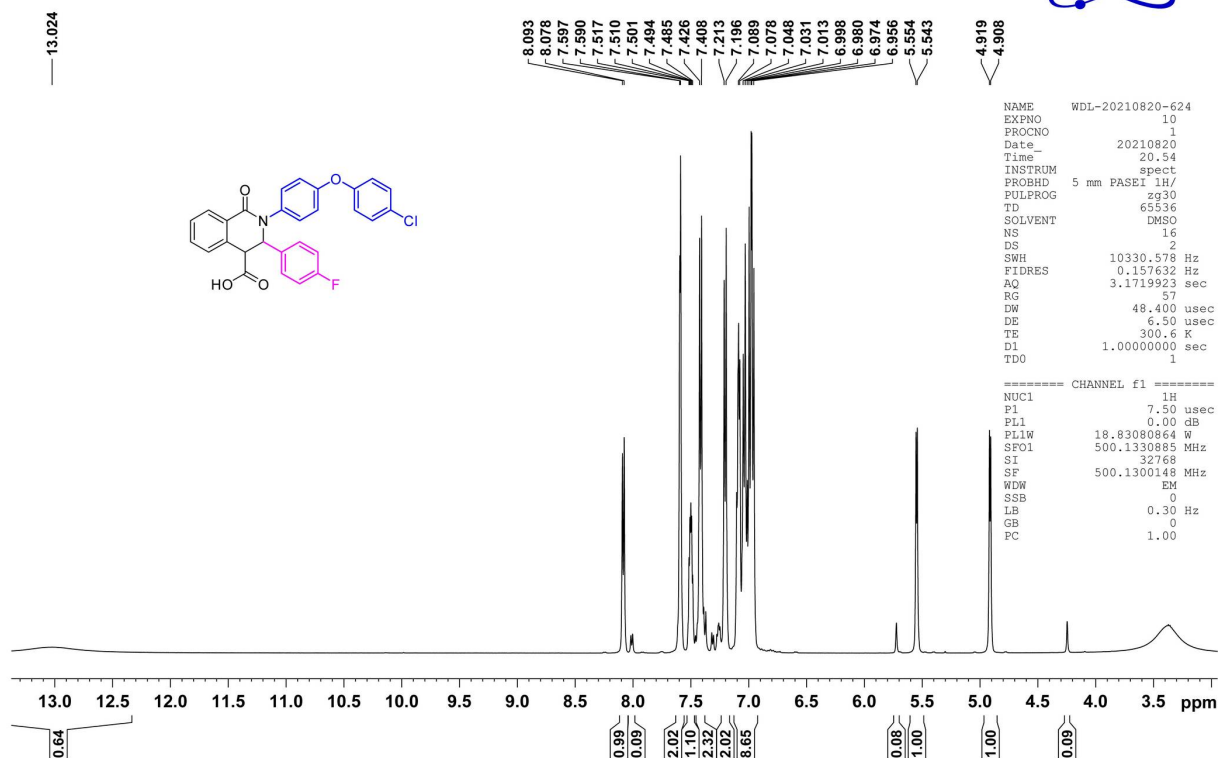


Figure S109. The ¹H NMR spectrum of compound II18

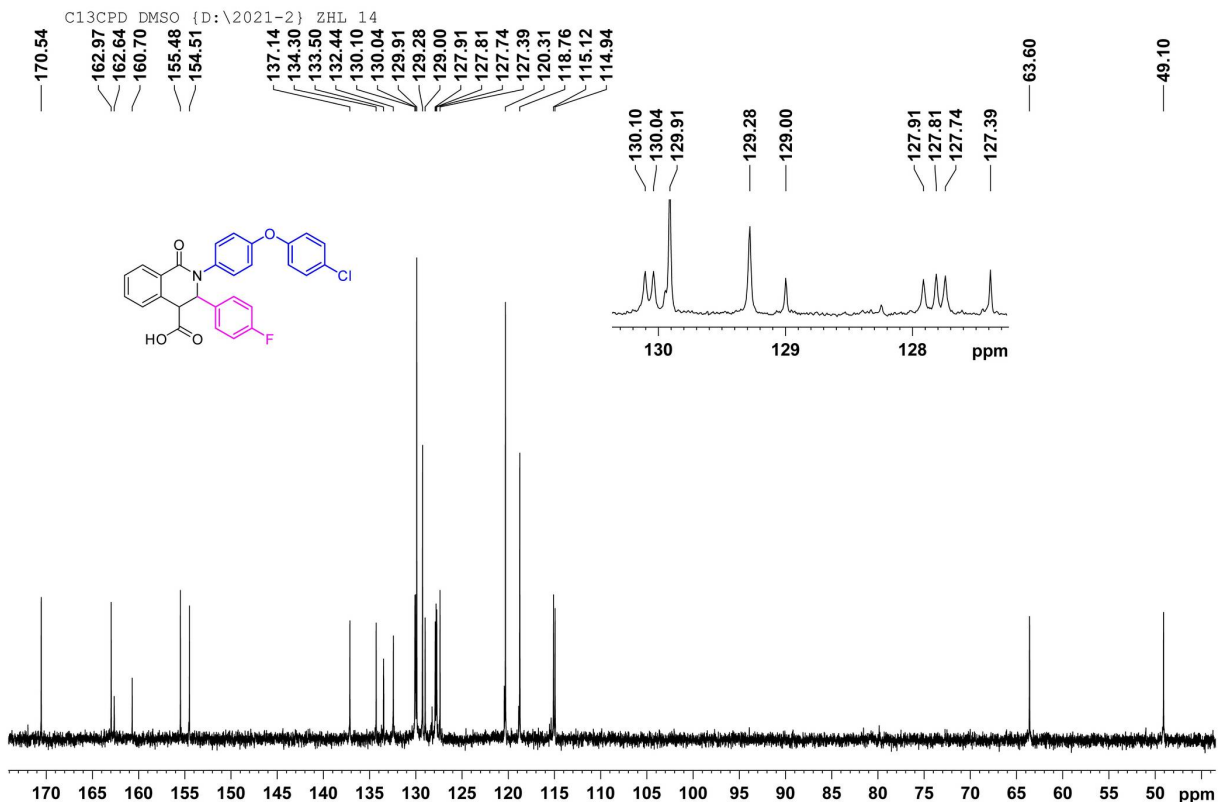


Figure S110. The ¹³C NMR spectrum of compound II18

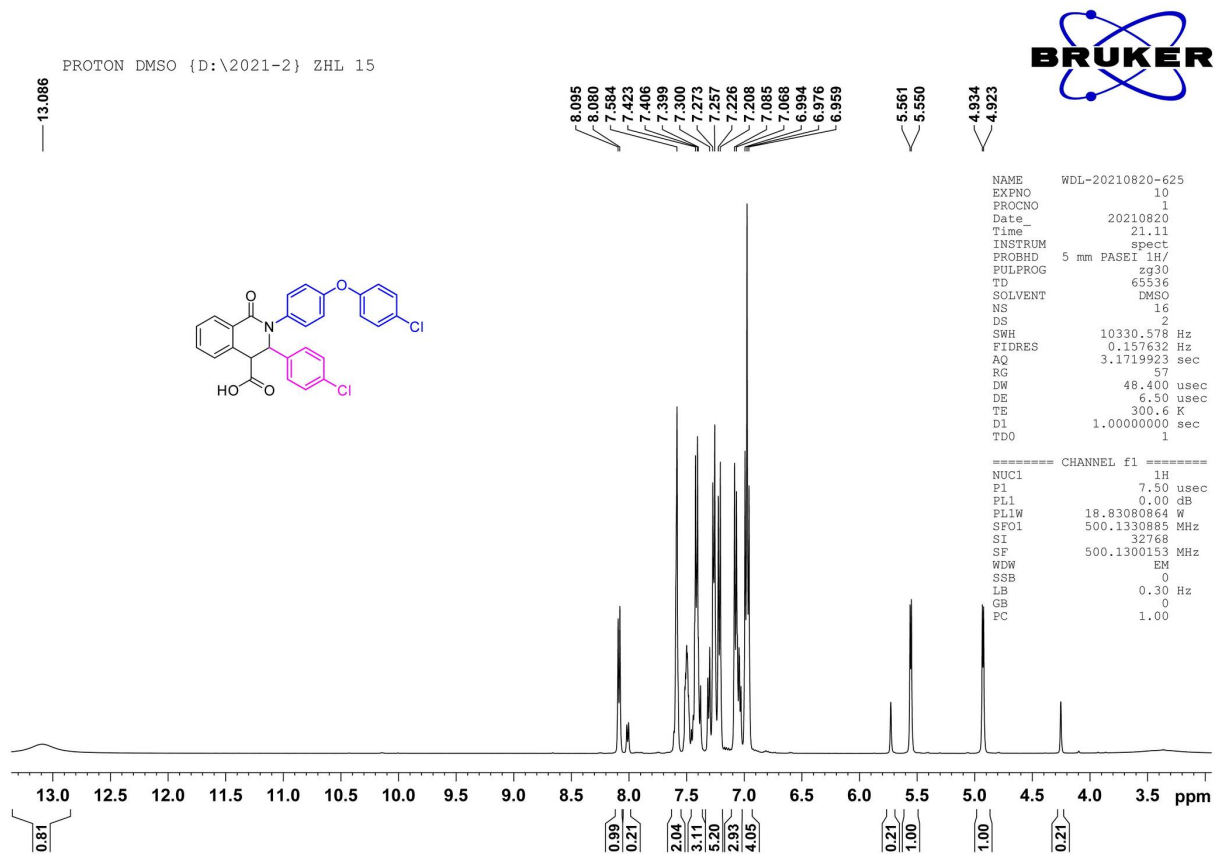


Figure S111. The ^1H NMR spectrum of compound II19

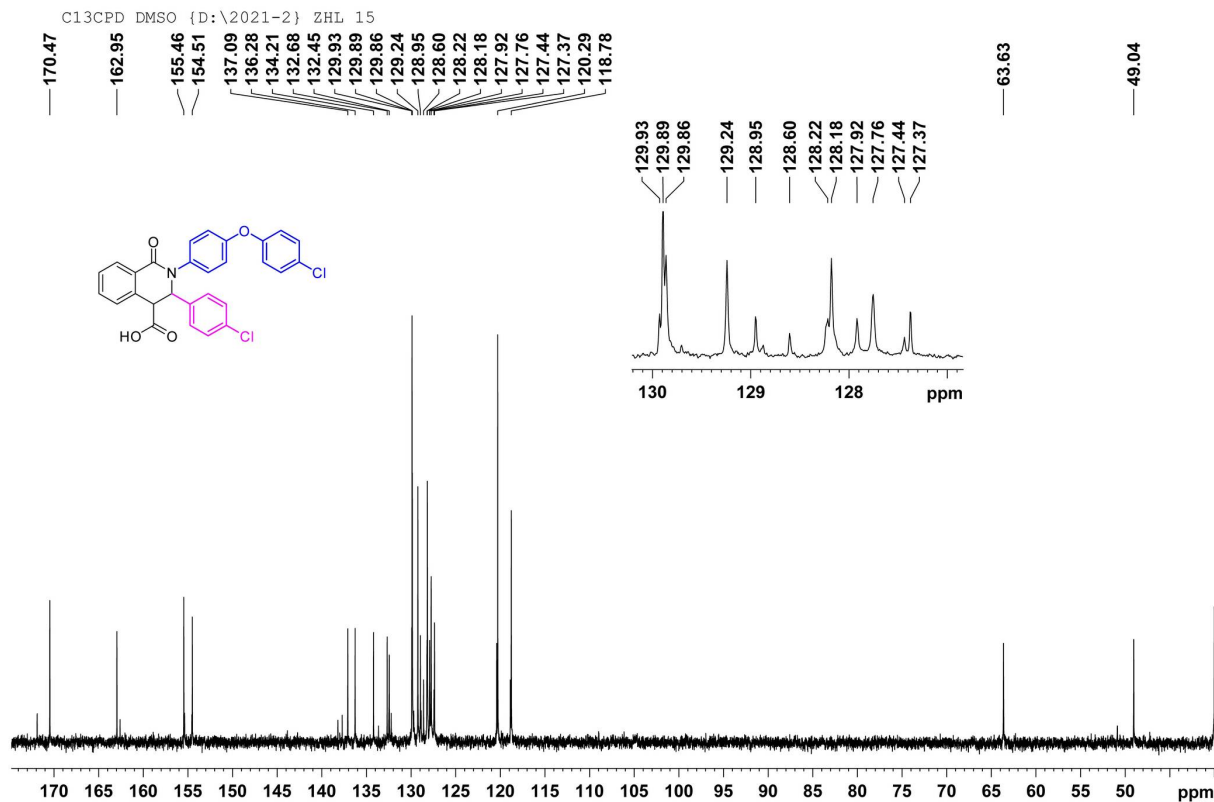


Figure S112. The ^{13}C NMR spectrum of compound II19

PROTON DMSO {D:\2021-2} ZHL 16

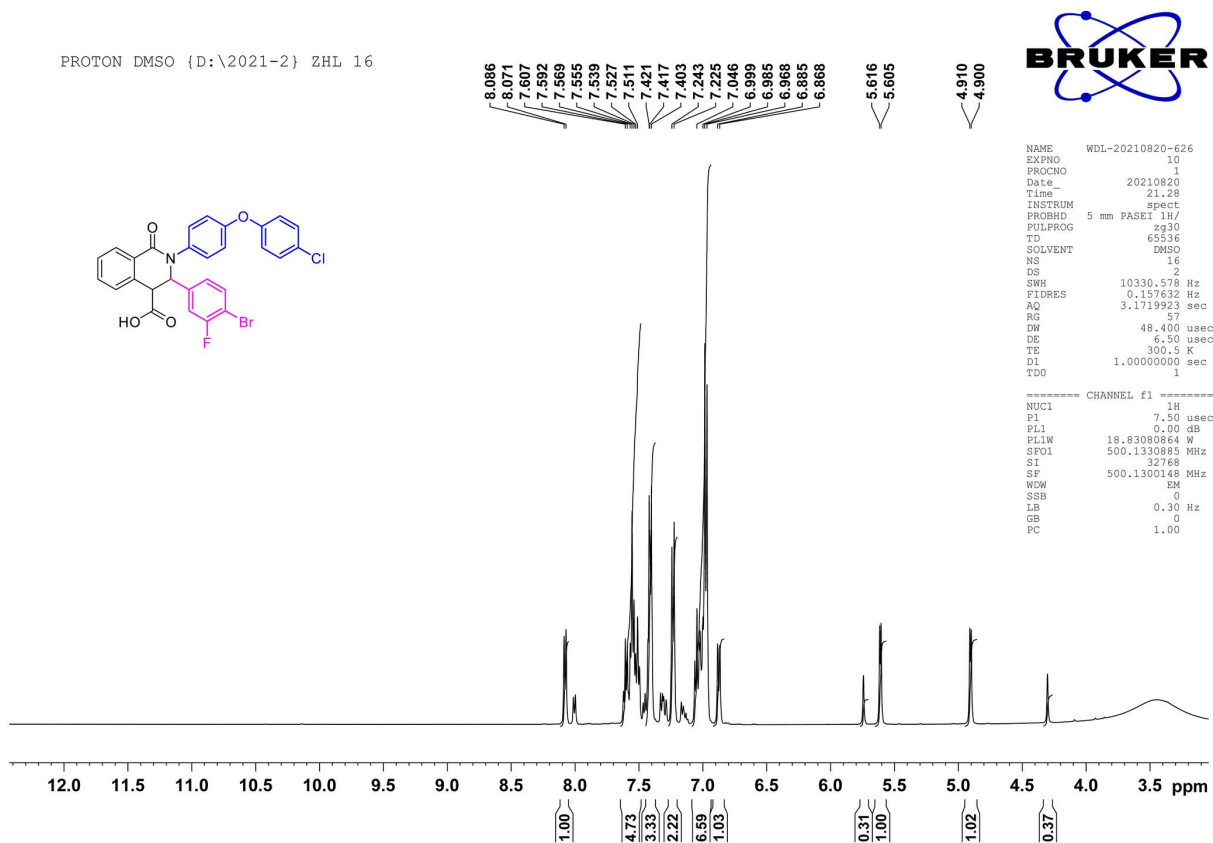


Figure S113. The ¹H NMR spectrum of compound II20

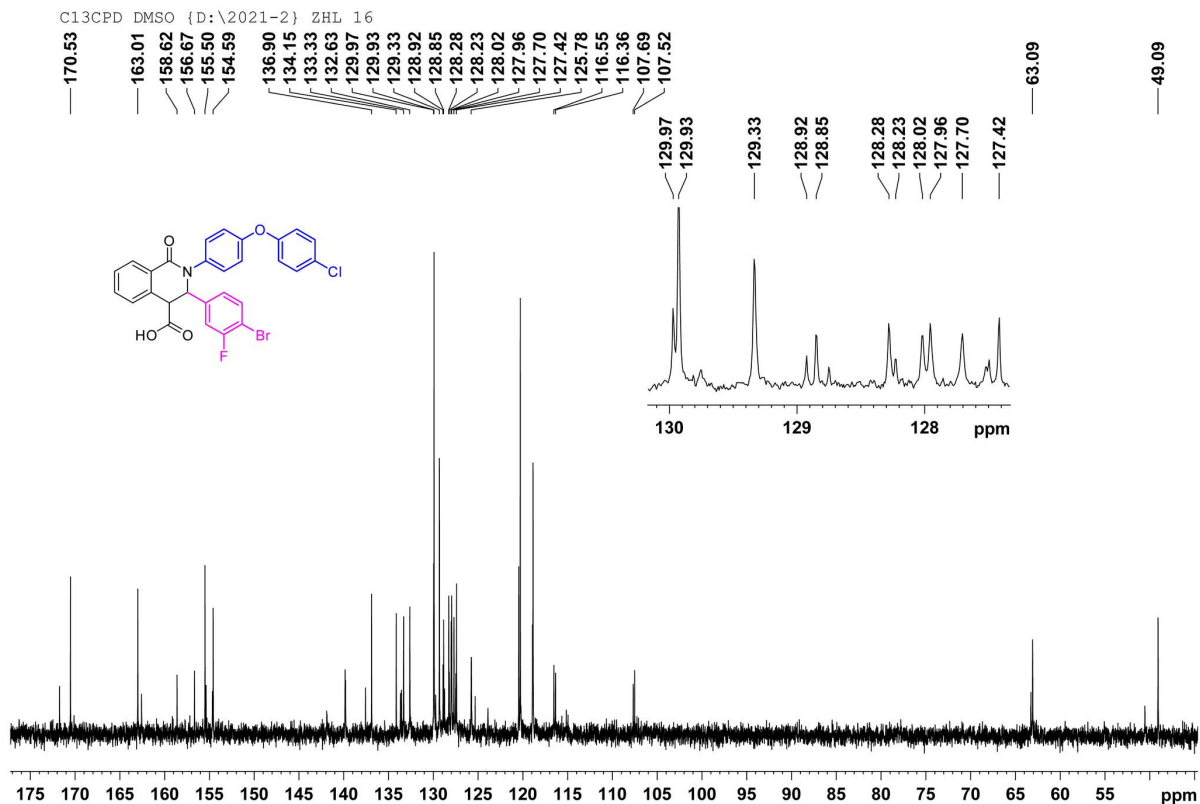


Figure S114. The ¹³C NMR spectrum of compound II20

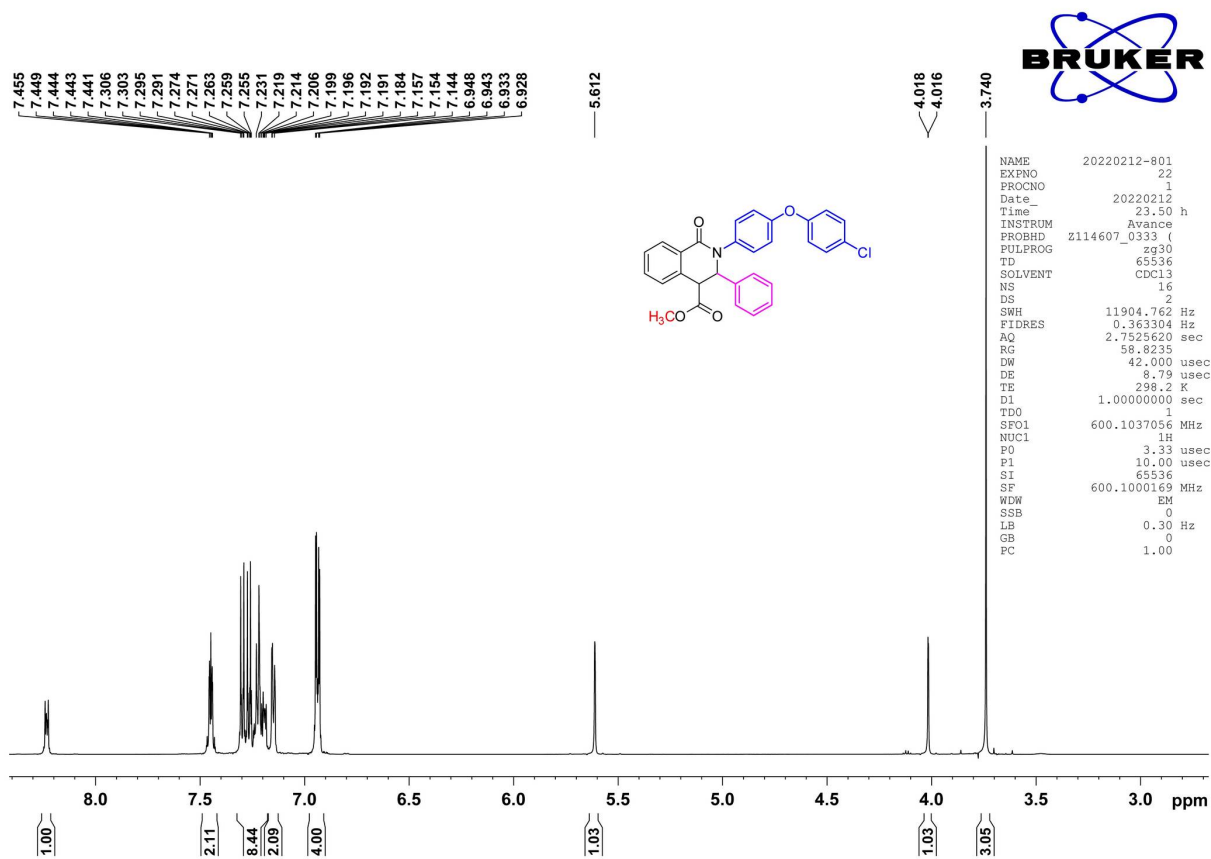


Figure S115. The ^1H NMR spectrum of compound III1

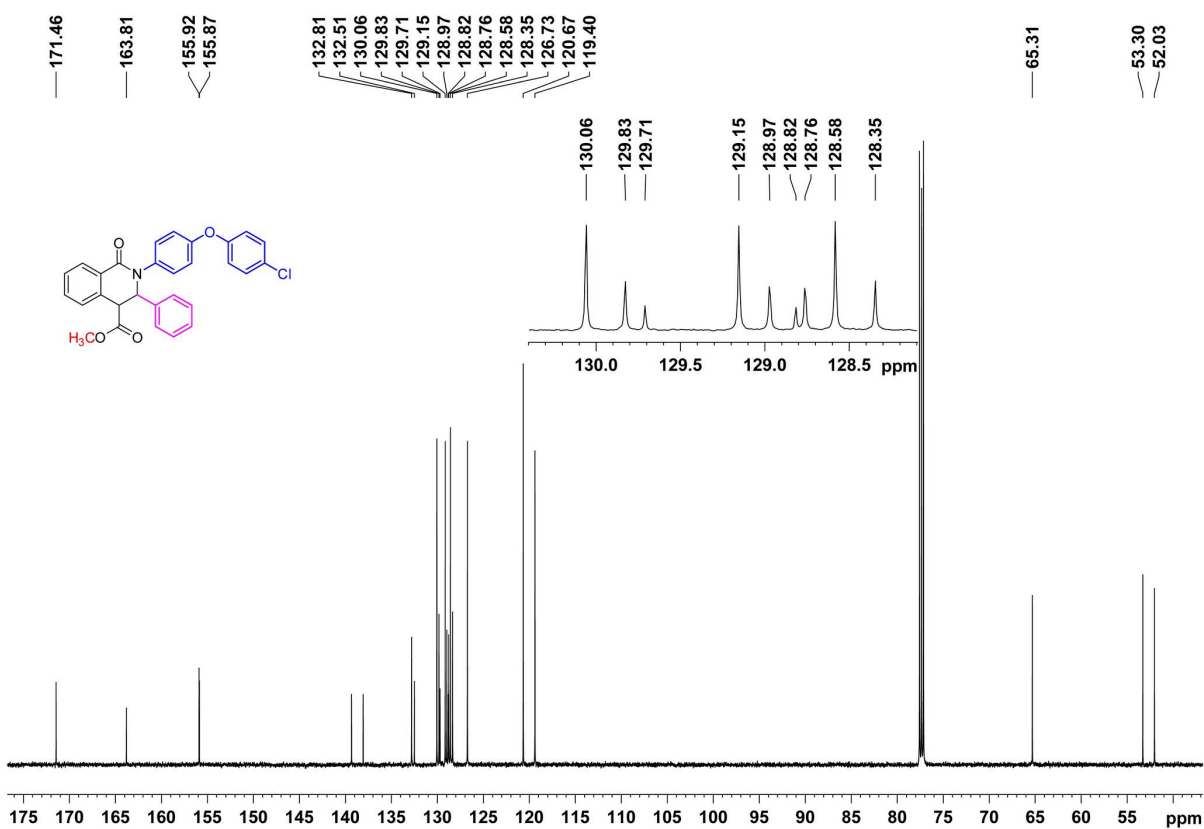


Figure S116. The ^{13}C NMR spectrum of compound III1

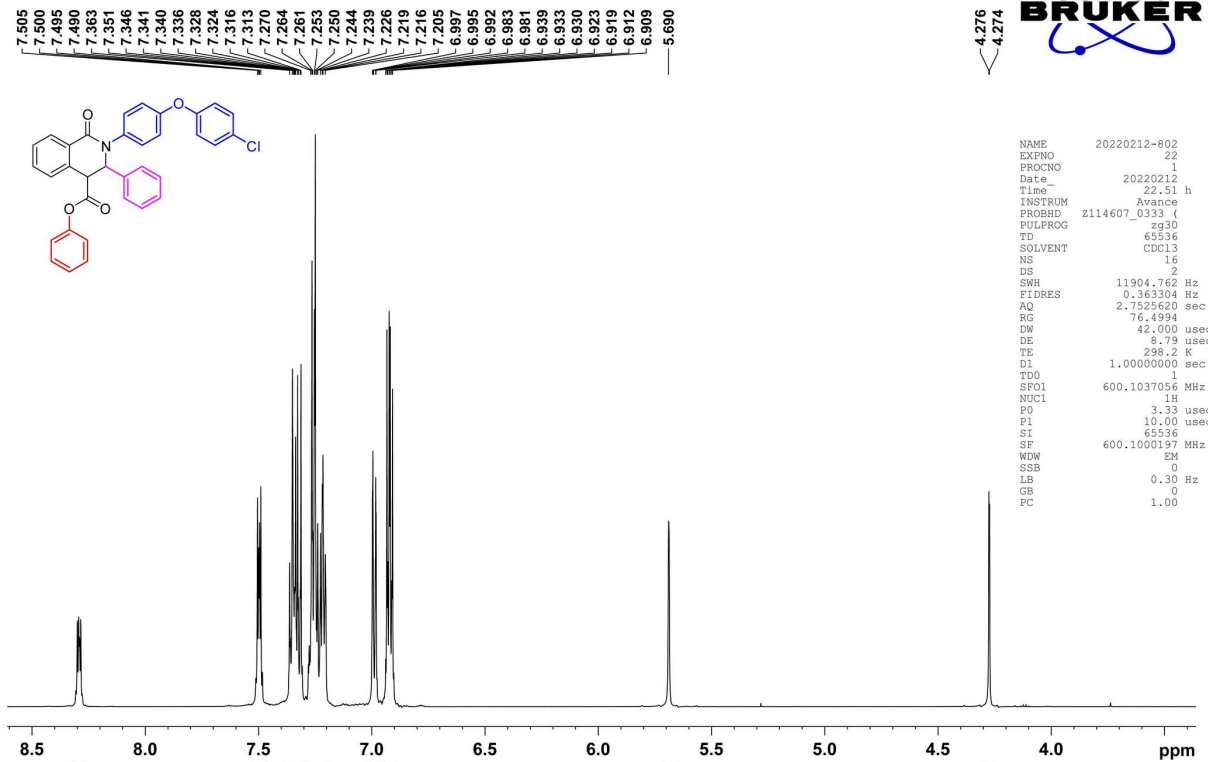


Figure S117. The ^1H NMR spectrum of compound III2

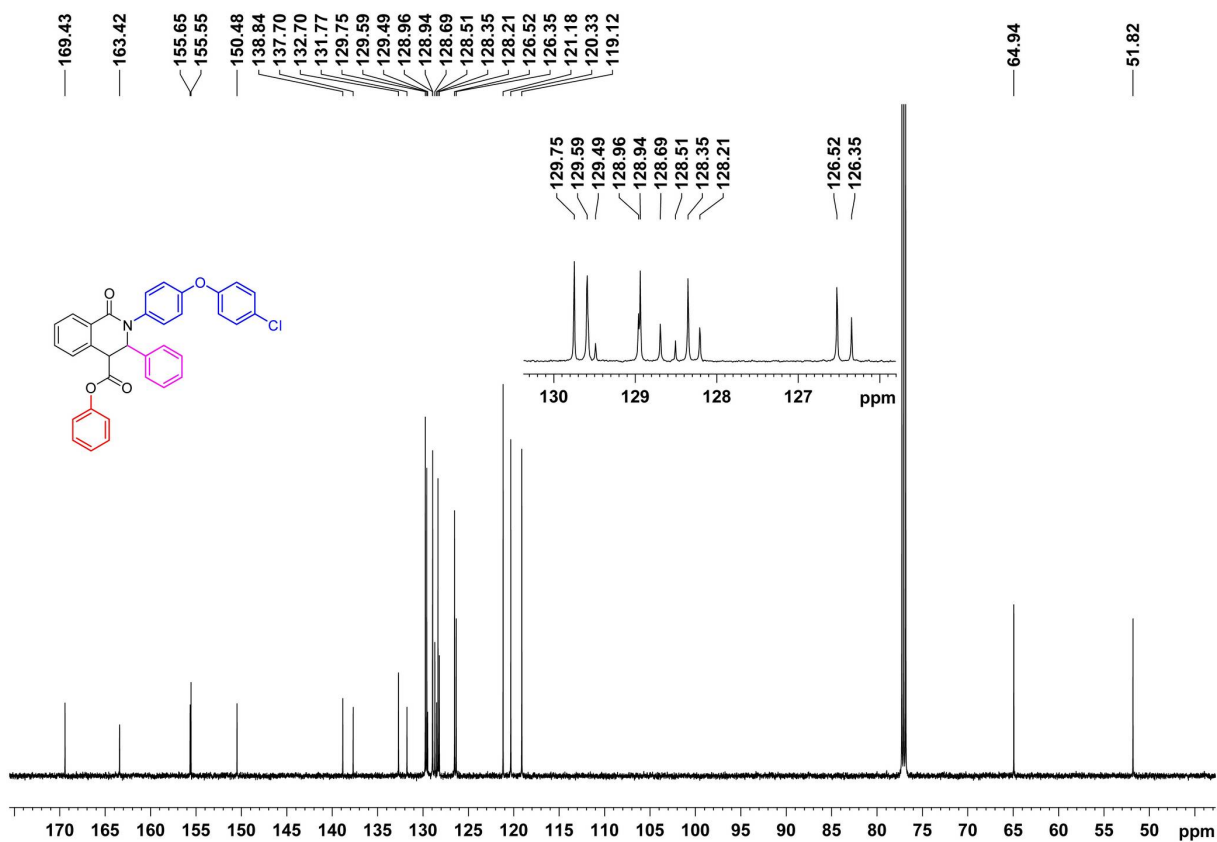


Figure S118. The ^{13}C NMR spectrum of compound III2

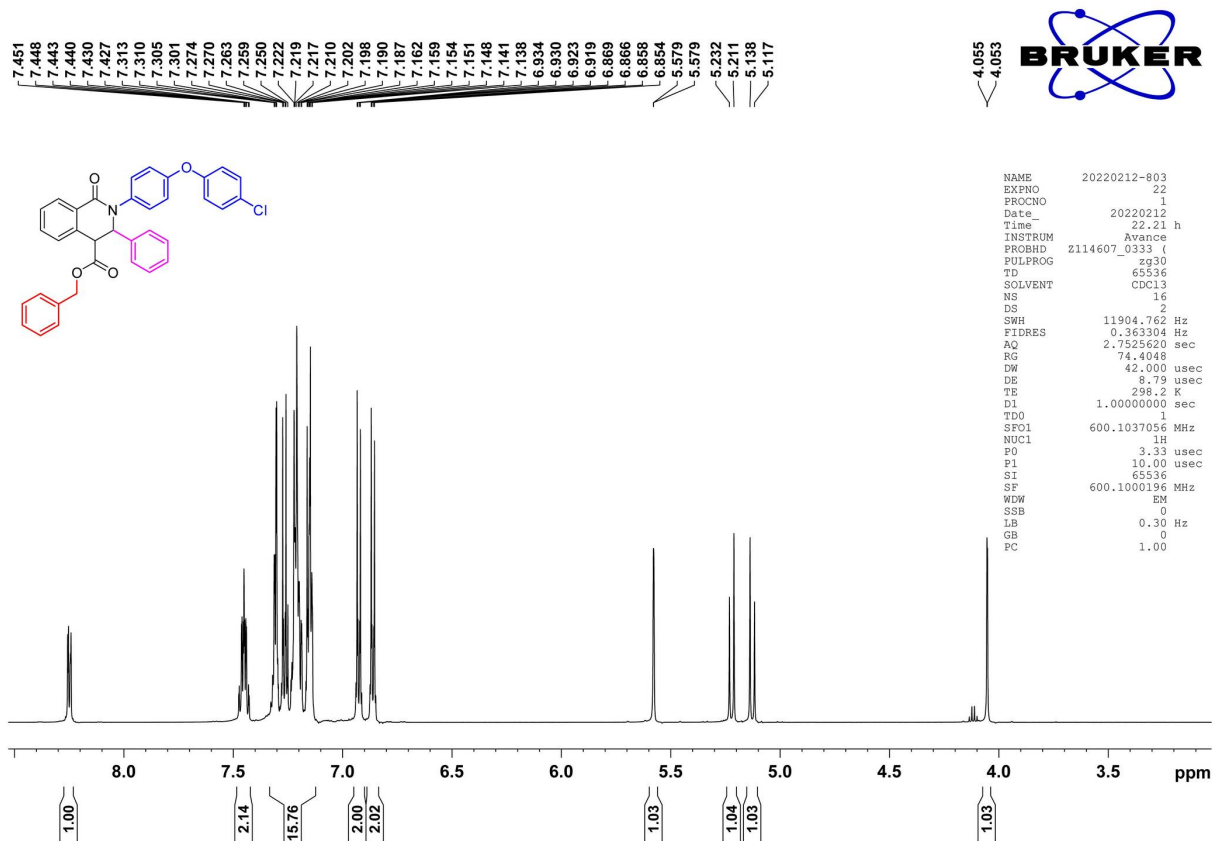


Figure S119. The ^1H NMR spectrum of compound III3

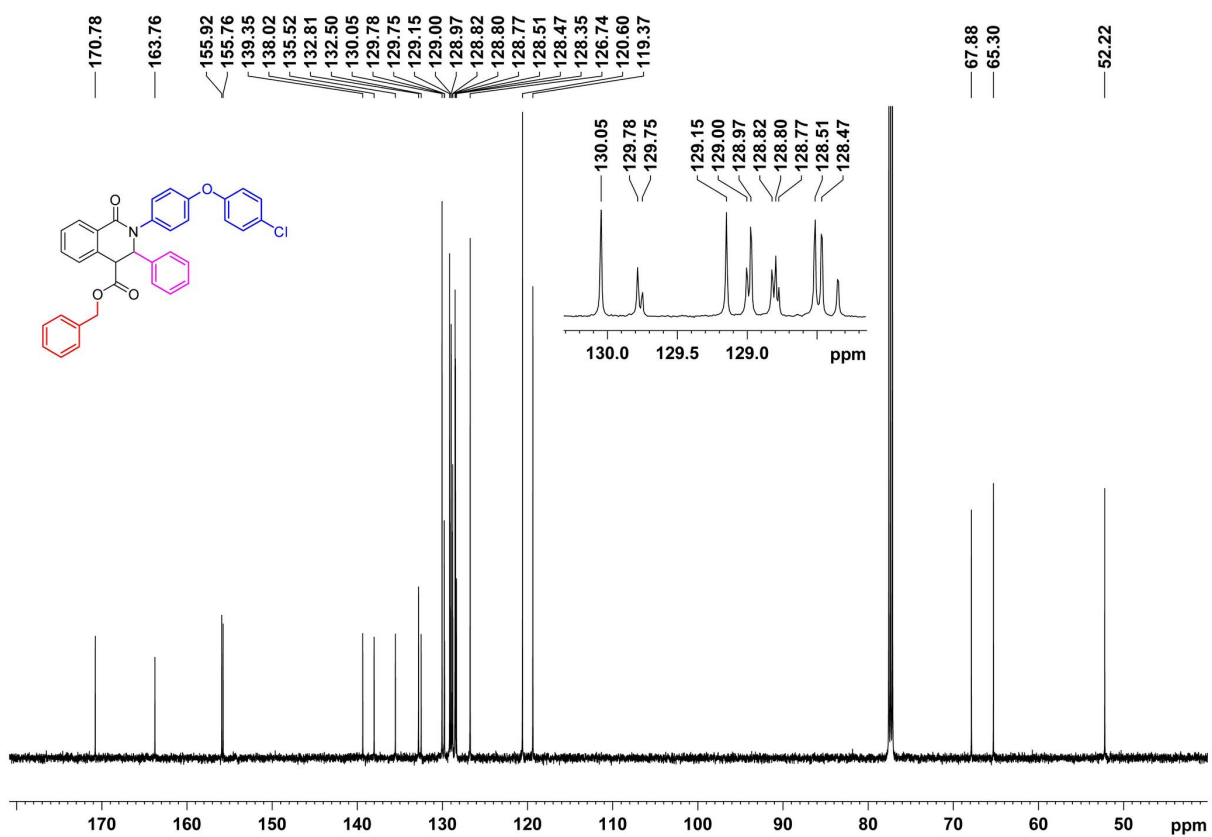


Figure S120. The ^{13}C NMR spectrum of compound III3

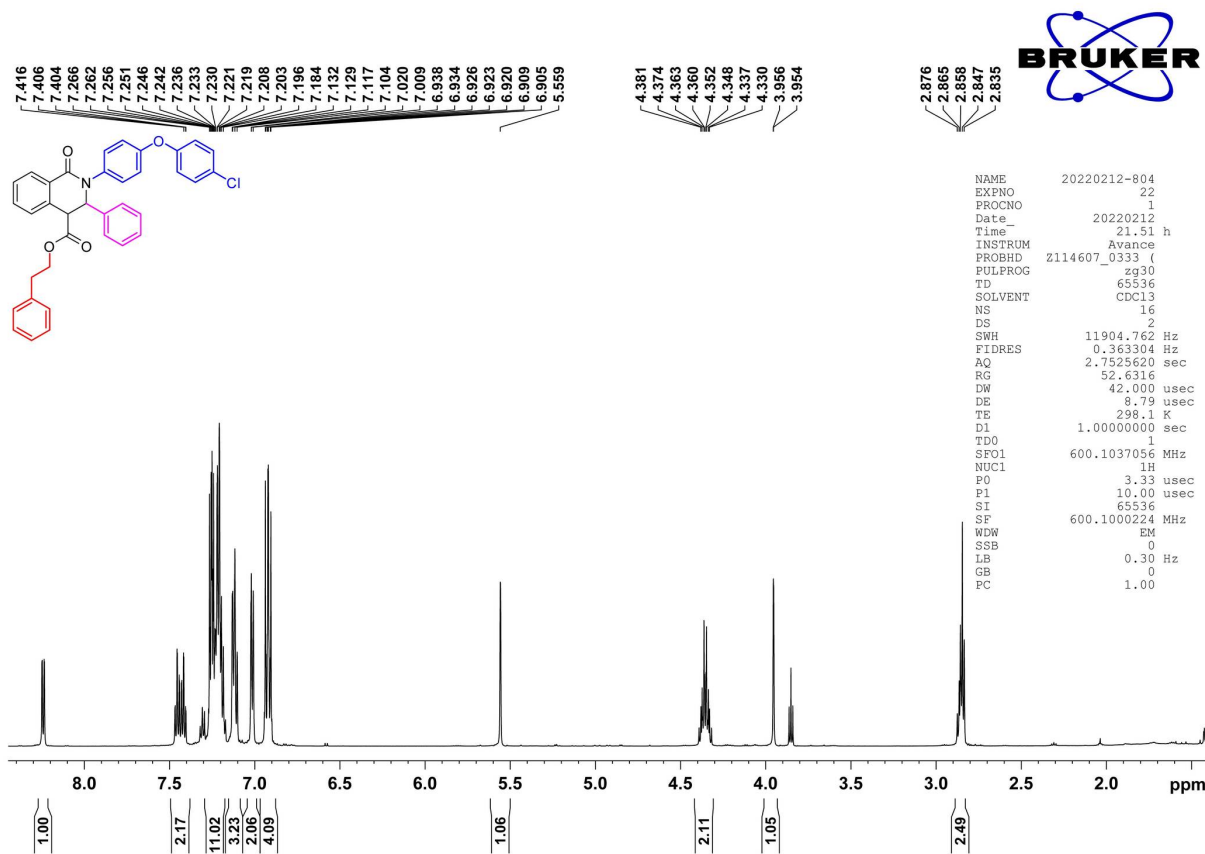


Figure S121. The ¹H NMR spectrum of compound III4

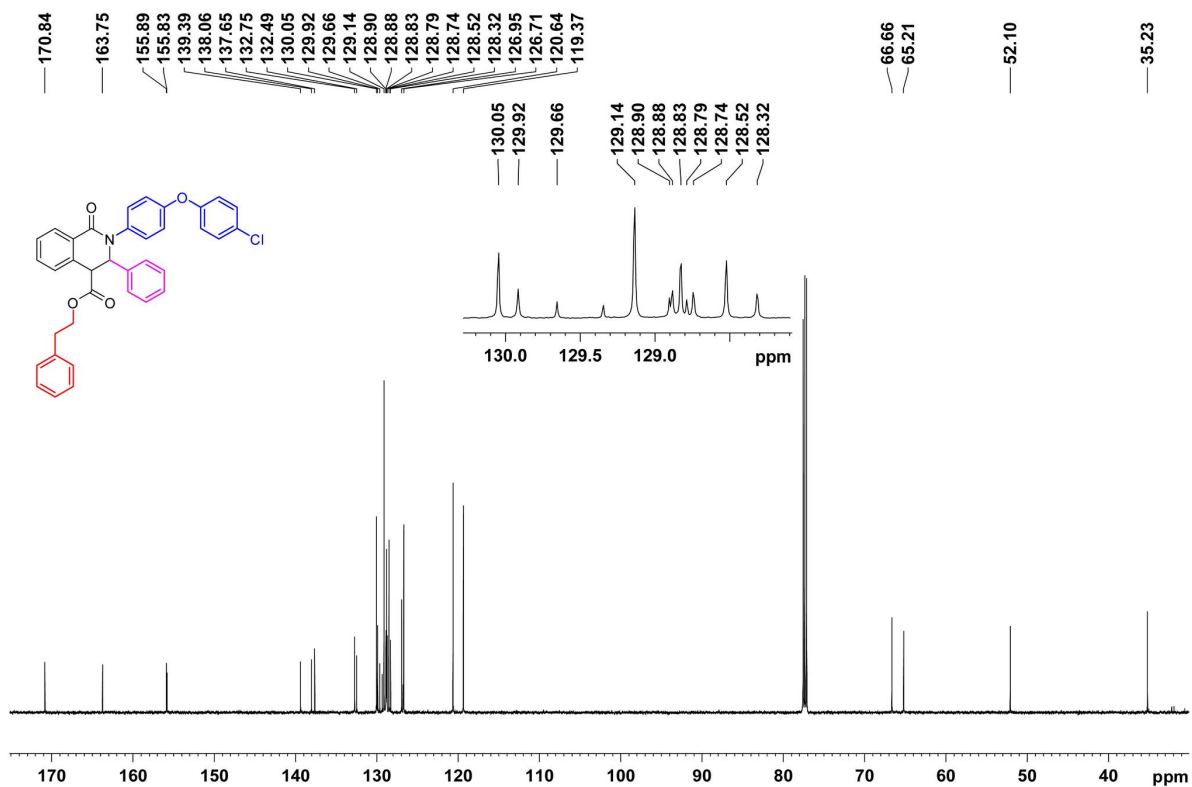


Figure S122. The ¹³C NMR spectrum of compound III4

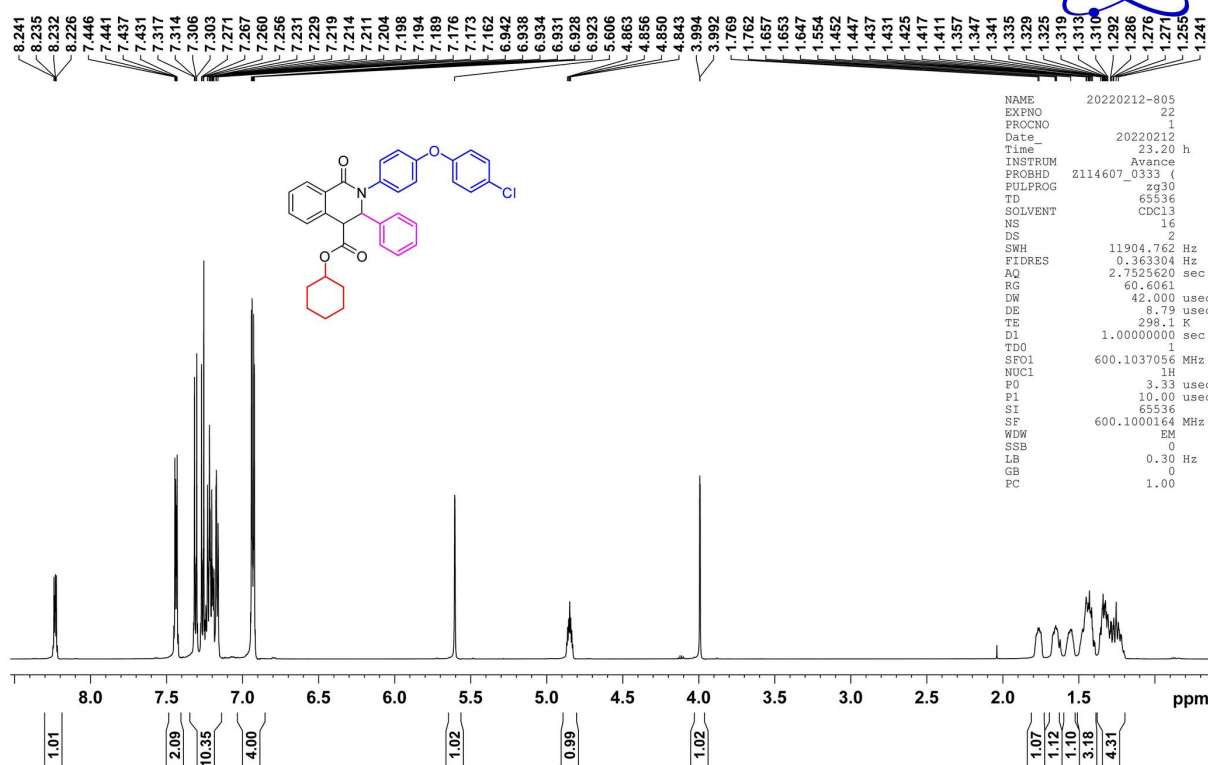


Figure S123. The ^1H NMR spectrum of compound III5

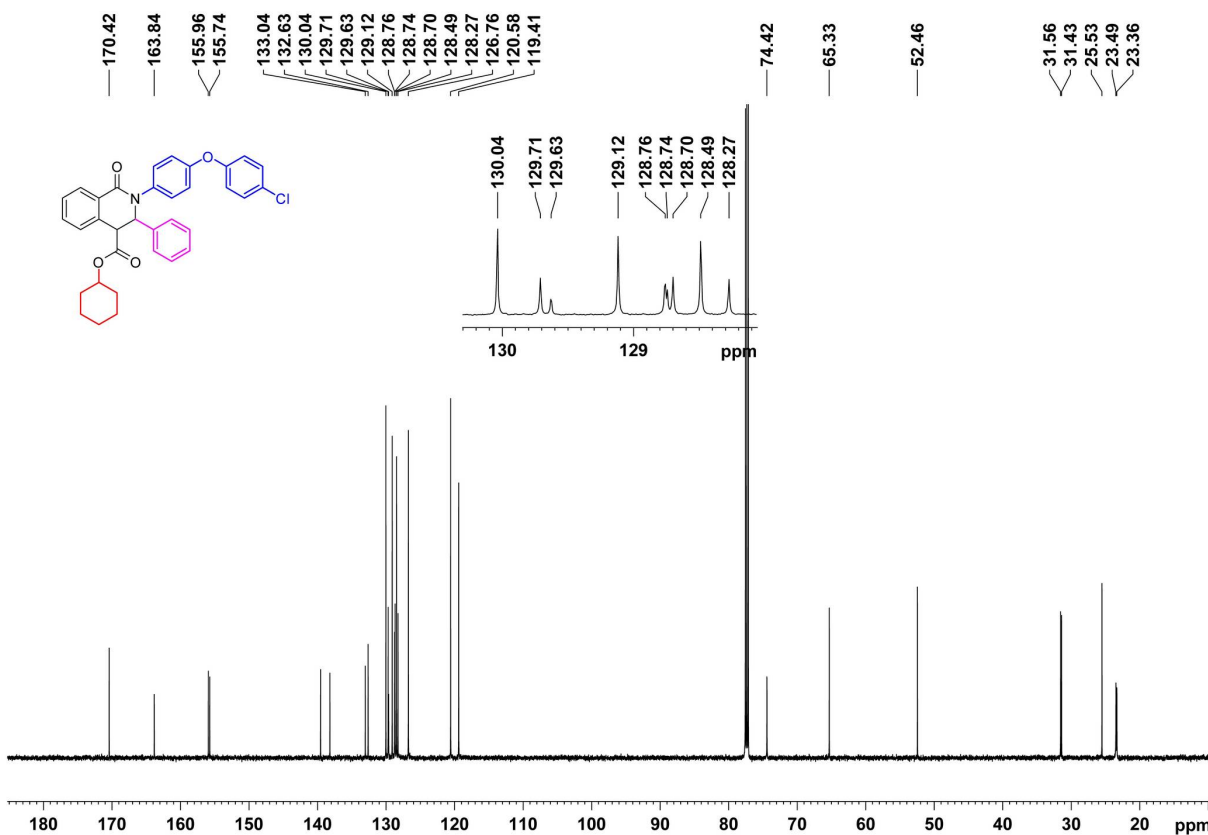


Figure S124. The ^{13}C NMR spectrum of compound III5